EINDHOVEN UNIVERSITY OF TECHNOLOGY

On mass transfer in extractive distillation with ionic liquids

Citation for published version (APA):
Quijada-Maldonado, E. (2013). *On mass transfer in extractive distillation with ionic liquids*. [Phd Thesis 1 (Research TU/e / Graduation TU/e), Chemical Engineering and Chemistry]. Technische Universiteit Eindhoven. https://doi.org/10.6100/IR760514

DOI:
10.6100/IR760514

Document status and date:
Published: 01/01/2013

Document Version:
Publisher's PDF, also known as Version of Record (includes final page, issue and volume numbers)

Please check the document version of this publication:

• A submitted manuscript is the version of the article upon submission and before peer-review. There can be important differences between the submitted version and the official published version of record. People interested in the research are advised to contact the author for the final version of the publication, or visit the DOI to the publisher's website.
• The final author version and the galley proof are versions of the publication after peer review.
• The final published version features the final layout of the paper including the volume, issue and page numbers.

Link to publication

General rights
Copyright and moral rights for the publications made accessible in the public portal are retained by the authors and/or other copyright owners and it is a condition of accessing publications that users recognise and abide by the legal requirements associated with these rights.

• Users may download and print one copy of any publication from the public portal for the purpose of private study or research.
• You may not further distribute the material or use it for any profit-making activity or commercial gain
• You may freely distribute the URL identifying the publication in the public portal.

If the publication is distributed under the terms of Article 25fa of the Dutch Copyright Act, indicated by the "Taverne" license above, please follow below link for the End User Agreement:

www.tue.nl/taverne

Take down policy
If you believe that this document breaches copyright please contact us at:

openaccess@tue.nl

providing details and we will investigate your claim.

Download date: 04. Oct. 2023

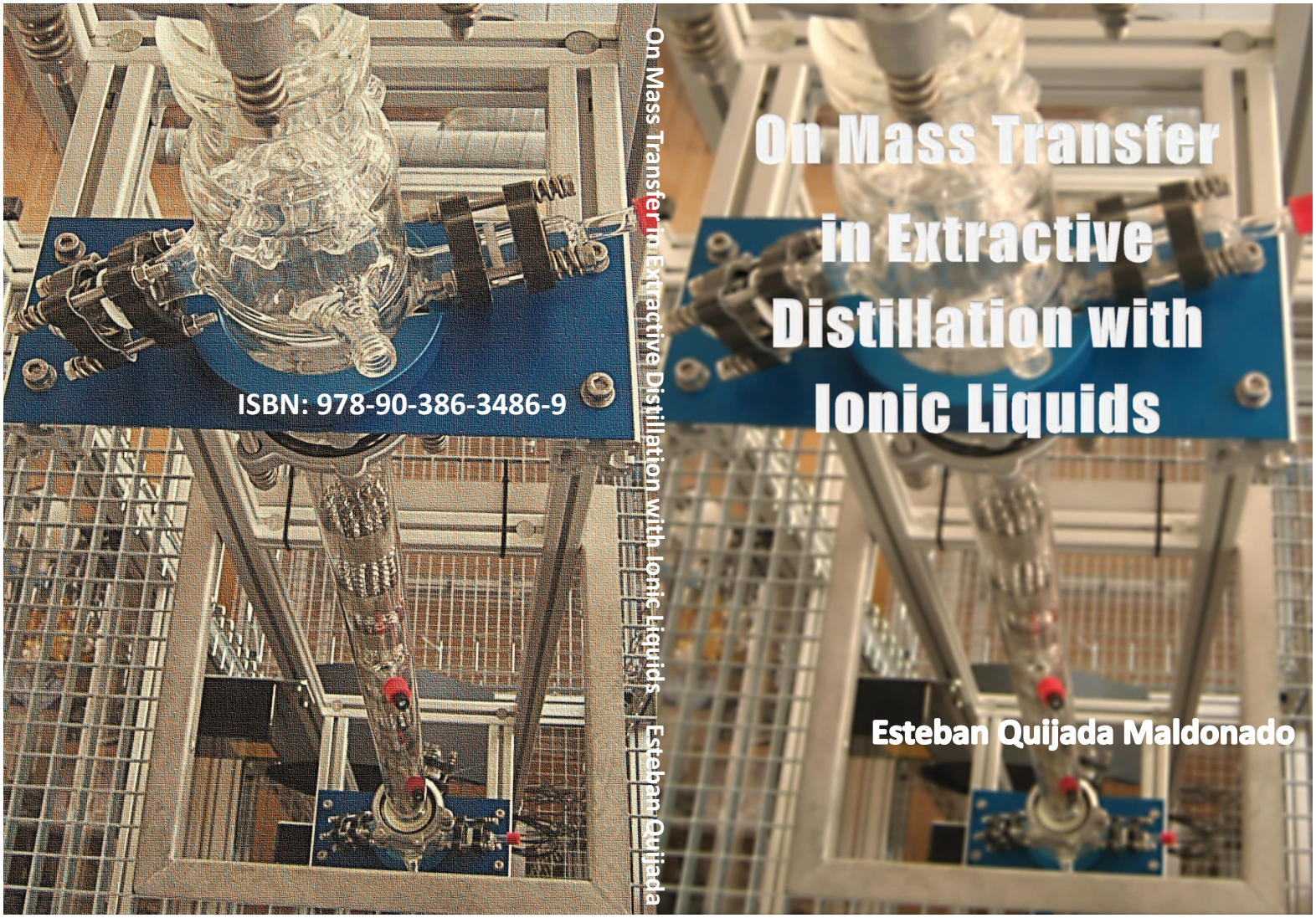

ISBN: 978-90-386-3486-9

On Mass Transfer in Extractive Distillation with Ionic Liquids

Esteban Quijada

On Mass Transfer in Extractive Distillation with Ionic Liquids

Esteban Quijada Maldonado

On Mass Transfer in Extractive Distillation with Ionic Liquids

Esteban Quijada Maldonado

Eindhoven University of Technology

This project has been financially supported by SenterNovem.

On Mass Transfer in Extractive Distillation with Ionic Liquids

Esteban Quijada Maldonado

ISBN: 978-90-386-3486-9

A catalogue record is available from the Eindhoven University of Technology Library.

Printed by Gildeprint Drukkerijen - Enschede

Cover photo by Jeoren Dergent

Copyright © Esteban Quijada Maldoinado, The Netherlands, 2013.

On Mass Transfer in Extractive Distillation with Ionic Liquids

PROEFSCHRIFT

ter verkrijging van de graad van doctor aan de Technische Universiteit Eindhoven, op gezag van de rector magnificus prof.dr.ir. C.J. van Duijn, voor een commissie aangewezen door het College voor Promoties, in het openbaar te verdedigen op dinsdag 5 november 2013 om 16:00 uur

door

Esteban de la Cruz Quijada Maldonado

geboren te Providencia, Chili

Dit proefschrift is goedgekeurd door de promotoren en de samenstelling van de promotiecommissie is als volgt:

voorzitter:	prof.dr.ir. J.A.M. Kuipers
1e promotor:	prof.dr.ir. A.B. de Haan
copromotor(en):	dr.ir. G.W. Meindersma
leden:	Prof.Dr.-Ing.habil. J.-U. Repke (TU Bergakademie Freiberg)
	prof.ir. G.J. Harmsen (RUG)
	Univ.-Prof.Dr.-Ing. A. Bardow (RWTH Aachen)
	Prof.Dr.-Ing. A. Górak (Technische Universität Dortmund)

Acknowledgments

Like in any society, this thesis is a result of a collective effort that I would like to thank. This thesis is dedicated to all the people who contributed with me during these years of research.

First of all I would like to thank my promotor prof.dr.ir Andre de Haan for give me the opportunity to carry out my Ph.D. at SPS group. Furthermore, I thank all his support, enthusiasm, professionalism, practicality, and of course all the provided coffee. But more importantly, I appreciate all the freedom that he gave to perform this research.

I would like to thank my co-promotor and daily supervisor dr.ir Wytze Meindersma for all his helpful advices and his nice company during the conferences. Also, for giving me all the confidence and telling me "go ahead" when I had to buy very expensive but necessary parts for the pilot plant.

I also thank very much all my examination committee for taking part of this thesis: J.A.M. (Hans) Kuipers; Prof. Jens-Uwe Repke for his helpful advices to construct the pilot plant; prof. G. Jan Harmsen for his nice thesis revision; Prof. André Bardow who I meet in Aachen at CAPE Forum and Prof. Andrzej Górak for allowing me to visit his facilities in Dortmund when I was starting the construction of the pilot plant. You all contributed me to make this thesis complete.

To my students and their enthusiasm and perseverance to work with a complicated daily supervisor that I am: Sander, Janneke, Jeroen Dergent and Tim. I say thank very much because you were an important part of this thesis.

To the technicians, many thanks Wilko and Wouter for all the support at the laboratory and also for sharing a talk at any moment. It was nice to know persons who always helped to find, request, and look for all kind of thing in the lab. I want to thank also the people from the metal workshop in the matrix building, especially Dolf van Liempt for supporting me with the construction of the pilot plant and providing tools when it was really necessary.

Pleunie and Caroline, I would like to thank you very much for organizing all the things that were unknown for me. You always solve everything. I do not forget Matthijs Lodewijks who helped with all the buying for the pilot plant.

To the members of the EPC (equipment and prototype center), ex-GTD, thank you for having an incredibly organized working place. Special thanks to Paul Aendenroomer, Frans Kuijpers, Harry de Laat and Peter Minten.

To all the members of the SuPerStars indoor soccer team I really have to thank very much, we are legends. I still remember when I score in the last minute giving hope to the team to win in the last second and became champions …. of the third division ☹. Thank all these nice moments, for 20 minutes I thought I was a professional soccer player and I forgot that I was a Ph.D. student. However, I will never be like Johan Cruyff.

Of course, I would like to thank all my colleagues from the glorious SPS group: Boelo, Edwin, Ana, Alex, Ferdy, Marjette, Esayas, Miguel, Bo, Lesly, Caecilia, Miran, Mark, Agnieszka, Antje and Martijn. I would like to thank my roommates, Mayank and JP for that very familiar atmosphere that we created in the office. Mayank: it was really nice to talk to you about life and the future. JP I have to say thank you so much because you helped me a lot with all the paperwork during the first days in The Netherlands.

Also, I would like to thank a colleague and also beer mate, Jeroen Bokhove for sharing all those depressive and negative talks at the F.O.R.T. and at the Bierprofessor. But especially for being a nice concert mate who was willing to go along to all those thrash, death and black metal gigs.

An especial dedication is to my parents. You were constantly supporting me to finish this very difficult step in my life. From you I have learnt to be perseverant and never give up.

The last and the most important dedication is for my daughter, Antonia, and my wife, Taty. Thank you very much for all that infinite patience that you had during these four years. I really think that without you I would never finished this long journey. You gave me the strength to continue in those dark moments.

Summary

The main objective of this study was to study the effect of the physical properties of ionic liquids as solvents on mass transfer efficiency of extractive distillation columns. Ionic liquids have been promoted as promising separating agents to be applied in this separation technology by means of vapor-liquid experiments. The water – ethanol mixture is commonly separated through extractive distillation using mainly glycols as solvents. To realize all the advantages that ionic liquids offer in the extractive distillation many potential ionic liquids were recommended as replacements of the organic solvent. However, the relatively high viscosity of this new class of solvents could bring mass transfer limitations to the separation process. The rate-based model is able to predict all these limitations while only knowing the physical properties of the system. Nevertheless, two new challenges arise: the scarcity of physical properties concerning ionic liquids and the possible deviation of ionic liquids properties from that predicted by mass transfer correlations. Therefore, the use of the rate-base model presented in this work comprised an experimental analysis on the physical and transport properties and pilot plant tests. After these steps, all the capabilities of the rate-based model can be exploited to quantify the extent in which physical properties may reduce the mass transfer efficiency of the extractive distillation column.

Analysis of physical properties for accurate prediction

The rate-based model requires physical and transport properties to solve the mass transfer across the vapor-liquid boundary through mass transfer correlations. These correlations describe the mass transfer process using physical and transport properties which are scarce for ionic liquids. Experimental work would be necessary to determine all the needed properties. However, this would be a time consuming step during the research. Therefore, the objective of this chapter is to establish the physical and transport properties that are necessary to correctly predict the mass transfer in extractive distillation with ionic liquids. Three ionic liquids were chosen for this purpose: 1-ethyl-3-methylimidazolum acetate, 1-ethyl-3-methylimidazolum chloride and 1-ethyl-3-methylimidazolum

dicyanamide. Furthermore, the reference solvent ethylene glycol was chosen to compare the mass transfer characteristic to the ionic liquids. From this analysis, ternary liquid viscosities, ternary surface tension and infinite dilution diffusion coefficients need to be experimentally determined to provide accurate predictions of the mass transfer characteristic. The rest of the properties can be predicted using common methods for conventional fluids from literature without producing deviations of the predictions.

Experimental determination physical properties

The previous analysis initiated the experimental determination of liquid viscosities, surface tension and infinite dilution diffusion coefficients. Therefore, the objective of this chapter is to experimentally determine the above properties using proven experimental methods from literature. Additionally, to enable the use of these properties in the simulation tool ASPEN® Plus, those properties have to be correlated with accurate models. As result, the above mentioned properties were measured over a wide range of temperatures and compositions of the ternary system water – ethanol – solvent. Additionally, ternary dynamic viscosities and surface tensions of the system water – ethanol – ethylene glycol were measured. The Patel-Teja model using Redlich-Kister and Margules types mixing rules was able to correlate very well the ternary dynamic viscosities over the whole range of compositions and temperatures. The Fu-Li-Wang mixing rule gave excellent results in correlating ternary surface tensions. From this work, the rate-based model can be built in order to predict the mass transfer performance of ionic liquids as solvents.

Rate-based model validation

The mass transfer efficiency of an extractive distillation column has been used to quantify the mass transfer limitations when using a more viscous solvent. This purely predicted result given by the developed rate-based model could be affected by viscosity of ionic liquids and may deviate from reality. Therefore an experimental validation of the model becomes necessary. The objective of this work is to validate the developed rate-

based model with experimental data from a pilot plant. A second objective of this work is to study the mass transfer efficiency of the pilot plant. To accomplish these objectives a pilot plant extractive distillation column was constructed at Eindhoven University of Technology. This plant is equipped with Mellapak® 750Y structured packing having 3.120 meters of height and was operated using a 70 wt% water – 30wt% ethanol feed mixture with 1-ethyl-3-methylimidazolium dicyanamide and ethylene glycol as solvents. The developed rate-based model describes the mass transfer using the Rocha et al. (1993,1996) mass transfer correlation. The results showed that the rate-based model gave excellent predictions of the experimental data for both solvents. The deviation between simulations and the pilot plant data was within 10% relative error. Finally, it was found that the ionic liquids produced better mass transfer efficiencies than the reference solvent for all studied operating conditions.

Effect of ionic liquid viscosities on mass transfer efficiency

Ionic liquids are promising solvents because they can outperform the common organic solvents by increasing relative volatilities. However, when using relatively viscous ionic liquids as separating agent in the extractive distillation of water – ethanol mixtures, the mass transfer efficiency of the column could be significantly reduced as it was previously demonstrated by Weiss and Arlt (1987). Many ionic liquids have been previously discarded due to relatively high viscosity values and so far it is not known the real effect of this property on mass transfer. The rate-based model is able to predict these decreases. This model was previously built with the information of physical and transport properties and validated for this specific purpose. The objective is to quantify the effect of the viscosity of ionic liquids on mass transfer efficiency using several ionic liquids for water – ethanol separation. In this chapter it was found that, for two chosen internals: Sieve trays and Mellapak® 250Y, the liquid phase viscosities affect the mass transfer efficiency. However, this effect can be decreased if the solvent is able to create improvements in relative volatility. This is of great importance since the main advantage of ionic liquids to be applied in extractive distillation is the better vapor-liquid performance than organic

solvents. These obtained conclusions are very important to discriminate ionic liquids during the solvent design.

Pilot plant separation of toluene-methylcyclohexane

Separation of aromatic – aliphatic mixtures by fractional distillation is very challenging due to the proximity of boiling points. The mixture of toluene – methylcyclohexane is separated using the organic solvent *N*-methyl-2-pyrrolidone. However, recently the ionic liquid 1-hexyl-3-methylimidazolium tetracyanoborate has been proposed as a promising replacement of the organic solvent. This ionic liquid is particularly good to separate the mixture due to the increased relative volatility over the common solvent. However, this ionic liquid exhibits limited solubility of the toluene – methylcyclohexane mixture and higher viscosity than the organic solvent. Therefore it is necessary to operate the extractive distillation unit with high solvent-to-feed ratios to avoid the occurrence of two liquid phases. This situation could bring high liquid phase viscosities and result in mass transfer limitations. The objective is to compare performances between the two solvent on the separation of toluene – methylcylcohexane under several operating conditions in the pilot plant and to study the mass transfer efficiency in this process. The results demonstrate that the proposed operating conditions formed only one liquid phase with high liquid phase viscosities. As a consequence, the HETP for the separation using 1-hexyl-3-methylimidazolium tetracyanoborate is twice as high compared to the separation with *N*-methyl-2-pyrrolidone. In spite of this decrease in mass transfer efficiency, the ionic liquid continues to be a promising solvent since high purities were achieve at the top of the column.

Contents

Summary ..... **VII**

1 General introduction **1**

1.1 Introduction 2

1.2 Extractive distillation with ionic liquids 2

1.3 The rate-based model in simulating the extractive distillation with ionic liquids 4

1.4 Ethanol – water separation 5

1.5 Toluene – methylcyclohexane separation 6

1.6 Problem statement 7

1.7 Approach and outline of the thesis 8

2 Physical property requirement analysis for using the rate-based model **17**

2.1 Introduction 18

2.2 The rate-based model 18

2.3 Mass transfer and interfacial area correlations 22

2.3.1 Sieve Trays 23

2.3.2 Mellapak® Structured packing 24

2.4 Property requirement for extractive distillation of water – ethanol with ionic liquids 25

2.5 Ionic liquids for water – ethanol separation 26

2.6 Properties to be studied 28

2.6.1 Liquid viscosity 28

2.6.2 Liquid diffusion coefficients 30

2.6.3 Surface tension 33

2.6.4 Liquid density 35

2.6.5 Liquid thermal conductivity 35

2.7 Conclusions 37

3 Experimental determination and modeling of the physical properties to develop a rate- based model for the separation of water – ethanol mixtures ... 49

3.1 Introduction ... 50

3.2 Experimental ... 51

3.2.1 Chemicals ... 51

3.2.2 Apparatus and procedure ... 52

3.2.2.1 Viscosity measurements ... 52

3.2.2.2 Infinite dilution diffusion coefficients measurements ... 53

3.2.2.3 Surface tension measurements ... 55

3.3 Results ... 57

3.3.1 Viscosity of pure solvents and in mixtures with water and/or ethanol ... 57

3.3.2 Infinite dilution diffusion coefficients ... 60

3.3.3 Surface tension measurements ... 62

3.3.4 Correlation of experimental data in mixtures ... 63

3.3.4.1 Density correlation ... 63

3.3.4.2 Viscosity correlation ... 64

3.4.4.3 Surface tension ... 70

3.4 Conclusions ... 71

4 Experimental determination and modeling of the physical properties to develop a rate- based model for the separation of water – ethanol mixtures ... 77

4.1 Introduction ... 78

4.2 Pilot-scale extractive distillation column ... 79

4.2.1 Experimental features and dimensions ... 79

4.2.2 Operating conditions ... 80

4.3 Experimental section ... 83

4.3.1 Materials ... 83

4.3.2 Analysis of the samples taken from the pilot plant ... 84

4.4 Set up of the rate-based model ... 84

4.4.1 Property methods 84
4.4.2 Mass transfer and interfacial area correlations 85
4.5 Results and discussion 86
4.5.1 Experimental versus simulated composition and temperature profiles 86
4.6 Experimental top purities 91
4.7 Mass transfer efficiency 92
4.8 Conclusions 95

5 Systematic analysis of ionic liquid effects on mass transfer efficiency in extractive distillation of water – ethanol mixtures 101

5.1 Introduction 102
5.2 Case study 103
5.3 Simulation setup 105
5.4 Results 108
5.4.1 Sieve tray column 108
5.4.2 Mellapak® structured packing 114
5.5 Conclusions 117

6 Pilot plant study on the separation of Toluene-Methylcyclohexane mixtures using NMP and the ionic liquid [HMIM][TCB] as solvents 121

6.1 Introduction 122
6.2 Operating parameters 123
6.3 Physical properties of the solvents 125
6.4 Liquid phase resistance 126
6.5 Results 129
6.5.1 Experimental profiles 129
6.5.2 Mass transfer 133
6.6 Conclusions 136

7 Conclusions and Outlook **139**

7.1 Conclusions 140

7.2 Outlook 142

Appendices **145**

Appendix A: Data physical properties 145

List of Publications **157**

Curriculum Vitae **161**

1

General Introduction.

1.1 Introduction

Distillation has been for years the most used and academically taught separation process. In words of Dr. James R. Fair (1990): "*Distillation, King of separations, will remain as the workhorse separation device of the process industries*". The first distillation practices date back to the Alexandrian chemists (100 – 900 A.D.) [1] and nowadays this technology is widely and intensively used in industry ranging from alcohol production to distillation of crude oil.

However, sometimes the production of high purity chemicals is not possible or economically unfeasible by means of a normal fractional distillation when trying to separate azeotropic and/or close boiling mixtures. For the separation of these complex mixtures, extractive distillation arises as an energy saving and advantageous alternative that produces high purity and valuable chemicals [2-5]. Furthermore, the use of ionic liquids has been recently proposed as a replacement of organic solvents due to their demonstrated high selectivities, enhancing the conventional extractive distillation process [6,7]. Despite of this merit, ionic liquids show very high viscosities [8-10], this could bring mass transfer limitations and mask all advantages gained by the use of this new class of promising solvents.

This chapter starts with a short state-of-the-art concerning the use of ionic liquids in extractive distillation. Next, a short review of rate-based modeling is given and linked with the simulation of extractive distillation processes. Besides that, a review of the current technologies for separating an azeotropic mixture like water – ethanol and a close boiling point mixture like toluene – methylcyclohexane is explained. Finally, the problem statement of this work is defined and followed by the outline of the thesis.

1.2 Extractive distillation with ionic liquids

The extractive distillation process allows separating complex mixtures by the addition of a third component having a high boiling point or so called "solvent" that modifies the activity coefficients at the liquid phase and thus increases the relative volatilities. This operation unit is well known and applied in the chemical and petrochemical industry.

Figure 1.1 shows a process flow sheet of a simple extractive distillation operation. The common solvents used for the separation of many mixtures are listed in literature [11]. Most of these solvents are organic while salts are used as a solvent in extractive distillation, but the latter in a less extent. Nowadays, the use of ionic liquids in extractive distillation is being extensively studied for many mixtures by means of thermodynamic vapor-liquid equilibria [12-34]. This opens the possibilities for process simulation, evaluation and optimization [35-37]. All of these investigations are driven by some excellent properties exhibited by ionic liquids such as: a non-detectable vapor pressure that would not pollute the top product; a wide liquid range offering good operational conditions; requirement of less complex regeneration steps than conventional solvents even though this is a matter of research; good chemical and thermal stability; non-flamability; non-toxicity; etc.

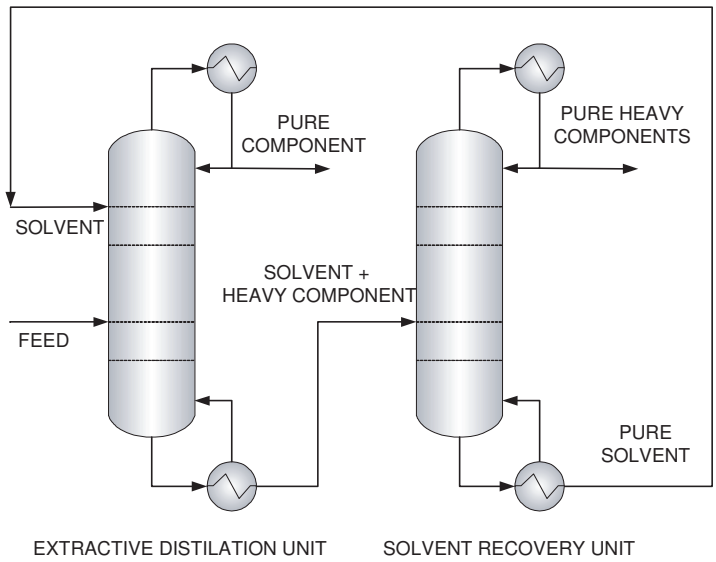

Figure 1.1. Scheme of a conventional extractive distillation unit and the solvent recovery step.

However, on top of those advantages, ionic liquids are molten salts and they could offer the same separation abilities as solid salts without the solubility issues. This generates improved selectivities than those produced by organic solvents which lead to a decrease in the use of solvent to achieve a certain separation. Furthermore, it was estimated that an

increase in selectivity brings a reduction in total annual cost [38] and a more promising separation scenario.

1.3 The rate-based model in simulating extractive distillation with ionic liquids

The equilibrium model (EQ) has been principally used to design, simulate and optimize the extractive distillation process [39-44] due to its simplicity and elegancy. Nevertheless, this model does not correctly describe the extractive distillation with ionic liquids. For example, the ideal representation of an equilibrium stage does not take into account the mass transfer limitations that a real stage normally has. This leads to defining efficiencies. Although there are methods to priory estimate efficiencies [45-48], this point can be very difficult to solve since the efficiencies varying from stage to stage ranging from $-\infty$ to $+\infty$ in multi-component systems. Therefore, the process of estimating efficiencies can become a mere parameter-fitting exercise.

To overcome these limitations, the non-equilibrium or rate-based model can be used for the above mentioned purposes. This model was proposed by Krishnamurthy and Taylor [49,50] and it is capable to accurately predict concentration profiles of several systems without the need of efficiencies. Since then, the rate-based model has been used to predict with great accuracy the behavior of many complex systems including azeotropic distillations [51-53], reactive distillations [54-56], absorption [57,58] and a few examples in extractive distillation [59,60]. However, due to the fact that ionic liquids are a new class of solvent, no studies on rate-based modeling of their use in extractive distillation can be found in literature. The use of the rate-based model could provide a very good and accurate approach to study the advantages and limitations of extractive distillation with ionic liquids, because the rate-based model accounts for the mass transfer limitations of a real distillation process and therefore it could account for the even larger mass transfer limitations of the ED process with ionic liquid could bring.

1.4 Water – ethanol separation

Ethanol is commonly known as alcohol in beverages and antiseptic. Ethanol is also a base component for many applications in the chemical industry. However, nowadays the main consuming area is bio-ethanol as fuel or fuel additive. Ethanol is produced from different resources such as sugarcane (mainly Brazil) [61-64], corn (mainly US) [65-67], cellulose [68,69], starch [70,71], and in a lesser extent from wheat and dairy. A fermentation of the hydrolyzed sugars produces a mixture of approximately 5 - 12 wt% of ethanol in water. Normally a distillation column is used after the fermentation step to increase the ethanol purity to roughly 95.6 wt% which is the azeotropic point of the water – ethanol mixture.

However, an extra step is required to completely dehydrate the ethanol. Due to the above mentioned azeotropic point, a normal fractional distillation is no longer a suitable and an alternative technology is required. Azeotropic distillation [72-75], adsorption [76-78], pervaporation [79-81], pressure swing distillation [82] and extractive distillation [3,41,83,84] have been extensively studied for water – ethanol separations. However, extractive distillation is advantageous over the rest of the mentioned technologies by the following reasons: For instance, azeotropic distillation requires significantly more energy than extractive distillation since the solvent is vaporized in the column. Adsorption processes are less energy intensive than extractive distillation and provide easier operation. However, the major energy consumption of this process occurs during the regeneration of the adsorptive medium where high temperatures or low pressures are required. This brings higher capital expenditures than ED because it needs an expensive heater for the regeneration. Pervaporation requires less energy since the separation is not based on differences in boiling point. Nevertheless, applications for pervaporators are limited to moderate volumes because the pieces of the membrane modules tend to be very high for large capacities while distillation allows higher throughputs. The case of pressure swing distillation is different. No solvent is needed, and previous studies [85,86] have claimed that this technology is more economical attractive than extractive distillation due to lower total annual cost or less Opex since ED requires a large amount of solvent. However, ionic liquids are designed to improve relative volatilities and reduce the amount of solvent

needed to achieve a certain separation. Therefore, extractive distillation continues to be an economically promising technology in separating complex mixtures.

1.5 Toluene – methylcyclohexane separation

Aromatic compounds like benzene, xylenes or toluene are important base chemicals for producing many starting materials for clothes, vehicles, cosmetics, computers, etc. Specially, from polyurethane is made from toluene and is used to produce building insulations, coatings for floor, refrigerators, and a variety of products. Aromatic compounds come from three main sources of feedstock: catalytic reformates or reforming of gasoline, pyrolysis gasoline and in minor percentage coke-oven light oil. In the reforming of the oil, alkyl-cyclopentanes are isomerized to substituted cyclohexanes and then aromatized by catalytic dehydrogenation [87,88]. Pyrolysis gasoline produces mainly benzene. Next, the obtained reformate compositions consists typically of a mixture of approximately 73% of aromatics and C_4-C_{10} paraffins and naphthenes (aliphatics)[88].

Separation of an aromatic/aliphatic mixture like toluene-methylcyclohexane is very complicated by normal fractional distillation due to the close boiling points of both components (b.p.: 110.8°C and 101°C respectively). Available processes for separating this mixture are divided according to the amount of aromatics present in a mixture. Thus, liquid-liquid extraction is used for a 20 – 65 wt% of aromatics, extractive distillation for a 65 – 90 wt% and azeotropic distillation for higher than 90 wt% of aromatics present in a mixture [87,89].

Commonly used organic solvents for extractive distillation of aromatic/aliphatic mixtures are published in literature [90-92] and include *N*-methyl-2-pirrolodone (NMP), Dimethylformamide (DMF), phenol and others. Lately ionic liquids have been proposed to separate these complex mixtures by extractive distillation due to their advantages [7,18,19,93-96].

1.6 Problem statement

In this thesis, a rate-based analysis will be carried out on the application of ionic liquids in extractive distillation for the separation of water – ethanol and toluene – methylcyclohexane mixtures. The aim is to determine the effects of the physical properties of ionic liquids on the mass transfer efficiency performance in an extractive distillation column. One of the important features of ionic liquids is their high viscosity. Although, ionic liquids are promoted to increase the selectivity over organic solvents, reported values of their viscosity range from approximately 15 [mPa s] to nearly 21.000 [mPa s] at 298.15 K [8,97-99]. These viscosities can induce serious mass transfer limitations. Indeed, a previous experimental study [100] shows a decrease in efficiency with the increase of solvent viscosity in extractive distillation.

The rate-based or nonequilibrium model enables the study of both the mass transfer characteristics in a distillation column. However, to give a real description of the process, it is necessary to provide reliable physical and transport property data of the ternary system formed by the constituents of the mixture to be separated and the solvent. Ionic liquids are a new class of solvent and although lately many of these properties have been experimentally determined, the knowledge on physical and transport properties in ternary mixtures remains scarce.

On the other hand, the reliability of the rate-based model relies on the accuracy offered by the mass transfer correlations under certain conditions. Correlations for trays and either random or structured packings are extensively reported in literature [59,101]. So far, ionic liquids have not been tested in distillation columns and their properties could result in inaccurate predictions by the mass transfer correlations and therefore the rate-based model. This could lead to erroneous conclusions about the mass transfer performance of using ionic liquids in extractive distillation. In this context, an extractive distillation pilot plant running with an ionic liquid as solvent is needed to evaluate the predictive ability of the rate-based model.

1.7 Approach and outline of the thesis

The objective is to study the effects of physical and transport properties of different ionic liquids on the separation of water – ethanol and toluene – methylcyclohexane mixtures by means of extractive distillation. For water ethanol separation, rate-based simulations are carried out in ASPEN Plus® Radfrac. Before performing any simulation, physical properties of ionic liquids need to be measured. These experiments include measuring viscosities, densities, surface tensions and diffusion coefficients. Additionally, to make these data usable in ASPEN Plus, models that correctly correlate the measured data are investigated. Based on these results, the effect of these physical properties on the mass transfer efficiency is investigated. Besides that, a chosen ionic liquid is tested in an extractive distillation pilot plant along with the reference solvent and commonly used ethylene glycol (EG) to validate the rate-based model for this process. Finally, the performance on a proposed ionic liquid to separate the toluene – methylcyclohexane mixture is studied in the extractive distillation pilot plant. This thesis is divided in seven chapters:

Chapter 2 describes the selection of physical properties to be measured in order to describe the mass transfer in an extractive distillation with ionic liquid without losing accuracy in the predictions.

Chapter 3 is about the experimental determination of physical and transport properties. This includes binary and ternary viscosities and densities of ionic liquids and EG in mixtures with water and/or ethanol, infinite dilution diffusion coefficients and ternary surface tension measurements. Also the modeling of these experimental data is carried out in this chapter.

Chapter 4 compares experimental data obtained from a pilot plant scale extractive distillation column that uses an ionic liquid, [EMIM][DCA], as solvent with the results obtained from the rate-based model for water – ethanol separation.

Chapter 5 investigates the effect of several ionic liquids viscosity on the mass transfer efficiency compared to the reference solvent EG.

Chapter 6 studies the performance of [HMIM][TCB] for the separation of toluene – methylcyclohexane in an pilot plant scale extractive distillation column.

Chapter 7 contains the major conclusions and future work.

Reference List

[1] R.J.Forbes, *A Short History of the Art of Distillation*, Brill, Leiden, 1970.
[2] R.P.Tripathi and J.M.Sagar, High purity cyclohexane from petroleum streams by extractive distillation, *J.Appl.Chem.Biotechn.*, 23, 2013, 581 - 588.
[3] A.Meirelles, S.Weiss, and H.Herfurth, Ethanol Dehydration by Extractive distillation, *J.Chem.Tech.Biotechnol.*, 53, 1992, 181 - 188.
[4] M.T.G.Jongmans, E.Hermens, M.Raijmakers, J.I.W.Maassen, B.Schuur, and A.B.de Haan, Conceptual process design of extractive distillation processes for ethylbezene/styrene separation, *Chem.Eng.Res.Des.*, 90, 2012, 2086 - 2100.
[5] M.Llano-Restrepo and J.Aguilar-Arias, Modeling and simulation of saline extractive distillation columns for the production of absolute ethanol, *Comput.Chem.Eng.*, 2003, 527 - 549.
[6] Z.Lei, C.Li, and B.Chen, Extractive Distillation: A Review, *Sep.Purif.Rev.*, 32, 2003, 121 - 213.
[7] A.B.Pereiro, J.M.M.Araújo, J.M.S.S.Esperança, I.M.Marrucho, and L.P.N.Rebelo, Ionic Liquid in separation of azeotropic system - A review, *J.Chem.Thermodyn.*, 46, 2012, 2 - 28.
[8] R.L.Gardas and J.A.P.Coutinho, A group contribution method for viscosity estimation of ionic liquids, *Fluid Phase Equilibr.*, 266, 2008, 195 - 201.
[9] N.Calvar, E.Gómez, B.González, and Á.Domínguez, Experimental Determination, Correlation, and Prediction of Physical Properties of the Ternary Mixtures Ethanol + Water with 1-Octyl-3-methylimidazolium Chloride and 1-Ethyl-3-methylimidazolium Ethylsulfate, *J.Chem.Eng.Data*, 52, 2007, 2529 - 2535.
[10] A.Galán-Sánchez, J.Ribé-Espel, F.Onink, G.W.Meindersma, and A.B.de Haan, Density, viscosity, and Surface Tension of Synthesis Grade Imidazolium, Pyridinium, and Pyrrolidinium Based Room Temperature ionic Liquids, *J.Chem.Eng.Data*, 54, 2009, 2803 - 2812.
[11] E.J.Henley, J.D.Seader, and D.K.Roper, *Separation Process Principles*, Wiley, Asia, 2011.
[12] Y.Ge, L.Zhang, X.Yuan, W.Geng, and J.Ji, Selection of ionic liquids as entrainers for separation of (water + ethanol), *J.Chem.Thermodyn.*, 40, 2008, 1248 - 1252.
[13] C.Jork, M.Seiler, Y.Beste, and W.Artl, Influence of Ionic Liquids on the Phase Behavior of Aqueous Aseotropic Systems, *J.Chem.Eng.Data*, 49, 2004, 852 - 857.
[14] N.Calvar, B.González, E.Gómez, and .Domínguez, Vapor-Liquid Equilibria for the Ternary System Ethanol + Water + 1-Ethyl-3-methylimidazolium Ethylsulfate and the Corresponding Binary System Containing the Ionic Liquid at 101.3 kPa, *J.Chem.Eng.Data*, 53, 2008, 820 - 825.
[15] V.K.Verma and T.Banarjee, Ionic liquids as entrainers for water + ethanol, water + 2-propanol, and water + THF systems: A quantum chemical approach, *J.Chem.Thermodyn.*, 42, 2010, 909 - 919.
[16] S.Nebig, R.Bölts, and J.Gmehling, Measurement of vapor-liquid equilibria (VLE) and excess enthalpies (H^E) of binary systems with 1-alkyl-3-methylimidazolium bis(trifluoromethylsulfonyl)imide and prediction of these properties and γ^∞ using modified UNIFAC (Dortmund), *Fluid Phase Equilibr.*, 258, 2007, 168 - 178.

[17] L.Zhang, B.Qiao, Y.Ge, D.Deng, and J.Ji, Effect of ionic liquids on (vapor + liquid) equilibrium behavior of (water + 2-methyl-2-propanol), *J.Chem.Thermodyn.*, 41, 2009, 138 - 143.

[18] B.Mokhtarani and J.Gmehling, (Vapour + liquid) equilibria of ternary system with ionic liquids using headspace gas chromatography, *J.Chem.Thermodyn.*, 42, 2010, 1036 - 1038.

[19] J.P.Gutierrez, W.Meindersma, and A.B.de Haan, Binary and ternary (liquid + liquid) equilibrium for {methylcyclohexane (1) + toluene (2) + 1-hexyl-3-methylimidazolium tetracyanoborate (3)/1-butyl-3-methylimidazolium tetracyanoborate (3)}, *J.Chem.Thermodyn.*, 43, 2011, 1672 - 1677.

[20] A.V.Orchillés, P.J.Miguel, E.Vercher, and A.Martínez-Andreu, Ionic Liquids as Entrainers in Extractive Distillation: Isobaric Vapor-Liquid Equilibria for Acetone + Methanol + 1-Ethyl-3-methylimidazolium Trifluoromethanesulfonate, *J.Chem.Eng.Data*, 52, 2007, 141 - 147.

[21] Q.Li, J.Zhang, Z.Lei, J.Zhu, J.Zhu, and X.Huang, Selction of Ionic Liquids as Entrainers for the Separation of Ethyl Acetate and Ethanol, *Ind.Eng.Chem.Res.*, 48, 2009, 9006 - 9012.

[22] A.V.Orchillés, P.J.Miguel, F.J Llopis, E.Vercher, and A.Martínez-Andreu, Influence of Some Ionic Liquids Containing the Trifluoromethanesulfonate Anion on the Vapor-Liuqid Equilibria of the Acetone + Methanol System, *J.Chem.Eng.Data*, 56, 2011, 4430 - 4435.

[23] L.Zhang, Y.Ge, D.Ji, and J.Ji, Experimental Measurements and Modeling of Vapor-Liquid Equilibrium for Ternary Systems Containing Ionic Liquids: A Case Study for the System Water + Ethanol + 1-Hexyl-3-methylimidazolium Chloride, *J.Chem.Eng.Data*, 54, 2009, 2322 - 2329.

[24] A.V.Orchillés, P.J Miguel, E.Vercher, and A.Martínez-Andreu, Using 1-Ethyl-3-methylimidazolium Trifluoromethanesulfonate as an Entrainer for the Extractive Distillation of Ethanol + Water Mixtures, *J.Chem.Eng.Data*, 55, 2010, 1669 - 1674.

[25] W.Geng, L.Zhang, D.Deng, Y.Ge, and J.Ji, Experimental Measurement and Modeling of Vapor-Liquid Equilibrium for the Ternary System Water + Ethanol + 1-Butyl-3-methylimidazolium Chloride, *J.Chem.Eng.Data*, 55, 2010, 1679 - 1683.

[26] A.V.Orchillés, P.J.Miguel, V.González-Alfaro, E.Vercher, and A.Martínez-Andreu, 1-Ethyl-3-methylimidazolium Dicyabamide as a Very Efficient Entrainer for the Extractive Distillation of the Acetone + Methanol System, *J.Chem.Eng.Data*, 57, 2012, 394 - 399.

[27] Q.Li, F.Xing, Z.Lei, B.Wang, and Q.Chang, Isobaric Vapor-Liquid Equilibrium for Isopropanol + Water + 1-Ethyl-3-methylimidazolium Tetrafluoroborate, *J.Chem.Eng.Data*, 53, 2008, 275 - 279.

[28] R.Li, X.Cui, Y.Zhang, T.Feng, and J.Cai, Vapor-Liquid Equilibrium and Liquid-Liquid Equilibrium of Ethyl Acetate + Ethanol + 1-Ethyl-3-methylimidazolium Acetate, *J.Chem.Eng.Data*, 57, 2012, 911 - 917.

[29] N.Calvar, B.González, E.Gómez, and Á.Domíngue, Vapor-Liquid Equilibria for the System Ethanol + Water + 1-Butyl-3-methylimidazolium Methylsulfate and the Corresponding Binary System at 101.3 kPa, *J.Chem.Eng.Data*, 54, 2009, 1004 - 1008.

[30] M.Döker and J.Gmehling, Measurement and prediction of vapor-liquid equilibria of ternary systems containing ionic liquids, *Fluid Phase Equilibr.*, 227, 2005, 255 - 266.

[31] B.Mokhtarami, L.Valialahi, K.T.Heidar, H.R.Mortaheb, A.Sharifi, and M.Mirzaei, Experimental study on (vapor + liquid) equilibria of ternary systems of hydrocarbons/ionic liquids using headspace gas chromatography, *J.Chem.Thermodyn.*, 51, 2012, 77 - 81.
[32] J.Zhao, C.Dong, C.Li, H.Meng, and Z.Wang, Isobaric vapor-liquid equilibria for ethanol-water system containing different ionic liquid at atmospheric pressure, *Fluid Phase Equilibr.*, 242, 2006, 147 - 153.
[33] C.Shen, X.Li, Y.Lu, and C.Li, Effect of ionic liquid 1-methylimidazolium chloride on the vapour liquid equilibrium of water, methanol, ethanol, and {water + ethanol} mixture, *J.Chem.Thermodyn.*, 43, 2011, 1748 - 1753.
[34] D.Deng, R.Wang, L.Zhang, Y.Ge, and J.Ji, Vapor-Liquid Equilibrium Measurements and Modeling for Ternary System Water + Ethanol + 1-Butyl-3-methylimidazolium Acetate, *Chinese J.Chem.Eng.*, 19, 2011, 703 - 708.
[35] V.H.Álvarez, P.Alijó, D.Serrão, R.M.Filho, M.Aznar, and S.Mattedi, Production of Anhydrous Ethanol by Extractive distillation of Diluted Alcoholic Solutions with Ionic Liquids, *Comput.Aided Chem.Eng.*, 27, 2009, 1137 - 1142.
[36] D.Valencia-Marquez, A.Flores-Tlacuahuac, and R.Zasquez-Medrano, Simultaneous Optimal Design of an Extractive Column and Ionic Liquid for the Separation of Bioethanol-Water Mixtures, *Ind.Eng.Chem.Res.*, (2012),
[37] L.M.Chávez-Islas, R.Vásquez-Medrano, and A.Flores-Tlacuahuac, Optimal Synthesis of a High Purity Bioethanol Distillation Column Using Ionic Liquids, *Ind.Eng.Chem.Res.*, 50, 2011, 5175 - 5190.
[38] S.O.Momoh, Assessing the Accuracy of Selectivity as a Basis for Solvent Screening in Extractive Distillation Processes, *Separ.Sci.Technol.*, 26, 1991, 729 - 742.
[39] E.Lladosa, J.B.Montón, and M.Burguet, Separation of di-n-propyl ether and n-propyl alcohol by extractive distillation ans pressure-swing distillation: Computer simulation and economic optimization, *Chem.Eng.Process*, 50, 2011, 1266 - 1274.
[40] P.Langston, N.Hilal, S.Shingfield, and S.Webb, Simulation and optimisation of extractive distillation with water as solvent, *Chem.Eng.Process*, 44, 2005, 345 - 351.
[41] M.A.S.S.Ravagnani, M.H.M.Reis, R.M.Filho, and M.R.Wolf-Maciel, Anhydrous ethanol production by extractive distillation: A solvent case study, *Process Saf.Environ.*, 88, 2010, 67 - 73.
[42] C.Ruiz, J.Coca, A.Vega, and F.Diez, Extractive Distillation of Hydrocarbons with Dimethylformamide: Experimental and Simulation Data, *Ind.Eng.Chem.Res.*, 36, 1997, 4934 - 4939.
[43] I.D.Gil, D.C.Botía, P.Ortiz, and O.F.Sánchez, Extractive Distillation of Acetone/Methanol Mixture Using Water as Entrainer, *Ind.Eng.Chem.Res.*, 48, 2009, 4858 - 4865.
[44] A.M.Emhamed, B.Czuczai, E.Rev, and Z.Lelkes, Analysis of Extractive Distillation with Mathematical Programming, *Ind.Eng.Chem.Res.*, 47, 2008, 9983 - 9995.
[45] D.L.Bennett, D.N.Watson, and M.A.Wiescinski, New Correlation for Sieve-Tray Point Efficiency, Entrainment, and Section Efficiency, *AIChE J.*, 43, 1997, 1611 - 1626.
[46] H.E.O'Connell, Plate efficiency of fractionating columns and absorbers, *Trans.AIChE.*, 42, 1946, 741 -
[47] S.A.MacFarland, P.M.Sigmund, and M.Van Winkle, Predict distillation efficiency, *Hydrocarb.Process.*, 51, 1972, 111 - 114.

[48] H.L.Toor, Prediction of Efficiencies and Mass Tranfer on a Stage with Multicomponent Systems, *AIChE J.*, 10, 1964, 545 - 548.
[49] R.Krishnamurthy and R.Taylor, A Nonequilibrium Stage Model of Multicomponent Separation Processes Part I: Model Description and Method of Solution, *AIChE J.*, 31, 1985, 449 - 456.
[50] R.Krishnamurthy and R.Taylor, A Nonequlibrium Stage Model of Multicomponent Separation Processes Part II: Comparison with Experiment, *AIChE J.*, 31, 1985, 456 - 465.
[51] E.Eckert and T.Vanek, Some aspects of rate-based modelling and simulation of three-phase distillation columns, *Comput.Chem.Eng.*, 25, 2001, 603 - 612.
[52] J.Repke, O.Villain, and G.Wozny, A nonequilibrium model for three-phase distillation in a packed column: modeling and expereiments, *Comput.Chem.Eng.*, 28, 2004, 775 - 780.
[53] J.Repke and G.Wozny, A Short Story of Modeling and Operation of Three-Phase Distillation in Phacked Columns, *Ind.Eng.Chem.Res.*, 43, 2004, 7850 - 7860.
[54] M.Klöker, E.Y.Kenig, A.Hoffmann, P.Kreis, and A.Górak, Rate-based modelling and simulation of reactive separations in gas/vapour-liquid systems, *Chem.Eng.Process.*, 44, 2005, 617 - 629.
[55] R.Taylor and R.Krishna, Modelling reactive distillation, *Chem.Eng.Sci.*, 55, 2000, 5183 - 5229.
[56] E.Y.Kenig, A.Górak, A.Pyhälahti, K.Jakobsson, and J.Aitamaa, Advanced Rate-Based Simulation Tool for Reactive Distillation, *Aiche.J.*, 50, 2004, 322 - 342.
[57] Z.Niu, Y.Guo, Q.Zeng, and W.Lin, Experimental Studies and Rate-Based Process Simulations of CO_2 Absorption with Aqueous Ammonia Solutions, *Ind.Eng.Chem.Res.*, 51, 2012, 5309 - 5319.
[58] J.Gabrielsen, H.F.Svendsen, M.L.Michelsen, E.H.Stenby, and G.M.Kontogeorgis, Experimental validation of a rate-based model for CO_2 capture using an AMP solution, *Chem.Eng.Sci.*, 62, 2007, 2397 - 2413.
[59] R.Taylor and R.Krishna, *Multicomponent Mass Transfer*, Wiley, New York, 1993.
[60] T.L.Junqueira, M.R.W.Maciel, and R.M.Filho, Evaluation of Barros and Wolf Efficiency Correlations for Conventional and Extractive Distillation Columns in Bioethanol Production Process, *Separ.Sci.Technol.*, (2012),
[61] P.Zuurbier and J.van de Vooren, *Sugarcane ethanol: Contributions to climate change mitigation and the environment*, Wageningen Academic Publishers, Wageningen, 2008.
[62] J.Goldemberg, S.T.Coelho, and P.Guardabassi, The sustainability of ethanol production from sugarcane, *Energ.Policy*, 36, 2008, 2086 - 2097.
[63] C.Rolz and R.León, Ethanol fermentation from sugarcane at different maturities, *Ind.Crop.Prod.*, 33, 2011, 333 - 337.
[64] J.D.van den Wall Bake, M.Junginger, A.Faaij, T.Poot, and A.Walter, Explaining the experience curve: Cost reductions of Brazilian ethanol from sugarcane, *Biomass Bioenerg.*, 33, 2009, 644 - 658.
[65] J.A.Quintero, M.I.Montoya, O.J.Sánchez, O.H.Giraldo, and C.A.Cardona, Fuel ethanol production from sugarcane and corn: Comparative analysis for Colombian case, *Energy*, 33, 2008, 385 - 399.
[66] R.K.Perrin, N.F.Fretes, and J.P.Sesmero, Efficiency in Midwest US corn ethanol plants: A plant survey, *Energ.Policy*, 37, 2009, 1309 - 1316.

[67] N.Kaliyan, R.V.Morey, and D.G.Tiffany, Reducing life cycle greenhouse gas emissions of corn ethanol by integrating biomass to produce heat and power at ethanol plants, *Biomass Bioenerg.*, 35, 2011, 1103 - 1113.
[68] J.Shen and F.A.Agblevor, Modeling semi-simultaneous saccharification and fermentation of ethanol production from cellulose, *Biomass Bioenerg.*, 34, 2010, 1098 - 1107.
[69] P.Christakopoulos, B.J Macris, and D.Kekos, Direct fermentation of cellulose to ethanol by *Fusarium oxysporum*, *Enzyme Microb.Technol.*, 11, 1989, 236 - 239.
[70] G.Verma, P.Nigam, D.Singh, and K.Chaudhary, Bioconversion of starch to ethanol in a single-step process by coculture of amylolyctic yeast and *Saccharomyces cerevisiae* 21, *Bioresource Technol.*, 72, 2000, 261 - 266.
[71] L.Jamai, K.Ettayebi, J.El Yamani, and M.Ettayebi, Production of ethanol from starch by free and immobilized *Candida tropicalis* in the presence of α-amylase, *Bioresource Technol.*, 98, 2007, 2765 - 2770.
[72] T.L.Junqueira, M.O.S.Dias, R.M.Filho, M.R.W.Maciel, and C.E.V.Rossell, Simulation of the Azeotropic Distillation fro anhydrous Bioethanol Production: Study on the Formation of a Second Liquid Phase, *Comput.Aided Chem Eng.*, 27, 2009, 1143 - 1148.
[73] H.R.Mortaheb and H.Kosuge, Simulation and optimization of heterogeneous azeotropic distillation process with a rate-based model, *Chem.Eng.Process*, 43, 2004, 317 - 326.
[74] V.Gomis, R.Pedraza, O.Francés, A.Font, and J.C.Asensi, Dehydration of Ethanol Using Azeotropic distillation with Isooctane, *Ind.Eng.Chem.Res.*, 46, 2007, 4572 - 4576.
[75] J.Li, Z.Lei, Z.Ding, C.Li, and B.Chen, Azeotropic Distillation: A Review of Mathematical Models, *Sep.Purif.Rev.*, 34, 2005, 87 - 129.
[76] T.Yamamoto, Y.H.Kim, B.C.Kim, A.Endo, N.Thongprachan, and T.Ohmori, Adsorption characteristics of zeolites for dehydration of ethanol: Evaluation of diffusivity of water in porous structure, *Chem.Eng.J.*, 181-182, 2012, 443 - 448.
[77] J.A.Delgado, M.A.Uguina, J.L.Sotelo, V.I.Águeda, A.García, and A.Roldán, Separation of ethanol-water liquids mixtures by adsorption on silicate, *Chem.Eng.J.*, 180, 2012, 137 - 144.
[78] S.Al-Asheh, F.Banat, and A.A.Fara, Dehydration of Ethanol-Water Azeotropic Mixture by Adsorption Through Phillipsite Packed-Column, *Separ.Sci.Technol.*, 44, 2009, 3170 - 3188.
[79] M.H.V.Mulder and C.A.Smolders, On the Mechanism of Separation of Ethanol/Water Mixtures by Pervaporation. 1. Calculations of Concentration Profiles, *J.Membrane Sci.*, 17, 1984, 289 - 307.
[80] J.Wang and T.Tsuru, Cobalt-doped silica membranes for pervaporation dehydration of ethanol/water solutions, *J.Membrane Sci.*, 369, 2011, 13 - 19.
[81] Q.G.Zhang, Q.L.Liu, A.M.Zhu, Y.Xiong, and L.Ren, Pervaporation performance of quaternized poly(vinyl alcohol) and its crosslinked membranes for the dehydration of ethanol, *J.Membrane Sci.*, 335, 2009, 68 - 75.
[82] J.F.Mulia-Soto and A.Flores-Tlacuahuac, Modeling, simulation and control of an internally heat integrated pressure-swing distillation process for bioethanol separation, *Comput.Chem.Eng.*, 35, 2011, 1532 - 1546.

[83] I.D.Gil, J.M.Gómez, and G.Rodríguez, Control of an extractive distillation process to dehydrate ethanol using glycerol as entrainer, *Comput.Chem.Eng.*, 39, 2012, 129 - 142.
[84] A.Yeh and L.Berg, The Dehydration of Ethanol by Extractive Distillation, *Chem.Eng.Commun.*, 113, 2007, 147 - 153.
[85] R.Muñoz, J.M.Montón, M.C.Burguet, and J.de la Torre, Separation of isobutyl alcohol and isobutyl acetate by extractive distillation and pressure-swing distillation: Simulation and optimization, *Sep.Purif.Technol.*, 50, 2006, 175 - 183.
[86] E.Llodosa, J.B.Montón, and M.C.Burguet, Separation of di-n-propyl ether and n-propyl alcohol by extractive distillation and pressure-swing distillation: Computer simulation and economic optimization, *Chem.Eng.Process*, 50, 2011, 1266 - 1274.
[87] K.Weissermel and H.-J.Arpe, *Industrial Organic Chemistry*, Wiley, Weinheim, 1997.
[88] P.R.Pujadó and M.Moser, Catalytic reforming, (2006), 217-237.
[89] G.W.Meindersma, A.Podt, and A.B.dec Haan, Selection of ionic liquids for the extraction of aromatic hydrocarbons from aromatic/aliphatic mixtures, *Fuel Process.Technology*, 87, 2005, 59 - 70.
[90] Z.Lei, C. Li and B.Chen, Extractive Distillation: A Review, *Sep.Purif.Rev.*, 32, 2003, 121 - 213.
[91] P.Le-utaiwan, B.Suphanit, P.L.Douglas, and N.Mongkolsiri, Design of extractive distillation for separation of close-boiling mixtures: Solvent selection and column optimization, *Comput.Chem.Eng*, 35, 2011, 1088 - 1100.
[92] J.R.Couper, R.Penney, and J.R.Fair, *Chemical Process Equipment: Selection and Design*, Butterworth-Heinemann, Waltham, USA, 2012.
[93] A.Westerholt, V.Liebert, and J.Gmehling, Influence of ionic liquids on the separation factor of three standard separation problems, *Fluid Phase Equilibr.*, 280, 2009, 56 - 60.
[94] E.Olivier, T.M.Letcher, P.Naidoo, and D.Ramjugernath, Activity coefficients at infinite dilution of organic solutes in the ionic liquid 1-butil-3-methylimidazolium hexafluoroantimoniate using gas-liquid chromatography, *J.Chem.Thermodyn.*, 43, 2011, 829 - 833.
[95] U.Domanska and A.Marciniak, Measurements of activity coefficients at infinite dilution of aromatics and aliphatics hydrocarbons, alcohol, and water in the new ionic liquid [EMIM][SCN] using GLC, *J.Chem.Thermodyn.*, 40, 2008, 860 - 866.
[96] U.Domanska and M.Laskowska, Measurements of activity coefficients at inffinite dilution of aliphatic and aromatic hydrocarbons, alcohol, thiophene, tetrahydrofuran, MTBE, and water in ionic liquids [BMIM][SCN] using GLC, *J.Chem.Thermodyn.*, 2009, 2009, 645 - 650.
[97] E.Quijada-Maldonado, S.van der Boogaart, J.H.Lijbers, G.W.Meindersma, and A.B.de Haan, Experimental densities, dynamic viscosities and surface tensions of the ionic liquids series 1-ethyl-3-methylimidazolium acetate and dicyanamide and their binary and ternary mixtures with water and ethanol at T = (298.15 K to 343.15 K), *J.Chem.Thermodyn.*, 51, 2012, 51 - 58.
[98] E.Gómez, B.González, Á.Domínguez, E.Tojo, and J.Tojo, Dynamic Viscosities of a Series of 1-Alkyl-3-methylimidazolium Chloride ionic Liquids and Their Binary Mixtures with Water at Several Temperatures, *J.Chem.Eng.Data*, 51, 2006, 696 - 701.

[99] M.H.Ghatee and M.Zare, Power-law behavior in the viscosity of ionci liquids: Existing a similarity in the power law and a new proposed viscosity equation, *Fluid Phase Equilibr.*, 311, 2011, 76 - 82.
[100] S.Weiss and R.Arlt, On the Modeling of Mass Transfer in Extractive Distillation, *Chem.Eng.Process.*, 21, 1987, 107 - 113.
[101] G.Q.Wang, X.G.Yuan, and T.Yu, Review of Mass-Tranfer Correlations for Packed Columns, *Ind.Eng.Chem.Res.*, 44, 2005, 8715 - 8729.

2

Physical property requirement analysis for using the rate-based model.

Abstract

The Rate-Based model requires reliable physical and transport properties to solve heat and mass transfer rates across the interphases by means of correlations. Ionic liquids are a new class of solvents whose properties are still under investigation even though their database has largely increased lately. Experimental methods are time consuming and expensive considering that these properties change with composition and temperature. The objective of this chapter is to determine which physical properties are required to be measured and which ones could be predicted to obtain sufficiently accurate information about changes in mass transfer. For the chosen ionic liquids for water – ethanol separation it was determined that ternary liquid dynamic viscosities have to be experimentally obtained. Liquid diffusion coefficients can be experimentally predicted very quickly to avoid the classical time consuming experiments that directly determine this property. Surface tension is a property that also has to be measured. However, measurements at room temperature suffice to provide reliability and time savings. Liquid densities and thermal conductivities are properties that can be estimated without losing accuracy in validating the rate-based model and reliability in the analysis of mass transfer efficiencies.

2.1 Introduction

Nowadays, the design or simulation/optimization of the extractive distillation (ED) process can be made by rigorous models available in commercial simulation tools. The rate-based model provides accurate predictions. In contrast to the equilibrium model, where only information of vapor-liquid equilibrium and the efficiencies are sufficient to perform simulations, the rate-based or non-equilibrium model requires a complete description of the physical and transport properties to produce reliable results [1]. This is a great problem because although the database containing relevant data of ionic liquids is increasing every day, many of the necessary properties to describe the mass transfer in extractive distillation are not available. This involves properties that must represent the multicomponent nature of the extractive distillation process. They should be measured and experimental methods are time consuming and expensive. Nevertheless, not all of the physical and transport properties need to be experimentally determined since some of the required properties only influence the mass transfer to a minor extent. Therefore, they could be estimated by methods available in the literature for common fluids. This brings time savings in both measuring properties and developing the rate-based model.

The objective of this chapter is to identify which of the physical and transport properties require high accuracy to properly describe the changes in mass transfer efficiency with increasing solvent viscosity for the separation of water – ethanol mixtures. This step is of crucial importance because it allows time savings by preventing the unnecessary experimental determination of properties without risking the loss of accuracy in describing the mass transfer in an extractive distillation column. To define these properties, this chapter will first provide the rate-based model and the mass transfer correlations. From this point, the different required properties are analyzed in terms of their importance for describing the mass transfer.

2.2 The rate-based model

Figure 2.1 shows a scheme of a non-equilibrium or real distillation stage which represents a single tray or a segment in packed columns. The mass and energy balances are

written for a respective phase present in the separation. Heat and mass transfer rates are defined across the interphase as a result of the exchange of mass and heat.

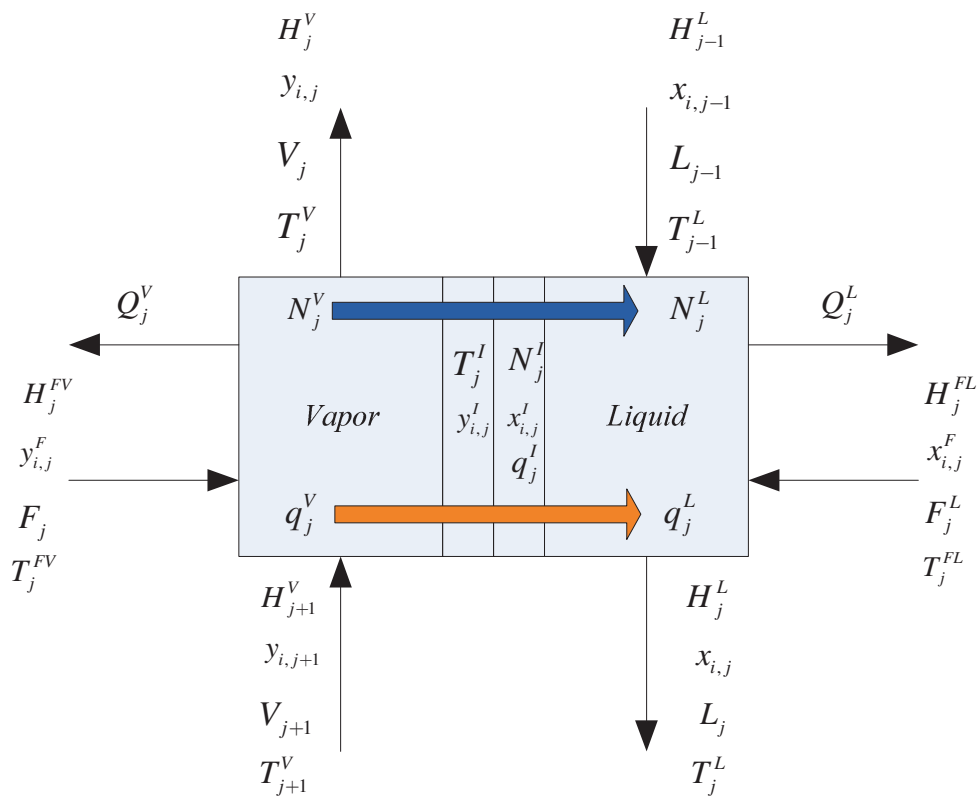

Figure 2.1. Scheme of a non-equilibrium stage.

The heat and mass balances for each phase are written in the following set of equations. Since we are dealing with extractive distillation, the reaction rates are not taken into account in these balances.

$$F_j^L x_{i,j}^F + L_{j-1} x_{i,j-1} + N_{i,j}^L - L_j x_{i,j} = 0 \qquad 2.1$$

$$F_j^V y_{i,j}^F + V_{j+1} y_{i,j+1} - N_{i,j}^V - V_j y_{i,j} = 0 \qquad 2.2$$

$$N_{i,j}^I - N_{i,j}^L = 0 \qquad 2.3$$

$$N_{i,j}^V - N_{i,j}^I = 0 \qquad 2.4$$

$$F_j^L H_j^{FL} + L_{j-1} H_{j-1}^L + Q_j^L + q_j^L - L_j H_j^L = 0 \qquad 2.5$$

$$F_j^V H_j^{FV} + V_{j+1} H_{j+1}^V + Q_j^V - q_j^V - V_j H_j^V = 0 \qquad 2.6$$

$$q_j^I - q_j^L = 0 \qquad 2.7$$

$$q_j^V - q_j^I = 0 \qquad 2.8$$

$$y_{i,j}^I - K_{i,j} x_{i,j}^I = 0 \qquad 2.9$$

$$\sum_{i=1}^{n} x_{i,j} = 1 \qquad 2.10$$

$$\sum_{i=1}^{n} y_{i,j} = 1 \qquad 2.11$$

$$\sum_{i=1}^{n} x_{i,j}^I = 1 \qquad 2.12$$

$$\sum_{i=1}^{n} y_{i,j}^I = 1 \qquad 2.13$$

The mass transfer rates of liquid across the interphase are defined as

$$\left[\Gamma_j^L\right]\left(\mathbf{x}_j^I - \mathbf{x}_j\right) - \left[\mathrm{R}_j^L\right]\left(\mathrm{N}_j^L - N_t^L \mathbf{x}_j\right) = 0 \qquad 2.14$$

$$\Gamma^L_{i,k,j} = \delta_{i,k} + x_{i,j} \left.\frac{\partial \ln \varphi^L_{i,j}}{\partial x_{k,j}}\right|_{T^L_j, P_j, \Sigma} \qquad 2.15$$

$$R^L_{i,i,j} = \frac{x_{i,j}}{\overline{\rho}^L_j a^I_j k^L_{i,n,j}} + \sum_{\substack{m=1 \\ m \neq i}}^{n} \frac{x_{m,j}}{\overline{\rho}^L_j a^I_j k^L_{i,m,j}} \quad \text{for } i = 1,\ldots, n\text{-}1 \qquad 2.16$$

$$R^L_{i,k,j} = -x_{i,j} \left(\frac{1}{\overline{\rho}^L_j a^I_j k^L_{i,k,j}} - \frac{1}{\overline{\rho}^L_j a^I_j k^L_{i,n,j}} \right) \quad \text{for } i = 1,\ldots, n\text{-}1,\ i \neq k \qquad 2.17$$

The mass transfer rates of vapor across the interphase are defined as

$$\left[\Gamma^V_j\right]\left(\mathbf{y}^I_j - \mathbf{y}_j\right) - \left[\mathrm{R}^L_j\right]\left(\mathrm{N}^V_j - N^V_t \mathbf{y}_j\right) = 0 \qquad 2.18$$

$$\Gamma^V_{i,k,j} = \delta_{i,k} + y_{i,j} \left.\frac{\partial \ln \varphi^V_{i,j}}{\partial y_{k,j}}\right|_{T^V_j, P_j, \Sigma} \qquad 2.19$$

$$R^V_{i,i,j} = \frac{y_{i,j}}{\overline{\rho}^V_j a^I_j k^V_{i,n,j}} + \sum_{\substack{m=1 \\ m \neq i}}^{n} \frac{y_{m,j}}{\overline{\rho}^V_j a^I_j k^V_{i,m,j}} \quad \text{for } i = 1,\ldots, n\text{-}1 \qquad 2.20$$

$$R^V_{i,k,j} = -y_{i,j} \left(\frac{1}{\overline{\rho}^V_j a^I_j k^V_{i,k,j}} - \frac{1}{\overline{\rho}^V_j a^I_j k^V_{i,n,j}} \right) \quad \text{for } i = 1,\ldots, n\text{-}1,\ i \neq k \qquad 2.21$$

The energy loss or gain due to interphase transfer is defined as

$$a^I_j h^L_j \left(T^I_j - T^L_j\right) - q^L_j + \sum_{i=1}^{n} N^L_{i,j} \overline{H}^L_{i,j} = 0 \qquad 2.22$$

$$a^I_j h^V_j \left(T^V_j - T^I_j\right) - q^V_j + \sum_{i=1}^{n} N^V_{i,j} \overline{H}^V_{i,j} = 0 \qquad 2.23$$

To solve this set of equations, the value of the mass transfer coefficients k^L, k^V, the heat transfer coefficients h^L, h^V, the interfacial area a^I and the distribution ratios K are required. The heat and mass transfer coefficients are obtained directly from correlations and the K-values are obtained from vapor-liquid equilibrium experiments. Mass transfer coefficients and interfacial areas depend upon physical and transport properties as well as the tray design and layout or the packing type and size. Distribution ratios are more easily found in the literature nowadays because many separation technologies where ionic liquids are involved require vapor-liquid or liquid-liquid equilibrium and some other thermodynamic properties for preliminary evaluation and equilibrium based simulations. However, when it comes to more rigorous rate-based modeling, no works are found in literature due to the difficulty of defining physical and transport properties. Due to this limitation, experimental work might be necessary to study the effect of physical and transport properties of ionic liquids on the mass transfer efficiency.

2.3 Mass transfer and interfacial area correlations

Due to their simplicity and availability of information in literature, two internals are used in this work: Sieve trays and Mellapak® structured packing. For the relevance of this work, the mass transfer coefficients are only analyzed in the liquid phase where the physical and transport properties of ionic liquids could influence the mass transfer. Therefore, below we emphasize the part of the correlations where physical and transport properties are involved. A more detailed description of these correlations is given in the literature presented in the sections below. Since ionic liquids do not vaporize, the vapor phase only contains water and ethanol whose physical and transport properties are well known and the heat and mass transfer coefficients easily calculated. Therefore, further analysis of this phase is not necessary.

2.3.1 Sieve trays

For Sieve trays, the Chan and Fair [2,3] mass transfer correlation is preferred over other correlations like Zuiderweg [4] because it gives a better description of the mass transfer characteristics in distillation [5,6]. This correlation is based on the previously published AIChE correlation [7].

$$k_{i,k}^{L} = 19700\left(Đ_{i,k}^{L}\right)^{0.5}\frac{0.4F_S + 0.17}{\bar{a}} \qquad 2.24$$

$$\bar{a} = \frac{a^I}{\xi A_b h_f} \qquad 2.25$$

$$\xi = \exp\left\{-12.55\left[u_s^V\left(\frac{\rho_t^V}{\rho_t^L - \rho_t^V}\right)^{0.5}\right]^{0.91}\right\} \qquad 2.26$$

To determine the interfacial area for mass transfer a^I the Zuiderweg correlation [4] is used:

$$a^I = \frac{40A_b}{\phi^{0.3}}\left(\frac{\left(u_S^V\right)^2\rho_t^V h_{cl} FP}{\sigma}\right)^{0.37} \quad \text{when } FP \le \frac{3l_w h_{cl}}{A_b}\text{,(spray regime)} \qquad 2.27$$

$$a^I = \frac{43A_b}{\phi^{0.3}}\left(\frac{\left(u_S^V\right)^2\rho_t^V h_{cl} FP}{\sigma}\right)^{0.53} \quad \text{when } FP > \frac{3l_w h_{cl}}{A_b}\text{,(froth emulsion regime)} \qquad 2.28$$

$$FP = \frac{Q_L}{Q_V}\left(\frac{\rho_t^L}{\rho_t^V}\right)^{0.5} \qquad 2.29$$

As it can be observed in the above set of equations, Maxwell-Stefan (MS) diffusion coefficients, liquid densities and surface tensions should be provided to determine the mass transfer on sieve trays.

2.3.2 Mellapak® structured packing

For corrugated metal sheet packing, the Rocha et al. correlation [8,9] has been developed based on the previous correlation from Bravo at al. [10], which considers that the packing surface was completely wetted. The improved correlation has several theoretical advantages that are worth to mention. Firstly, it takes into account the partial wetting over the packing. This is especially important when having aqueous systems like water – ethanol. Water has a relatively high surface tension and this decreases the wetting of packing surface reducing the interfacial area for mass transfer. A second important point is that the penetration theory is used to evaluate mass transfer coefficients that are able to account for the increase in liquid phase resistance when using viscous solvents. In distillation it has been assumed that the main resistance to mass transfer resides in the vapor phase. However, some studies have shown that the liquid phase resistance cannot be neglected in distillation systems [11]. The Rocha et al. mass transfer correlation is the following.

$$k_{i,k}^{L} = 2\left(\frac{Đ_{i,k}^{L} u_{Le}}{\pi S C_E}\right)^{0.5} \qquad 2.30$$

$$a^{I} = a_e A_t h_P \qquad 2.31$$

$$u_{Le} = \frac{u_S^L}{\varepsilon h_t \sin\theta} \qquad 2.32$$

$$h_t = \left(4\frac{F_t}{S}\right)^{0.67}\left(\frac{3\eta^L u_S^L}{\rho_t^L g_{eff}\varepsilon \sin\theta}\right)^{0.33} \qquad 2.33$$

$$F_t = \frac{29.12\left(We_L Fr_L\right)^{0.15} S^{0.359}}{\mathrm{Re}_L^{0.2}\, \varepsilon^{0.6} \left(\sin\theta\right)^{0.3} \left(1-0.93\cos\gamma\right)} \qquad 2.34$$

$$We_L = \frac{\left(u_S^L\right)^2 \rho_t^L S}{\sigma} \qquad 2.35$$

$$\mathrm{Re}_L = \frac{u_S^L S \rho_t^L}{\eta^L} \qquad 2.36$$

$$\cos\gamma = 5.211x10^{-16.835\sigma} \qquad 2.37$$

for $\sigma \geq 0.0055$

$$\cos\gamma = 0.9 \qquad 2.38$$

for $\sigma < 0.0055$

$$a_e = F_t F_{se} a_P \qquad 2.39$$

Equations 2.30 to 2.39 define the liquid phase mass transfer correlation and all the physical and transport properties. The same physical properties as the case with sieve trays; liquid viscosity, density and surface tension should be provided to the rate-based model for correct predictions. Although the correlation of Billet and Schultes [12,13] is also able to describe the mass transfer in Mellapak structured packing, this correlation needs confidential parameters to be provided and was therefore discarded.

2.4 Property requirements for extractive distillation of water – ethanol mixtures with ionic liquids

The non-equilibrium or rate-based model is able to predict the performance of distillation processes by solving the mass transfer rate equations simultaneously with the stage conservation equations (equations 2.1 to 2.23). Mass transfer correlations are used to calculate mass transfer rates across the boundary phases (equations 2.24 to 2.38). These correlations require accurate physical and transport properties of the system in study. As

noted above, this point is very important since an incorrect description of the physical properties or using the wrong assumptions could bring erroneous predictions.

Since extractive distillation is a thermal separation process involving multicomponent mixtures, the physical properties presented here must be well defined as function of temperature and concentration. Nowadays, physical properties for binary mixtures are scarce and barely found for ternary mixtures. This problem could be overcome by using semi-empirical methods such as group contribution methods [14]. Nevertheless, ionic liquids are a new class of fluids and these methods need experimental data to be developed. Therefore, in the absence of either experimental data or accurate estimative methods, an experimental determination would be necessary. A second step, after collecting the experimental data, is their correlation with available models.

2.5 Ionic liquids for water ethanol separation

Before discussing the physical properties that need to be measured, it is important to take into consideration one very important point in order to properly evaluate the extent to which the ionic liquid viscosities could affect the mass transfer efficiency:

- The range of viscosities must be large enough to produce an effect on the liquid phase resistance.

Nevertheless, a suitable ionic liquid for the separation of a specific mixture is chosen by the improvements in relative volatility. This last property also influences the mass transfer efficiency calculations. High relative volatilities improve the mass transfer efficiency. Therefore, a second point has to be taken into account in order to study the mass transfer efficiency:

- A wide range of relative volatilities to study the effect of this property on the mass transfer efficiency.

So far, many ionic liquids have been proposed to separate the water – ethanol mixture by means of extractive distillation. A suitable selection of these solvents can be obtained from the work of Ge et al. [15] where the effect of the solvent concentration on relative volatility is experimentally studied. Figure 2.2, shows this effect for three solvents plus the reference solvent ethylene glycol, EG: 1-ethyl-3-methyimidazolium chloride, [emim][Cl]; 1-ethyl-3-methyimidazolium acetate [emim][OAc]; and 1-ethyl-3-methyimidazolium dicyanamide, [emim][DCA] [16].

In figure 2.2 it is observed that all the chosen ionic liquids show improvements over the reference solvent ethylene glycol (EG) and the effect of the solvent concentration is also clearly seen. The ionic liquids do not show large advantages at low solvent mass fractions. However, the differences appear at higher solvent mass fractions where for instance the relative volatility of [emim][Cl] is 1.75 times higher than that of EG. Table 2.1 gives the dynamic liquid viscosity of these solvents at 298.15 K.

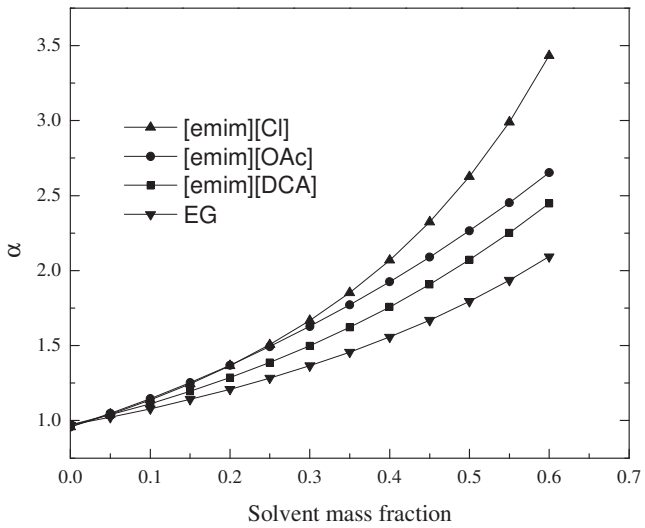

Figure 2.2. Relative volatility of the water – ethanol system in function of different solvents mass fractions. [15,16]

Table 2.1. Solvent viscosities at T = 298.15 K.

Solvent	M_w [g mol^{-1}]	η [mPa s]	References
[emim][Cl]	142	2597.69[a]	[17]
[emim][OAc]	171	132.91	[18]
[emim][DCA]	177	14.90	[18]
EG	62	16.61	[19]

[a] Extrapolated viscosity from three experimental data points.

In this table it is observed that the viscosity of [emim][Cl] is around 150 times higher than that of EG. Therefore, in this case it is possible to analyze the effect of viscosity on the mass transfer efficiency in an extractive distillation column since this solvent on one side eases the separation but on the other side the increased viscosity could create mass transfer limitations. [emim][OAc] also shows good improvements in relative volatility with a viscosity 8 times higher than the reference solvent EG. Here, less mass transfer limitations are expected. The case of [emim][DCA] is different because the viscosity of this ionic liquid is similar to EG and the relative volatilities are moderately higher. Therefore, improvements in mass transfer efficiency can be expected.

2.6 Properties to be studied

As observed above, the rate-based equations require physical and transport properties: liquid viscosity, MS diffusion coefficients, surface tension, liquid densities and liquid thermal conductivities.

2.6.1 Liquid viscosity

Since the dynamic liquid viscosity is the property under study in this work, high accuracy is needed. In the set of equations described above this property is furthermore needed in the estimation of MS diffusion coefficients, determination of liquid holdup in

packing (equation 2.33) and in the Reynolds dimensionless number (equation 2.36). Previous work by Weiss and Arlt [20] demonstrated a decrease in mass transfer efficiency with increased solvent viscosity in extractive distillation. The liquid phase viscosity increases the resistance to mass transfer and although in distillation it is accepted that the main resistance to mass transfer is in the vapor phase [21], the liquid phase resistance could become important at high liquid viscosities [22]. To quantify this, it is necessary to provide reliable liquid phase viscosities. This means that the dynamic viscosities must be estimated, predicted or measured as function of concentration and temperature. In the literature, several semi-predictive methods are available to estimate liquid phase viscosities such as UNIFAC-VISCO [23] or ASOG-VISCO [24]. However, no group contributions for mixtures containing ionic liquids have been developed so far. Although, experimental data for pure ionic liquids are nowadays fairly well known, in an extractive distillation column a ternary mixture is formed by the system water – ethanol – IL, for which experimental dynamic viscosity data are very scarce. Only a few experimental works have been published at 298.15 K [25-28] and one at several low temperatures [29] where water and ethanol are combined with the ionic liquids listed in table 2.1. In conclusion, experimental determination is necessary. At the same time, an accurate model to correlate this experimental data is needed as well. Since aqueous and polar mixtures show strong hydrogen bonding interactions the classical models [30,31] could fail in correlating the experimental data. Lately, the use of the Eyring theory in combination with an equation of state and a mixing rule gives very good results in multicomponent mixtures. The Eyring-Patel-Teja model with a Redlich-Kister type mixing rule is able to represent aqueous and polar multicomponent mixtures with great accuracy [32]. The model is described by the following equations:

$$(\eta V)_{mixture} = (\eta V)_{ideal} \exp\left(\frac{G^{ex}}{RT}\right) \qquad 2.40$$

$$(\eta V)_{ideal} = \exp\left(\sum_{i=1}^{n} x_i \ln\left[\eta_i V_i\right]\right) \qquad 2.41$$

$$G^{ex} = RT\sum_{i=1}^{n} x_i \left(\ln \varphi_i - \ln \varphi_i^0\right) \qquad 2.42$$

and the Redlich-Kister mixing rule[33]:

$$a_{i,k} = \left[\left(1 - l_{i,j}\right) - \left(x_i - x_k\right) l_{k,i}\right]\left(a_i a_k\right)^{0.5} \qquad 2.43$$

Additionally, Margules-type mixing rules could be used [34,35]:

$$a_{i,k} = \left[1 - x_i l_{i,k} - x_k l_{k,i}\right](a_i a_k)^{0.5} \qquad 2.44$$

$$a_{i,k} = \left[1 - \overline{l_{i,k}}(1 - x_i - x_k) - x_i l_{i,k} - x_k l_{k,i}\right](a_i a_k)^{0.5} \qquad 2.45$$

The viscosity of ionic liquids strongly decreases with increasing temperature. To better represent these changes, temperature-dependent interactions parameters $k_{i,k}$ are introduced in this work:

$$l_{i,k} = l_{i,k}^{(1)} + \frac{l_{i,k}^{(1)}}{T} \qquad 2.46$$

2.6.2 Liquid diffusion coefficients

Liquid diffusion coefficient represents the resistance to mass transfer. A more viscous liquid phase is reflected by lower diffusion coefficients. The rate-based model uses the Maxwell-Stefan theory of diffusion to determine the mass transfer rates (equation 2.18). More importantly, MS diffusion coefficients are required to calculate mass transfer coefficients (equations 2.24 and 2.30). To calculate these coefficients in a ternary mixture, infinite dilution diffusion coefficients are firstly needed and secondly a mixing rule allows

to calculate MS diffusion coefficients at any concentration. Kooijman and Taylor [36] developed a Vignes-type geometrically-consistent mixing rule to estimate MS diffusion coefficients in multicomponent mixtures:

$$Đ_{i,k} = \left(Đ^0_{i,k}\right)\left(Đ^0_{k,i}\right)\prod_{\substack{m=1\\ m\neq i,k}}^{n}\left(Đ^0_{i,m}Đ^0_{m,i}\right)^{1/2} \qquad 2.47$$

Although, some authors have recommended this mixing rule [37], the research in this area is still progressing [38]. This section is dedicated to infinite dilution diffusion coefficients in the liquid phase. This does not mean that no vapor phase diffusion coefficients are required. They are needed to calculate mass transfer coefficients in the vapor phase and the mass transfer efficiency. These coefficients are calculated internally by ASPEN® Plus using the Chapman-Enskog-Wilke-Lee equation[39].

The infinite dilution diffusion coefficient is a rather unknown property for systems containing ionic liquids. A few experimental studies can be found in literature [40-46], mainly of ionic liquids infinitely diluted in water and some polar solvents. In absence of experimental data, the Wilke-Chang equation (Equation 2.48) is normally used to predict infinite dilution diffusion coefficients with very poor and underestimated results [42].

$$Đ^0_{i,k} = 7.4x10^{-12}\frac{\left(\Phi M_{w,k}\right)^{0.5}T}{\eta_k V^{0.6}_{b,i}} \qquad 2.48$$

This is explained by the fact that in the Wilke-Chang equation the molar volume at the normal boiling point of the solute $V_{b,i}$ has to be provided (See equation 2.48). In the case of any ionic liquid infinitely diluted in water or ethanol the information of the molar volume at the normal boiling point of that ionic liquid is required. However, ionic liquids do not have an atmospheric boiling point or they decompose before reaching that point [47]. This is the source of the large deviations mentioned above. In literature, only data for [emim][DCA] in water is found. No information is encountered for the rest of ionic liquids listed in table 2.1. Therefore, an experimental determination of the infinite dilution diffusion coefficient of the ionic liquids in water or ethanol would be necessary. A second problem is that, the

experimental methods like the Taylor dispersion method are rather complicated and time consuming. An easier way to obtain these diffusion coefficients is by taking the advantage of the electrolyte nature of dissolved ionic liquids. By measuring the electrical conductivity of the ionic liquid infinite diluted in water or ethanol and the help of the Nerst-Haskell equation it is possible to determine the binary diffusion coefficients of the ionic liquids presented here infinite diluted in water or ethanol [42,48]. Equation 2.49 describes the Nerst-Haskell equation:

$$Đ_{i,k}^{0} = \frac{R_u T}{F^2} \frac{|z_+| + |z_-|}{|z_+ z_-|} \frac{\Lambda_+^0 \Lambda_-^0}{\Lambda_+^0 + \Lambda_-^0} \qquad 2.49$$

where Λ_+^0 and Λ_-^0 are the molar conductivities that are obtained from electrical conductivity measurements. The mathematical procedure to convert electrical conductivities into molar conductivities is described in detail elsewhere [42].

On the other side, to predict the diffusion coefficient of water or ethanol infinitely diluted in ionic liquids the Wilke-Chang equation could be used. Now, the limitation of the molar volume at the normal boiling point is not present since this value for water and ethanol is well documented. Predictions are compared with experimental values reported in literature. Table 2.2 contains reported experimental data of water infinite diluted in 1-butyl-3-methylimidazolium dicyanamide [bmim][DCA] and water in 1-n-butyl-3-methylimidazolium bis(trifluoromethanesulfonyl)imide [bmim][NTf_2] and results given by the Wilke-Chang equation. It gives acceptable approximations as it can be observed in the table 2.2 and it can be used as a predictive method for the infinite dilution diffusion coefficients of water or ethanol in the ionic liquids presented here. Unfortunately, no more experimental data is available to test the predictive capabilities of this equation. In conclusion, the infinite dilution diffusion coefficients of ionic liquids in water or ethanol can be predicted via the Nerst-Haskell equation supported by conductivity experiments and the infinite dilution diffusion coefficients of water or ethanol in ionic liquid can be estimated by using the Wilke-Chang relation.

For the case of EG, the infinite dilution diffusion coefficients of water or ethanol in EG and in the other side EG in water or ethanol are found in literature [49-51], except for the infinite dilution diffusion coefficient of EG in ethanol which is predicted by using the

Wilke-Chang equation. Finally, the infinite dilution diffusion coefficient pair water in ethanol and vice versa can be found in literature [52,53].

Table 2.2. Infinite dilution diffusion coefficient of water in [bmim][DCA] at T = 298.15 K.

	Literature	Wilke-Chang	
	$Đ^0_{i,k}$ x10^9/ m^2 s^{-1}	$Đ^0_{i,k}$ x10^9/ m^2 s^{-1}	Ref.
[bmim][DCA]	2.08	1.96	[44]
[bmim][Ntf_2]	3.92	1.54	[44]

2.6.3 Surface tension

The effect of the liquid surface tension in distillation is mainly on the interfacial area for mass transfer and in the calculation of the liquid holdup when using the Rocha et al. mass transfer correlation. In packing for example, the surface tension determines the wetted area of the packing surface (equation 2.50). More importantly, when using structured packing to separate aqueous mixtures, the information of surface tension becomes crucial to determine the changes in wetting degree with composition [54]. Therefore, this information is important in calculating the mass transfer efficiency but it does not play any role when comparing different solvents since the values of surface tension with ionic liquids do not differ much from those of regular solvents. Table 2.3 depicts typical values of surface tension of some ionic liquids and the benchmark solvent ethylene glycol.

Table 2.3. Surface tension of ethylene glycol and some ionic liquids at T = 298.15 K.

Solvent	σ / mN m^{-1}	References
EG	47.89	[55]
[bmim][$MeSO_4$][a]	43.3	[56]
[bmim][DCA][b]	48.6	[57]
[bmim][Cl][c]	48.2[f]	[58]
[emim][$EtSO_4$][d]	46.96	[59]
[emim][BF_4][e]	50.1	[60]

[a] 1-butyl-3-methylimidazolium methylsulfate

[b] 1-butyl-3-methylimidazolium dicyanamide

[c] 1-butyl-3-methylimidazolium chloride

[d] 1-ethyl-3-methylimidazolium ethylsulfate

[e] 1-ethyl-3-methylimidazolium tetrafluoroborate

[f] Value measured at 298.1K

Various studies have shown the importance of surface tension in mass transfer efficiency when having the so-called Maragoni effect [61,62]. However, in this work the analysis is limited to one system (ethanol-water) and the comparisons of different solvents are carried out at comparable operating conditions using the same column internals. Since the system in this study is aqueous, the information of surface tension should be accurate enough to quantify the expected changes in surface wetting. To predict the surface tension of pure ionic liquids as well as in mixtures group contribution methods are available [14]. However, when ionic liquids are present, the lack of interaction parameters makes these methods inadequate. Therefore, experimental determination is necessary. This experimental determination should represent the change of this property with composition more than with temperature because the surface tension only decreases slightly and linearly with temperature. This is observed in pure ionic liquids [57,63], water and ethanol [64]. Therefore, the changes in composition are much more relevant and the surface tension could be only measured at room temperature. Secondly, a model to accurately correlate the

experimental data is required. The Fu-Li-Wang mixing rule [65], which is depicted in equation 2.50, allows correlating polar and aqueous systems.

$$\sigma = \sum_{i=1}^{n} \frac{x_i \sigma_i}{\sum_{j=1}^{n} l_{ij} x_j} - \sum_{i=1}^{n} \sum_{j=1}^{n} \frac{x_i x_j \left| \sigma_i - \sigma_j \right|}{\sum_{m=1}^{n} l_{im} x_m \sum_{r=1}^{n} l_{jr} x_r} \qquad 2.50$$

2.6.4 Liquid density

The fourth physical property is the liquid density. This is the most abundant and simple to measure property that can be found in literature. Furthermore, it is not a crucial property to determine mass transfer even though this property is required in many equations within the rate-based model. Liquid density is mainly necessary for equipment sizing. Therefore, it can be predicted. The manner of predicting this property is discussed in chapter 3.

2.6.5 Liquid thermal conductivity

Liquid thermal conductivity is a transport property that accounts for the resistance to heat transfer. Specifically, this property must be defined in the heat transfer correlation. In distillation, the Chilton-Colburn analogy is used:

$$h^L = \overline{k}^L \overline{\rho}^L C_P^L \left(\frac{\lambda^L}{\overline{\rho}^L C_P^L \overline{Đ}^L} \right)^{0.67} \qquad 2.51$$

$$\overline{Đ}^L = \frac{\sum_{i=1}^{n-1} \sum_{k=i+1}^{n} (x_i + \delta)(x + \delta) Đ_{i,k}}{\sum_{i=1}^{n-1} \sum_{k=i+1}^{n} (x_i + \delta)(x_k + \delta)} \quad \text{with } \delta \text{ being } 10^{-4}. \qquad 2.52$$

Equation 2.52 also applies for the average mass transfer coefficient $\overline{k}^L$. Despite of the importance of thermal conductivity in heat transfer processes, the experimental information

about this property is very limited and even scarcer in mixtures. However, in distillation the temperature gradients between phases are not high enough to consider the thermal contributions to mass fluxes [39]. Therefore, this property can be predicted using the classical methods from literature. The Sato-Reidel equation is capable to estimate thermal conductivities of liquids with only knowing the molecular weight, boiling point and critical temperatures of the fluids [14]. It is important to say that, boiling point and critical temperatures concern information that does not exist for ionic liquids. However, these points can be somehow predicted by a group contribution method available in literature [66]. Typical values for liquid thermal conductivity of ionic liquids range from 0.1 to 0.22 $W \cdot m^{-1} \cdot K^{-1}$ approximately and they are almost independent with temperature [67-72]. Experimental data and predicted values are presented in table 2.4.

Table 2.4 shows that the predictions underestimate the experimental values and the deviations are relatively large. However, the errors are acceptable for distillation processes due to the reasons discussed above. In mixtures, the thermal conductivity can be calculated by using the Li mixing rule [73].

Table 2.4. Thermal conductivity of two ionic liquids and the predicted values at T = 293.15 K.

	Literature	Sato-Riedel	
	λ / W m^{-1} K^{-1}	λ / W m^{-1} K^{-1}	Ref.
[emim][OAc]	0.2110	0.130	[71]
[emim][DCA]	0.2021	0.141	[71]

$$\lambda^L = \sum_i \sum_k \vartheta_i \vartheta_k \lambda_{ik} \qquad 2.52$$

$$\lambda_{ik} = 2\left(\lambda_i^{-1} + \lambda_k^{-1}\right)^{-1} \qquad 2.53$$

$$\vartheta_i = \frac{x_i V_i}{\sum_m x_m V_m} \qquad 2.54$$

$$\sum_i \vartheta_i = 1 \qquad 2.55$$

2.7 Conclusions

The rate-based model provides reliable predictions for the extractive distillation process to separate water – ethanol mixtures only when reliable physical and transport properties are provided. In this chapter, the required physical and transport properties were evaluated according to the needs of the rate-based model in order to correctly describe the mass transfer efficiency changes when using ionic liquids as solvents.

Two internals were chosen: Sieve trays and Mellapak® 250Y. Mass transfer correlations for those internal were also chosen: Chan & Fair [2,3] and Rocha et al. [8,9] respectively.

For water – ethanol separation the ionic liquids 1-ethyl-3-methyimidazolium chloride, [emim][Cl]; 1-ethyl-3-methyimidazolium acetate [emim][OAc]; and 1-ethyl-3-methyimidazolium dicyanamide, [emim][DCA] were chosen. Furthermore, ethylene glycol was selected as the reference solvent.

Reliable dynamic viscosities for all the solvents have to be provided by means of experimental determination. Besides that, this data must be provided as function of temperature and concentration in the ternary mixture water – ethanol – solvent. To represent correctly the experimental viscosity data the Eyring-Patel-Teja model was selected from literature.

Infinite dilution diffusion coefficients of ionic liquids in water or ethanol are determined by measuring electrical conductivities and the help of the Nerst-Haskell equation. The Wilke – Chang correlation can be used in the case of infinite dilution

diffusion coefficients of water or ethanol in ionic liquids. When using ethylene glycol as solvent, most values can be obtained from literature. To determine the Maxwell-Stefan diffusion coefficient in mixtures the Kooijman and Taylor mixing rule [36] is used.

In the case of liquid densities, this property can be predicted.

Liquid surface tension is another property that has to be accurately provided. This property needs to be experimentally determined only as function of concentration. The Fu-Li-Wang mixing rule [65] is used to correlate the experimental data.

Finally, liquid thermal conductivity of a pure solvent is a property that can be predicting using the Sato-Reidel [14] method for common fluids. The Li mixing rule [73] is used to represent the changes of this property with composition.

Nomenclature

a	Constant in Patel-Teja equation of state
$\bar{a}$	Interfacial per unit of volume of liquid, $m^2\ m^{-3}$
a_e	Effective surface area per volume of the column, $m^2\ m^{-3}$
a^I	Interfacial area, m^2
a_P	Specific area of the packing, $m^2\ m^{-3}$
A_b	Total active bubbling area on the tray, m^2
A_t	Cross-sectional area of the column, m^2
a_i	Constant in the Patel-Teja equation of state
C_E	Correction factor for surface renewal
C_P	Specific molar heat capacity, $J\ kmol^{-1}\ K^{-1}$

$Đ^L$	Maxwell-Stefan Diffusion coefficient, m s^{-1}
F	Faraday's constant, C mol^{-1}
F^L	Feed molar flow rate of liquid, kmol s^{-1}
F_S	Superficial F-Factor, $kg^{0.5}$ $m^{-0.5}$ s^{-1}
F_{SE}	Factor for surface enhancement
F_t	Correction factor for total holdup due to effective wetted area
FP	Flow parameter
Fr_L	Dimensionless Froude number
g_{eff}	Effective gravity, m^2 s^{-1}
G^{ex}	Excess Gibbs free energy of mixture, J $kmol^{-1}$
h	Heat transfer coefficient, J m^{-2} K^{-1} s^{-1}
h_{cl}	Clear liquid height, m
h_f	Froth height, m
h_P	Height of a packing section, m
h_t	Fractional holdup
H	Enthalpy, J $kmol^{-1}$
$\overline{H}$	Partial enthalpy, J $kmol^{-1}$
k^L	Mass transfer coefficient, m s^{-1}
K	Distribution coefficient
l	Binary parameter in mixing rules
$\bar{l}$	Averaged binary parameter, $\bar{l} = \left(l_{i,k} + l_{k,i}\right)/2$
l_w	Average weir length (per liquid pass), m

L	Liquid molar flow rate, kmol s^{-1}
M_w	Molecular weight, kg $kmol^{-1}$
N	Mass transfer rate, kmol s^{-1}
q	Heat transfer rate, J s^{-1}
Q	Heat input to stage, J s^{-1}
Q_L	Total volumetric flow rate for the liquid, m^3 s^{-1}
R	Inverse of the mass transfer coefficient matrix, s $kmol^{-1}$
R_G	Universal gas constant, J $kmol^{-1}$ K^{-1}
R_u	Universal gas constant in Nerst-Haskell equation, J mol^{-1} K^{-1}
Re_L	Dimensionless Reynolds number in liquid phase
S	Slant height of a corrugation, m
T	Temperature, K
u_S	Superficial velocity for the liquid, m s^{-1}
u_{Le}	Effective velocity through the channel for liquid, m s^{-1}
V	Liquid molar volume, m^3 $kmol^{-1}$
V_b	Liquid molar volume at the normal boiling point, m^3 $kmol^{-1}$
x	Molar fraction of the liquid
y	Molar fraction of the vapor
z_+, z_-	Charge number of ion

Greek letters

α	Relative volatility

δ	Delta kronecker
ε	Void fraction of packing
ϕ	Fractional hole area per unit bubbling area
Φ	Association factor for the solvent (2.26 for water; 1.9 for methanol, 1.5 for ethanol and 1 for unassociated solvents)
Γ	Matrix of thermodynamic factors
γ	Contact angle between solid and liquid film, deg
η	Liquid viscosity, mPa s
φ	Fugacity coefficient
φ^0	Fugacity of the pure component
ϑ	Volume fraction
λ	Thermal conductivity, W m^{-1} K^{-1}
Λ_+^0, Λ_-^0	Molar conductivities, m^2 S mol^{-1}
θ	Angle with horizontal of falling film or corrugation channel, deg
ρ_t	Mass density, kg m^{-3}
$\overline{\rho}$	Molar density, kmol m^{-3}
σ	Surface tension, nN m^{-1}
ξ	Relative froth density

Subscripts

i, k, m, n	Component indices
j	Stage indice

Superscripts

FL, FV	Liquid feed, vapor
I	Interface
L	Liquid
V	Vapor
0	Infinite dilution

Reference List

[1] H.Kooijman, R.Krishna, and R.Taylor, Real World Modeling of Distillation, *CEP Magazine: An AIChE Publication*, (2003), 28-39.

[2] H.Chan and J.R.Fair, Prediction of point efficiencies on sieve trays. 1. Binary systems, *Ind.Eng.Chem.Process Des.Dev.*, 23, 1984, 814 - 819.

[3] H.Chan and J.R.Fair, Prediction of point efficiencies on sieve trays. 2. Multicomponent systems, *Ind.Eng.Chem.Process Des.Dev.*, 23, 1984, 820 - 827.

[4] F.J.Zuiderweg, Sieve trays: A view on the state of the art, *Chem.Eng.Sci.*, 37, 1982, 1441 - 1464.

[5] H.A.Kooijman and R.Taylor, Modelling mass transfer in multicomponent distillation, *Chem.Eng.J.*, 57, 1995, 177 - 188.

[6] R.Taylor and R.Krishna, *Multicomponent Mass Transfer*, Wiley, New York, 1993.

[7] AIChE, *Bubble-tray Design Manual: prediction of fractional efficiency*, American Institute of Chemical Engineers, New York, 1958.

[8] J.A.Rocha, J.L.Bravo, and J.R.Fair, Distillation Columns Containing Structured Packings: A Comprehensive Model for Their Performance. 1. Hydraulic Models, *Ind.Eng.Chem.Res.*, 1993, 1993, 641 - 651.

[9] J.A.Rocha, J.L.Bravo, and J.R.Fair, Distillation Columns Containing Strictured Packings: A Comprehensive Model for Their Performance. 2. Mass-Tranfer Model, *Ind.Eng.Chem.Res.*, 35, 1996, 1660 - 1667.

[10] J.L.Bravo, J.A.Rocha, and J.R.Fair, Mass Tranfer in Gauze Packings, *Hydrocarbon Process.*, 64, 1985, 91 - 95.

[11] G.X.Chen and K.T.Chuang, Liuqid-Phase Resistance to Mass Transfer on Distillation Trays, *Ind.Eng.Chem.Res.*, 34, 1995, 3078 - 3082.

[12] R.Billet and M.Schultes, Predicting Mass Transfer in Packed Columns, *Chem.Eng.Technol.*, 16, 1993, 1 - 9.

[13] R.Billet and M.Schultes, Prediction of Mass Tranfer Columns with Dumped and Arranged Packings: Updated Summary of the Calculations Method of Billet and Schultes, *Chem.Eng.Res.Des.*, 77, 1999, 498 - 504.

[14] B.E.Poling, J.M.Prausnitz, and J.P.O'Connell, *The Properties of Gases and Liquids*, McGraw-Hill, London, 2001.

[15] Y.Ge, L.Zhang, X.Yuan, W.Geng, and J.Ji, Selection of ionic liquids as entrainers for separation of (water + ethanol), *J.Chem.Thermodyn.*, 40, 2008, 1248 - 1252.

[16] A.V.Orchillés, P.J.Miguel, F.J.Llopis, E.Vercher, and A.Martínez-Andreu, Isobaric Vapor-Liquid Equilibria for the Extractive Distillation of Ethanol + Water Mixtures Using 1-Ethyl-3-methylimidazolium Dicyanamide, *J.Chem.Eng.Data*, xx, 2012, xxx - xxx.

[17] S.Fendt, S.Padmanabhan, H.W.Blanch, and J.M.Prausnitz, Viscosities of Acetate or Chloride-Based Ionic Liquids and Some of Their Mixtures with Water or Other Common Solvents, *J.Chem.Eng.Data*, 56, 2011, 31 - 34.

[18] E.Quijada-Maldonado, S.van der Boogaart, J.H.Lijbers, G.W.Meindersma, and A.B.de Haan, Experimental densities, dynamic viscosities and surface tensions of the ionic liquids series 1-ethyl-3-methylimidazolium acetate and dicyanamide and their binary and ternary mixtures with water and ethanol at T = (298.15 K to 343.15 K) 19, *J.Chem.Thermodyn.*, 51, 2012, 51 - 58.

[19] E.Quijada-Maldonado, G.W.Meindersma, and A.B.de Haan, Viscosity and density data for the ternary system water(1) - ethanol(2) - ethylene glycol(3) between 298.15 and 328.15K, *J.Chem.Thermodyn.*, 2012,

[20] S.Weiss and R.Arlt, On the Modeling of Mass Transfer in Extractive Distillation, *Chem.Eng.Process.*, 21, 1987, 107 - 113.

[21] P.Harriott, The Effect of Liquid-Phase Resistance on the Efficiency of Distillation Plates, *Ind.Eng.Chem.Res.*, 44, 2005, 5298 - 5303.

[22] R.F.Strigle Jr., *Packed Tower Design and Applications: Random and Structured Packings*, Gulf, Houston, Texas, 1994.

[23] Y.Gaston-Bonhomme, P.Petrino, and J.L.Chavalier, UNIFAC-VISCO group contribution method for predicting kinematic viscosity: Extension and temperature dependence, *Chem.Eng.Sci.*, 49, 1994, 1799 - 1806.

[24] K.Tochigi, K.Yoshino, and V.K.Rattan, Prediction of Kinematic Viscosities for Binary and Ternary Liquid Mixtures with an ASOG-VISCO Group Contribution Method, *Int.J.Thermophys.*, 26, 2005, 413 - 419.

[25] N.Calvar, E.Gómez, B.González, and Á.Domínguez, Experimental Determination, Correlation, and Prediction of Physical Properties of the Ternary Mixtures Ethanol + Water with 1-Octyl-3-methylimidazolium Chloride and 1-Ethyl-3-methylimidazolium Ethylsulfate, *J.Chem.Eng.Data*, 52, 2007, 2529 - 2535.

[26] E.Gómez, B.González, N.Calvar, and Á.Domínguez, Excess molar properties of ternary system (ethanol + water + 1,3-dimethylimidazolium methylsulphate) and its binary mixtures at several temperatures, *J.Chem.Thermodyn.*, 40, 2008, 1208 - 1216.

[27] B.González, N.Calvar, E.Gómez, and Á.Domínguez, Physical properties of the ternary system (ethanol + water + 1-butyl-3-methylimidazolium methylsulphate) and its binary mixtures at several temperatures, *J.Chem.Thermodyn.*, 40, 2008, 1274 - 1281.

[28] N.Calvar, E.Gómez, B.González, and Á.Domínguez, Experimental Determination, Correlation, and Prediction of Physical Properties of the Ternary Mixtures Ethanol and 1-Propanol + Water + 1-Ethyl-3-methylpyridinium at 198.15 K, *J.Chem.Eng.Data*, 54, 2009, 2229 - 2234.

[29] J.Zhang, W.Wu, T. Jiang, H.Gao, Z.Liu, J.He, and B.Han, Conductivities and Viscosities of the Ionic Liquids [bmim][PF_6] + Water + Ethanol and [bmim][PF_6] + Water + Acetone Ternary Mixtures, *J.Chem.Eng.Data*, 48, 2003, 1315 - 1317.

[30] L.Grunberg and A.H.Nissan, Mixture Law for Viscosity, *Nature*, 164, 1949, 799 - 800.

[31] A.S.Teja and P.Rice, Generalized corresponding states method for the viscosities of liquid mixtures, *Ind.Eng.Chem.Fundamen.*, 20, 1981, 77 - 81.

[32] M.Lee, J.Chiu, S.Hwang, and H.Lin, Viscosity Calculations with Eyring-Patel-Teja Model for Liquid Mixtures, *Ind.Eng.Chem.Res.*, 38, 1999, 2867 - 2876.

[33] Y.Adachi and H.Sugie, A New Mixing Rule - Modified Conventional Mixing Rule, *Fluid Phase Equilibr.*, 28, 1986, 103 - 118.

[34] R.Stryjek and J.H.Vera, PRSV - An Improved Peng-Robinson Equation of State with New Mixing Rules for Strongly Nonideal Mixtures, *Can.J.Chem.Eng.*, 64, 1986, 334 - 340.

[35] R.Sandoval, G.Wilczek-Vera, and J.H.Vera, Prediction of Ternary Vapor-Liquid Equilibria with the PRSV Equation of State, *Fluid Phase Equilibr.*, 52, 1989, 119 - 126.

[36] H.A.Kooijman and R.Taylor, Estimation of Diffusion Coefficients in Multicomponent Liquid Systems, *Ind.Eng.Chem.Res.*, 30, 1991, 1217 - 1222.
[37] A.Bardow, E.Kriesten, M.A.Voda, F.Casanova, B.Blümich, and W.Marquardt, Predictions of multicomponent mutual diffusion in liquids: Model discrimination using NMR data, *Fluid Phase Equilibr.*, 278, 2009, 27 - 35.
[38] X.Liu, T.J.H.Vlugt, and A.Bardow, A predictive Darken Equation for Maxwell-Stefan Diffusivities in Multicomponent Mixtures, *Ind.Eng.Chem.Res.*, 50, 2011, 10350 - 10358.
[39] R.Taylor and R.Krishna, *Multicomponent Mass Transfer*, Wiley, New York, 1993.
[40] A.Heintz, R.Ludwig, and E.Schmidt, Limiting diffusion coefficients of ionic liquids in water and methanol: a combined experimental and molecular study, *Phys.Chem.Chem.Phys.*, 13, 2011, 3268 - 3273.
[41] A.Heintz, J.K.Lehmann, E.Schmidt, and A.Wandschneider, Diffusion coefficients of Imidazolium Based Ionic Liquids in Aqueous Solutions, *J.Solution Chem.*, 38, 2009, 1079 - 1083.
[42] C.Wong, A.N.Soriano, and M.Li, Diffusion coefficients and molar conductivities in aqueous solutions of 1-ethyl-3-methylimidazolium-based ionic liquids, *Fluid Phase Equilibr.*, 271, 2008, 43 - 52.
[43] S.Sarraute, M.F.C.Gomes, and A.A.H.Pádua, Diffusion Coefficients of 1-alkyl3-methylimidazolium Ionic Liquid in Water, Methanol, and Acetonitrile at Infinite Dilution, *J.Chem.Eng.Data*, 54, 2009, 2389 - 2394.
[44] C.A.Nieto de Castro, E.Langa, A.L.Morais, M.L.M.Lopes, M.J.V.Lourenço, F.J.V.Santos, M.S.C.S.Santos, J.N.C.Lopes, H.I.M.Veiga, M.Macatrão, J.M.S.S.Esperança, C.S.Marques, L.P.N.Rebelo, and C.A.M.Afonso, Studies on the density, heat capacity, surface tension and infinite dilution diffusion with the ionic liquds [C_4mim][NTf_2], [C_4mim][dca], [C_2mim][$EtOSO_3$] and [*Aliquat*][dca], *Fluid Phase Equilibr.*, 294, 2010, 157 - 179.
[45] W.C.Su, C.H.Chou, D.S.H.Wong, and M.H.Li, Diffusion coefficients and conductivities of alkylimidazolium tetrafluoroborate and hexafluorophosphates, *Fluid Phase Equilibr.*, 252, 2007, 74 - 78.
[46] C.Wong, A.N.Soriano, and M.Li, Infinite dilution diffusion coefficients of [Bmim]-based ionic liquids in water and its molar conductivities, *J.Taiwan Inst.Chem.E.*, 40, 2009, 77 - 83.
[47] J.A.Lazzús, A group contribution method to predict the thermal decomposition temperature of ionic liquids, *J.Mol.Liq.*, 168, 2012, 87 - 93.
[48] A.Soriano, A.Agapito, L.Lagumbay, A.Caparanga, and M.Si, Diffusion Coefficients of Aqueous Ionic Liquid Solutions at Infinite Dilution Determined from Electrolytic Conductivity Measurements, *J.Taiwan Inst.Chem.E.*, 42, 2011, 258 - 264.
[49] G.Ternström, A.Sjöstrand, G.Aly, and Å.Jernqvis, Mutual Diffusion Coefficients of Water + Ethylene Glycol and Water + Glycerol Mixtures, *J.Chem.Eng.Data*, 41, 1996, 876 - 879.
[50] C.H.Byers and C, J. King, Liquid Diffusivities in the Glycol-Water System, *J.Phys.Chem.*, 70, 1966, 2499 - 2503.
[51] T.Tominaga and S.Matsumoto, Diffusion of Polar and Nonpolar Molecules in water and Ethanol, *Bull.Chem.Soc.Jpn.*, 63, 1990, 533 - 537.
[52] M.T.Tyn and W.F.Calus, Temperature and Concentration Dependence of Mutual Diffusion Coefficients of Some Binary Liquids Systems, *J.Chem.Eng.Data*, 20, 1975, 310 - 316.

[53] S.F.Y.Li and H.M.Ong, Infinite Dilution Diffusion Coefficients of Several Alcohol in Water, *J.Chem.Eng.Data*, 35, 1990, 137 - 140.
[54] A.P.Boyes and A.B.Ponter, Prediction of Distillation Column Performance for Surface Tension Positive and Negative Systems, *Ind.Eng.Chem.Process Des.Develop.*, 10, 1971, 140 - 143.
[55] A.A.Rafati, E.Ghasemian, and M.Abdolmaleki, Surface Properties of Binary Mixtures of Ethylene Glycol with a Series of Aliphatic Alcohols (1-Pentanol, 1-Hexanol, and 1-Heptanol), *J.Chem.Eng.Data*, 53, 2008, 1944 - 1949.
[56] A.B.Pereiro, P.Verdía, E.Tojo, and A.Rodríguez, Physical Properties of 1-Butyl-3-methylimidazolium Methyl Sulfate as a Function of Temperature, *J.Chem.Eng.Data*, 52, 2007, 377 - 380.
[57] A.Galán-Sánchez, J.Ribé-Espel, F.Onink, G.W.Meindersma, and A.B.de Haan, Density, viscosity, and Surface Tension of Synthesis Grade Imidazolium, Pyridinium, and Pyrrolidinium Based Room Temperature ionic Liquids, *J.Chem.Eng.Data*, 54, 2009, 2803 - 2812.
[58] M.H.Ghatee and A.R.Zolghadr, Surface tension measurements of imidazolium-based ionic liquids at liquid vapor equilibrium , *Fluid Phase Equilibr.*, 263, 2008, 168 - 175.
[59] E.Gómez, B.González, N.Calvar, E.Tojo, and Á.Domínguez, Physical Properties of Pure 1-Ethyl-3-methylimidazolium Ethylsulfate and Its Binary Mixtures with Ethanol and Water at Several Temperatures, *J.Chem.Eng.Data*, 51, 2006, 2096 - 2102.
[60] W.Xu, L.Li, X.Ma, J.Wei, W.Duan, W.Guan, and J.Yang, Density, Surface Tension, and Refractive Index of Ionic Liquids Homologue of 1-alkyl-3-methylimidazolium Tetrafluoroborate [$C_n$mim][BF_4], *J.Chem.Eng.Data*, 57, 2012, 2177 - 2184.
[61] S.J.Proctor, M.W.Biddulph, and K.R.Krishnamurphy, Effects of Maragoni Surface Tension Forces on Modern Distillation Packings, *AIChE J.*, 44, 1998, 831 - 835.
[62] Z.Stefanov and M.K.Karaivanova, Influence of the Maragoni Effect on the Efficiency of Plate Columns for Binary Distillation, *Chem.Eng.Technol.*, 34, 2011, 2029 - 2032.
[63] M.G.Freire, P.J.Carvalho, A.M Fernandes, I.M Marrucho, A.J.Queimada, and J.A.P.Coutinho, Surface tensions of imidazolium based ionic liquids: Anion, cation, temperature and water effect, *J.Colloid Interf.Sci.*, 314, 2007, 621 - 630.
[64] G.Vázquez, E.Alvarez, and J.M.Navaza, Surface Tension of Alcohol + Water from 20 to 50 ºC, *J.Chem.Eng.Data*, 40, 1995, 614 -
[65] J.Fu, B.Li, and Z.Wang, Estimation of Fluid-Fluid Interfacial Tensions of Multicomponent Mixtures, *Chem.Eng.Sci.*, 41, 1986, 2673 - 2679.
[66] J.O.Valderrama and R.E.Rojas, Critical Properties of Ionic Liquids. Revisited, *Ind.Eng.Chem.Res.*, 48, 2009, 6890 - 6900.
[67] M.E.Van Valkenburg, R.L.Vaughn, M.Williams, and J.S.Wilkes, Thermochemistry of ionic liquid heat-transfer fluids, *Thermochim.Acta*, 425, 2005, 181 - 188.
[68] R.Ge, C.Hardacre, P.Nancarrow, and D.W.Rooney, Thermal Conductivities of Ionic Liquids over the Temeprature Range from 293 K to 353 K, *J.Chem.Eng.Data*, 52, 2007, 1819 - 1823.
[69] D.Tomida, S.Kenmochi, T.Tsukada, K.Qiao, and C.Yokoyama, Thermal Conductivities of [bmim][PF6], [hmim][PF6], and [omim][PF6] from 294 to 335 K at Pressures up to 20 MPa, *Int.J.Thermophys.*, 28, 2007, 1147 - 1160.

[70] C.A.Nieto de Castro, M.J.V.Lourenco, A.P.C.Ribeiro, E.Langa, and S.I.C.Vieira, Thermal Properties of Ionic Liquids and IoNanofluids of Imidazolium and Pyrrolidinium Liquids , *J.Chem.Eng.Data*, 55, 2010, 653 - 661.

[71] A.P.Fröba, M.H.Rausch, K.Krzeminski, D.Assenbaum, P.Wasserscheid, and A.Leipertz, Thermal Conductivity of Ionic liquids: Measurement and Prediction, *Int.J.Thermophys.*, 31, 2010, 2059 - 2077.

[72] H, Chen, Y.He, J.Zhu, H.Alias, Y.Ding, P.Nancarrow, C.Hardacre, D.Rooney, and C.Tan, Rheological and heat transfer behaviour of the ionic liquid, $[C_4mim][NTf_2]$, *Int.J.Heat.Fluid Fl.*, 29, 2008, 149 - 155.

[73] C.C.Li, Thermal Conductivity of Liquid Mixtures, *AIChE J.*, 22, 1976, 927 - 930.

3

Experimental determination and modeling of the physical properties to develop a rate-based model for the separation of water – ethanol mixtures

Abstract

To use the rate-based model in predicting the performance of the extractive distillation with ionic liquids and studying the mass transfer efficiency of the process, several physical and transport properties are necessary. The scarcity of experimental data or mathematical models model to predict this data leads to measure it experimentally. It was determined before that, only liquid dynamic viscosities, infinite dilution diffusion coefficients and surface tension should be measured in a wide range of temperature and concentration to provide reliability in the predictions given by the rate-based model. In this work these properties were measured in the established ranges. However, to make these properties usable in ASPEN® Plus, the experimental data was correlated with models. The Vogel equation [1] correlated very well pure viscosities and polynomials correlated diffusion coefficients at infinite dilution and densities. The Eyring-Patel-Teja model [2]and the Fu-Li-Wang mixing rule [3] correlated very well the viscosities and the surface tension respectively.

3.1 Introduction

In the previous chapter, it was established which physical and transport properties are necessary to provide accuracy in mass transfer analysis when using the rate-based model. The properties are: liquid viscosity, infinite dilution diffusion coefficients and surface tension. Additionally, liquid densities are measure since this property is required to obtain dynamic viscosities. The first property has to be provided as function of concentration and temperature. The second property only depends on temperature and then a mixing rule describes this property as function of concentration. And finally, the surface tension has to be provided as function of concentration at room temperature. Additionally, the ionic liquids to study the effect of the physical and transport properties on the mass transfer efficiency of an extractive distillation column were defined. These ionic liquids are: 1-ethyl-3-methylimidazolium acetate [emim][OAc], 1-ethyl-3-methylimidazolium dicyanamide [emim][DCA] and 1-ethyl-3-methylimidazolium chloride [emim][Cl]. Their performance is finally compared with ethylene glycol EG. A few experimental works are already available in literature containing the required data.

Pure dynamic viscosities of [emim][OAc] [4-6], [emim][DCA] [5,7-10] and [emim][Cl] [4] can be found in literature. However, as function of concentration only one work is found for the mixture [emim][OAc] – water [4]. To our knowledge, no experimental binary and ternary mixture water – ethanol – solvent is reported in literature. For the case of EG, pure dynamic viscosities and binary mixture water – EG at several temperatures as are well known [11-15]. Experimental ternary dynamic viscosities as function of temperature are only published in a previous study for a limited range of compositions and temperatures [16]. On the other hand, the case of the infinite dilution diffusion coefficients the available literature is fairly limited and in the previous chapter it was established that this property should be experimentally determined. Finally, the surface tension of the pure solvents to be analysed can be found in literature [8,9,12,17], except for [emim][OAc] and [emim][Cl] which is solid at room temperature. However, in mixtures, only water – ethylene glycol can be found in literature [12].

The objective of this chapter is to experimentally determine the mentioned properties of the solvent for both pure and in binary and /or ternary mixtures. Additionally, the modelling of this experimental data with available model from literature is carried out to in order to use all the measured data in ASPEN® Plus.

3.2 Experimental

3.2.1 Chemicals

The ionic liquids 1-ethyl-3-methylimidazolium acetate with a mass fraction purity higher than 95 wt%, 1-ethyl-3-methylimidazolium dicyanamide with a mass fraction purity higher than 98 wt% and 1-ethyl-3-methylimidazolium chloride with a mass fraction purity higher than 98 wt% were purchased from Ionic Liquids Technologies GmbH. The initial water content of these ionic liquids in mass fraction was 0.13 wt% for [emim][OAc] and 0.17 wt% for [emim][DCA]. The rest of the components present in the ionic liquids are unreacted ethylimidizadole and their salts. [emim][Cl] is solid at room temperature, therefore the water content was not measured. The ionic liquids (except for [emim][Cl]) were dried under vacuum (~7 mbar) and a temperature of ~ 343.15 K in a rotary evaporator for 24 hours to reduce the initial water content. The water content was measured by using 796 Karl Fisher analysis. After drying, the water content of the ionic liquids was 0.13 wt% and 0.09 wt% in [emim][OAc] and [emim][DCA], respectively. It was not possible to dry [emim][OAc] due to its highly hydrophilic character. Anhydrous grade ethylene glycol was purchased from Sigma Aldrich with mass fraction purity higher than 99.8 wt%. The water content of this solvent was 0.02 wt% measured with a 796 Karl Fisher analysis and no further drying was performed. Ethanol was purchased from Merck with mass fraction purity higher than 99.5 wt% and a water content of 0.04 wt%. This ethanol was used without further purification in measurements with EG and the water content was removed using molecular sieves (3Å) purchased from Sigma Aldrich for the measurements with ionic liquids. The final water content of this ethanol in mass fraction was 0.02 wt%. Finally,

deionized ultrapure water was used (18.2 MΩ·cm, Milli-Q system, Millipore, Billerica, USA).

For the infinite dilution diffusion coefficients measurements, Potassium chloride (KCl) standards, Certipur®, were purchased from Merck KGaA. Table 3.1 summarizes the purity of the used chemicals.

Table 3.1. Sample purity description.

Chemical name	Source	Initial mass fraction purity	Initial water mass fraction	Purification method	Final Water mass fraction
[emim][OAc]	Iolitec GmbH	> 0.95	0.0013	Vacuum evaporation	0.0013
[emim][DCA]	Iolitec GmbH	> 0.98	0.0017	Vacuum evaporation	0.0009
Ethanol	Merck	> 0.9995	0.0005	Molecular Sieves (3Å)	0.0002

3.2.2 Apparatus and procedure

3.2.2.1 Viscosity measurements

The samples were prepared in an Erlenmeyer flask with a NS top. Nitrogen was fed into the Erlenmeyer to avoid water uptake by the ionic liquids and EG. After this step, the closed flask was filled with solvent, water and/or ethanol until reaching the desired concentration. A stirring magnet assured good mixing (10 minutes). The composition of the mixture was determined using a Mettler Toledo AT200 high precision balance (±0.0001 g). This flask was kept closed to prevent water uptake and ethanol vaporization.

Densities were measured using an Anton Paar DMA-5000 densimeter. This was first calibrated using air and standard ultra-pure water provided by Anton Paar GmbH in the temperature range of T = 293.15 K to T = 333.15 K and compared with values reported in the densimeter instruction manual. The uncertainty in density provided in the apparatus is $5x10^{-6}$ g·cm^{-3}. The densimeter automatically corrects the effect of viscosity on the density. Additionally, the temperature is controlled automatically by the densimeter with a

resolution of ±0.001 K. During the experiments, densities were measured three times. The measured density was compared with literature data of a known ionic liquid and the results are shown in Table 3.2. To do this, 1-ethyl-3-methylimidazolium ethylsulfate, [emim][EtSO4] was taken as a reference with a water content of 0.01wt% mass fraction. Comparison between these measurements and existing experimental data show good agreement with deviations less than 0.1%.

Kinematic viscosities were determined using an automatic and PC-controlled viscosimeter Lauda iVisc with Ubbelhode capillary viscosimeters from Schott. The measuring principle is gravity fall and the equipment measures the falling time. To ensure accurate results, the falling time has to be between 200 and 1000 seconds. Therefore, to correctly measure these two ionic liquids in the given range of temperatures, a complete series of eight capillary diameters from 0.36 mm to 1.50 mm (referenced at Schott-Geräte GmbH) were used. These viscosimeters calibrated and credited by the supplier with a relative uncertainty of 0.65% at a confidence level of 95%. The equipment has a software control unit to measure the falling time with a resolution of 0.01s. Temperature was kept with a LAUDA E200 thermostat with resolution of 0.01K by using a LAUDA 015T water bath. To avoid water uptake during the measurements, the viscosimeter was constantly fluxed with nitrogen at a pressure of 30 mbar. Measurements were compared with existing pure ionic liquids [emim][EtSO4], [emim][OAc], [emim][DCA] and EG from literature and the results are shown in Table 3.2. The measurements show good agreement with literature data. The falling times were measured between 3 and 5 times.

3.2.2.2 Infinite dilution diffusion coefficients measurements

Electrical conductivities were measured using a Cole-Parmer conductivity meter (model 1481-90) with a platina dip cell (model 1481-95). The measuring resolution is 1 μS cm^{-1} for conductivities between 200-2000 μS cm^{-1} and 0.1 μS cm^{-1} for conductivities between 20-200 μS cm^{-1}. A secondary conductivity meter (model MultiLine P4) was used to validate the results of the first meter at 298.15 K. Temperatures were measured using an IKA® ETS-D6 thermocouple with a measuring resolution of 0.01 K.

Table 3.2. Comparison of the measured values for pure components and literature data.

	ρ [g cm^{-3}]		η [mPa s]	
	Experimental	literature	Experimental	literature
[emim][EtSO4]	1.240184	1.23915[a]	101.42	100.77[a]
		1.23763[b]		97.58[b]
[emim][OAc]	1.09778	1.0993[c]	132.91	143.61[c]
		1.102[d,•]		162.00[e]
		1.0997[f]		162.00[g,★]
[emim][DCA]	1.10198	1.1008[h]	14.90	14.50[h]
		1.10891[i]		18.76[i]
		1.104[c]		16.088[c]
		1.1084[m]		20.99[o]
		1.1092[p]		
Water	0.997039	0.99705[q]	0.89	0.89[q]
ethanol	0.78507	0.78546[q]	1.087	1.082[q]
EG	1.10989	1.1100[r]	16.61	16.474[u]
		1.1085[s]		
		1.1084[t]		

Ref. a[18], Ref. b[19], Ref. c[5], Ref. d[20], Ref. e[4], Ref. f[21], Ref.g[6], Ref. h[7], Ref. i[9], Ref. m[17], Ref. o[10], Ref. p[22], Ref. q[23], Ref. r[24], Ref. s[13], Ref. t[25], Ref. u[16].
Standard uncertainties u are $u(T)$ = 0.003, $u(\rho)$ = 1E-05 and the relative standard uncertainty u_r in $u_r(\eta)$ = 0.0033.
[•] Literature data reported at T = 298.1 K.
[★] Literature data reported at T = 293.15 K.

The conductivity meter is calibrated before each measuring sequence. The actual cell constant is specified by a rotating button during the calibration. Certipur® KCl standards are used with a concentration of 0.01 mol L^{-1} at 1.41 mS cm^{-1} nominal and 0.001 mol L^{-1} at 0.147 mS cm^{-1} nominal. A sample with a stirrer is placed in a heating bath. The conductivity dip cell and the thermocouple are submerged in the solution, after which it is sealed. This is done in order to minimize evaporation of the solvent, and thereby change the concentration, when increasing the temperature. The measuring range of the equipment is set manually. Electrical conductivities are measured while gradually increasing the temperature of the water bath. Calibration of equipment followed the same procedure. The cell constant was fixed at the reference temperature, 298.15 K. Afterwards the temperature was increased to check that conductivities at higher temperatures were consistent with reported values. The error on measuring accuracy is less than 1% for the entire temperature

range. The reliability of the results are tested with reported in literature [22] and given in Table 3.3. The maximum relative error from the literature data is 17%.

3.2.2.3 Surface tension measurements

The surface tension of the ternary system water – ethanol – solvent was measured at 298.15 K with a Kruss K11 tensiometer using a ring of 9.545 mm radius certified by Kruss GmbH. The ternary samples were prepared in an Erlenmeyer flask with a NS top to minimize the water uptake and ethanol vaporization. The closed flask was filled with ionic liquid or EG, water and ethanol until reaching the desired concentration. A stirring magnet assured good mixing (10 minutes). The composition of the mixture was determined using a Mettler Toledo AT200 high precision balance (±0.0001 g). Right after this step, the prepared samples were placed into the tensiometer to determine the surface tension. The surface tension measurements were corrected using the Huh&Manson method that is already implemented in the tensiometer and has a large range of validity. This method corrects the surface distortion when the ring pulls the liquid surface. The tensiometer resolution is 0.1 mN m^{-1} and 0.1 K. For validation the surface tension of pure water, ethanol, [emim][EtSO4], [emim][DCA] and EG were measured at around 298.15 K and compared to values reported in literature. These comparisons are reported in Table 3.4. Deviations from literature data are less than 1% except when comparing the measurements of [emim][DCA] with literature data that show larger deviations. During the experimental procedure, the surface tension was measured three times. The measured ternary compositions cover the region where the extractive distillation takes place.

Table 3.3. Binary diffusion coefficients of [emim][DCA](3) at infinite diution in water(1) at several temperatures.

T [K]	$Đ^0_{31}$ x10E09 [m^2 s^{-1}]	$Đ^0_{31}$ x10E09 [m^2 s^{-1}] [22]	RD [a] [%]
298.15	1.259		
303.15	1.429	1.253	14.05
308.15	1.604	1.407	14.00
313.15	1.785	1.538	16.06
318.15	1.971	1.706	15.53
323.15	2.164	1.849	17.04

[a] $RD\ [\%] = 100 \left| Đ^0_{i,j,lit} - Đ^0_{i,j,pred} \right| / Đ^0_{i,j,lit}$

Table 3.4. Comparisons of measured surface tension of pure water and ethanol with literature data at T = 298.15 K and experimental surface tension for the system water(1) – ethanol(2) – solvent(3) at room temperature.

	σ [mN m^{-1}]	
	Experimental	Literature
Water	71.5	71.35[a]
		72.01[b]
Ethanol	22.0	22.0[a]
		21.8[c]
[emim][EtSO4]	46.9*	46.96[d]
[emim][DCA]	40.3*	44.14[e,★]
		64[f +]
		60.06[g]

Ref. a[26], Ref. b[27], Ref. c[28], Ref. d[19], Ref. e[9], Ref. f [8], Ref. g[17].

* Standard uncertainties u are $u(T)$ = 0.03 K and $u(\sigma)$ = 0.12 [mN m^{-1}].

★ Literature data reported at T = 293.15 K.

+ Literature data reported at T = 293 ± 0.5 K.

3.3 Results

3.3.1 Viscosity of pure solvents and in mixtures with water and/or ethanol

Density ρ and dynamic viscosities η of pure [emim][OAc], [emim][DCA] and EG from T = 298.15 K to T = 343.15 K for the ionic liquids and from T = 298.15 K to T = 328.15 K for EG are reported in Table 3.5. The density ρ values are fitted as a function of temperature by the method of the least squares using the linear expression given by Equation 3.1. Dynamic viscosities η are fitted as a function of temperature using the Vogel equation [1] (3.2) and Andrade equation [29] (3.3). The parameters in these equations were fitted with the by the method of the least squares. The obtained value of these parameters is given in Table 3.6 along with the sum of square error (SSE) with a 95% confidence. [emim][Cl] was not measured due to it is solid at room temperature. Figure 3.1 shows a comparison between the experimental dynamic viscosities (points) of the three solvents and the regression with the Vogel equation. The Vogel equation agrees very well with experimental data.

$$\rho = a + bT \tag{3.1}$$

$$ln(\eta) = c_1 + \frac{c_2}{T + c_3} \tag{3.2}$$

$$ln(\eta) = c_1 + \frac{c_2}{T} + c_3 ln(T) \tag{3.3}$$

In general, both three-parameter equations represent the marked decrease of viscosity with temperature in ionic liquids well. Also, the equations describe very well the viscosity of EG as function of temperature. However, the Vogel equation shows a better agreement with experimental data.

In appendix A.3 the binary and ternary dynamic viscosities for the system (x_1 water + ($1-x_1$) IL), (x_2 ethanol + ($1-x_2$) IL) and (x_1 water + x_2 ethanol + 1-(x_1+x_2) IL) between the temperatures 298.15 K and 343.15 K at atmospheric pressure are reported from table A.3.1 to A.3.3. These tables show an important decrease in viscosities with increasing water or ethanol mole fraction. However, this decrease is sharper in mixtures containing ethanol. The decrease in viscosities with increasing temperatures is well noticeable in the ternary mixtures. However, when the concentration of any of ionic liquid presented here is low, this decrease is less marked. Also, in table A.3.4, ternary dynamic viscosities and densities are presented for the system (x_1 water + x_2 ethanol + 1-(x_1+x_2) EG).

Table 3.5. Densities, ρ and dynamic viscosities, η, of [emim][OAc], [emim][DCA] and EG at several temperatures[a].

	ρ [g cm^{-3}]			η [mPa s]		
T/(K)	[emim][OAc]	[emim][DCA]	EG	[emim][OAc]	[emim][DCA]	EG
303.15	1.09472	1.09866	1.10638	97.98	12.93	13.58
308.15	1.09167	1.09537	1.10286	74.34	11.36	11.24
313.15	1.08862	1.09209	1.09931	57.72	10.07	9.40
318.15	1.08558	1.08883	1.09575	45.76	8.98	7.95
323.15	1.08255	1.08558	1.09216	36.92	8.05	6.77
328.15	1.07953	1.08236	1.08856	30.31	7.26	5.83
333.15	1.07653	1.07915		25.19	6.58	
338.15	1.07353	1.07595		21.24	5.99	
343.15	1.07054	1.07277		18.10	5.48	

[a] Standard uncertainties u are $u(T)$ = 0.003 [K] and $u(\rho)$ = 1E-05 [g cm^{-3}], and the relative standard uncertainty u_r is $u_r(\eta)$ = 0.0034.

Table 3.6. Fitted parameters of equation 3.1 to 3.3 for pure density ρ, and viscosity η, of the solvents.

Property	ρ [g cm^{-3}]			
Solvent	a	b		SSE
[emim][OAc]	1.278	-0.0006054		$1.20\cdot10^{-8}$
[emim][DCA]	1.295	-0.000649		$3.71\cdot10^{-8}$
EG	1.322	-0.000711		8.04E-09
Property	η [mPa s]			
	Vogel			
Solvent	c_1	c_2	c_3	SSE
[emim][OAc]	-1.621	664.5	-196.1	0.008184
[emim][DCA]	-1.719	682.4	-143.7	0.001755
EG	-3.755	1038	-140.1	1.65E-05
	Andrade			
Solvent	c_1	c_2	c_3	SSE
[emim][OAc]	-342.7	20190	49.11	0.2193
[emim][DCA]	-84.9	6040	11.82	0.003149
EG	-130.7	9071	18.09	0.0001248

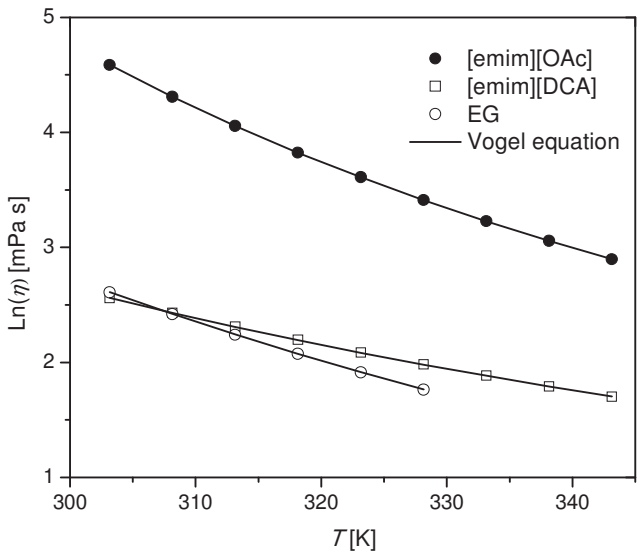

Figure 3.1. Comparison between the experimental viscosities of the three solvents and the Vogel equation.

3.3.2 Infinite dilution diffusion coefficients

In this section the results of the experimentally determined infinite dilution diffusion coefficients are shown. These values are obtained using the Nerst-Haskell relation for electorlites. However, we limit the results to those coefficients and the measured electrical conductivities an all the intermediate calculation steps to arrive to the final diffusion coefficients are left out. Anyhow, a complete description on how to obtain this property is explained elsewhere [22,30]. In the appendix section, Table A.3.5 shows the obtained molar conductivities from electrical conductivity measurements. That experimental data leads to obtain infinite dilution diffusion coefficients that are shown in Table 3.7 for an IL in water or in ethanol at several temperatures.

Table 3.7. Infinite dilution diffusion coefficients $D^0_{i,j}$ x10E09 [m^2 s^{-1}] of the ionic liquids in water or ethanol.

	Solvent					
T [K]	Water			Ethanol		
	[emim][OAc]	[emim][DCA]	[emim][Cl]	[emim][OAc]	[emim][DCA]	[emim][Cl]
298.15	1.042	1.259	1.462	0.553	0.651	0.582
303.15	1.183	1.429	1.666	0.617	0.724	0.648
308.15	1.329	1.604	1.877	0.682	0.799	0.715
313.15	1.479	1.785	2.094	0.751	0.876	0.785
318.15	1.633	1.971	2.319	0.821	0.955	0.857
323.15	1.791	2.164	2.551	0.894	1.035	0.932

The conductivities of ionic liquids were measured in water and in ethanol to obtain the infinite dilution diffusion coefficients presented in Table 3.7. As observed in this table, these values are lower in ethanol compared to water, which is as expected. Li et al. [31] reported that organic solvents have a strong influence on physical properties, depending on the dielectric constant of the solvent. The molar conductivity, and therefore diffusion, decreases with increasing organic solvent compared to the pure ionic liquid. It was confirmed that the solvents enhance the association of ionic liquids to aggregates, which results in a lower mobility. This is in agreement with the results obtained in this work. In contrast, the molar conductivity increases with increasing the amount of water. This solvent is able to break ionic aggregates by enhancing the dissociation, leading to an increase of the

ionic mobility. From Table 3.7, Diffusion coefficients follow the trends: [emim][Cl] > [emim][DCA] > [emim][OAc] for these ionic liquids diluted in water. This trend was expected as [emim][Cl] is the strongest electrolyte, whereas the [emim][OAc] is the weakest. Acetate, with a pK_a value of 4,76 in water [32], is subjected to an acid-base equilibrium, leading to a decrease in conductivity. In ethanol, a polar protic solvent, these effects are different. Here [emim][DCA] > [emim][Cl] ≈ [emim][OAc]. A possible explanation for the change of order between the ionic liquids, is the low solubility of chlorine in ethanol [33]. This could promote the association of the ionic liquid, leading to larger aggregates and decreased mobility.

The infinite dilution diffusion coefficients $Đ^0_{i,j}$ values are fitted as a function of temperature by the method of the least squares using the quadratic expression given by Equation 3.4. The found parameters are shown in Table 3.8 along with the sum of square errors at 95% of confidence.

$$Đ^0_{i,j} = a + bT + cT^2 \qquad 3.4$$

Table 3.8. Fitted parameters of equation 3.4.

solvent	water			
solute	*a*	*b*	c	SSE
[emim][OAc]	0.1577	-0.02195	8.357e-005	1.786e-007
[emim][DCA]	1.414	-0.03438	0.0001136	4.071e-007
[emim][Cl]	1.967	-0.04343	0.00014	3.429e-007
solvent	ethanol			
solute	*a*	*b*	c	SSE
[emim][OAc]	0.9613	-0.01521	4.643e-005	5.214e-007
[emim][DCA]	-0.4223	-0.007262	3.643e-005	1.786e-007
[emim][Cl]	0.8865	-0.01486	4.643e-005	4.071e-007

Finally, a summary of the source of all the infinite dilution diffusion coefficients is given in Table 3.9.

Table 3.9. Literature review and prediction of infinite dilution diffusion coefficients $Đ_{ij}^{0} \neq Đ_{ji}^{0}$ for the system water – ethanol – solvent.

$Đ_{ij}^{0}$	Water	Ethanol	EG	[emim][Cl]	[emim][OAc]	[emim][DCA]
Water		[34,35]	[36]	(w&ch)	(w&ch)	(w&ch)
Ethanol	[34,35]		(w&ch)	(w&ch)	(w&ch)	(w&ch)
EG	[36]	[37]				
[emim][Cl]	(n&h)	(n&h)				
[emim][OAc]	(n&h)	(n&h)				
[emim][DCA]	[22]	(n&h)				

(w&ch) = predicted using the Wilke-Chang equation.
(n&h) = Obtained by using the method presented here.

3.3.3 Surface tension

The surface tensions of the pure ionic liquid were measured at T = 298.15 K. At higher temperatures, the surface tension can be predicted by the method of Macleod-Sudgen and presented by Fröba et al. [9] only by knowing the surface tension at a given temperature and the density in function of temperature. This is represented by equation 3.5:

$$\sigma = (\sigma_{298.15\ \mathrm{K}}) \cdot \left(\frac{\rho}{\rho_{298.15\ \mathrm{K}}} \right) \qquad 3.5$$

Results given by this semi-predictive equation were compared with literature data [21] giving average deviations less than 4%. This relation can overcome the lack of experimental data at higher temperatures.

In Tables A.3.6 to A.3.9, the surface tensions for the system (x_1 water + x_2 ethanol + 1-($x_1 + x_2$) solvent) at around T = 298.15 K are reported. From these tables it is observed that, in the water-rich zone, high surface tensions are reported. However, the use of [emim][Cl] produces the highest values since high degree of association between water and the ionic liquid. The information of ternary surface tension is very valuable to determine the mass transfer in structured packing in extractive distillation.

3.3.4 Correlation of experimental data in mixtures

To correlate the binary and ternary experimental data presented in sections above and find the binary parameters associated to the models, we use the non-linear least square method. The used objective function is given by equation 3.6, where γ_i represents any property. Equation 3.7 represents the overall average deviation.

$$obj = \sum_{i=1}^{n_{exp}} \frac{\left|\gamma_{i,exp} - \gamma_{i,calc}\right|}{\gamma_{i,exp}} \qquad 3.6$$

$$\%ADD = \frac{100}{n_{exp}} \sum_{i=1}^{n_{exp}} \frac{\left|\gamma_{i,exp} - \gamma_{i,calc}\right|}{\gamma_{i,exp}} \qquad 3.7$$

3.3.4.1 Density correlation

Experimental binary and ternary liquid densities are normally correlated by a Redlish-Kister polynomial expansion at one temperature using the excess molar volume data. In this work a simple quadratic mixing rule [38] is applied to correlate these data at any temperature:

$$V_m = \sum_i x_i V_i^l + \sum_i x_i \sum_j x_j K_{ij} (V_i^l V_j^l)^{0.5} \qquad 3.8$$

with ($K_{ij} = K_{ji}; K_{ii} = K_{jj} = 0$). Table 3.10 lists the obtained binary parameters for the mixture water – ethanol – EG between T = 298.15 K and T = 328.15 K and the overall average deviation. In general, this quadratic mixing rule correlates the ternary liquid densities very well. This is not a surprise, since the deviations from ideality are usually negligible. This shows that the ideal term of equation 3.8 could be used alone for predictive purposes without losing accuracy when there is lack of experimental data. This fact can be seen in Table 3.10 where the found binary parameters are very small. In this table, *%ADD ideal* is the overall average deviation for the ideal term solely. It is important to notice that,

the density of [emim][OAc] and [emim][DCA] was measured in binary as well as in ternary mixtures. Both were regressed all together.

Table 3.10. Binary parameters K_{ij} of the quadratic mixing rule given by equation 3.8.

Interaction parameter	EG	[emim][OAc]	[emim][DCA]	[emim][Cl]
K_{12}	-0.0751	-0.0787	-0.060	0
K_{13}	-0.0276	-0.0611	0.019	-0.0413
K_{23}	-0.0126	-0.0214	-0.025	-0.0508
%ADD	**0.15**	**0.25**	**0.89**	**0.56**[a]
%ADD ideal	**2.15**	**1.59**	**1.06**	

[a] Some density points of pure [emim][Cl] were measured near T = 373.15 K. The final polynomial is: $\rho = 0.0009819T^2 - 0.6609T + 242.9$.

3.3.4.2 Viscosity correlation

In Chapter 2, it was establish that the Eyring-Patel-Teja [2] model with the help of a temperature-dependent Redlish-Kister mixing rule and two Margules-type mixing rules was able to correlate very well these highly polar and aqueous systems. The experimental data were regressed using the non-linear least-squares method. Equations 3.6 and 3.7 are the objective function and the overall average deviation respectively.

When regressing the experimental viscosities of the systems containing water, the binary mixture water – ethanol was included in the optimizations and taken from literature [39] (from T = 293.15 to T = 343.15 K). So then, three binary mixtures and the respective ternary mixture were regressed together to obtain the binary parameters. In total, 176 and 175 data points are used to find the optimized binary parameters for mixtures containing [emim][OAc] and [emim][DCA], respectively. For the case of [emim][Cl], only binary data was measured. Therefore, ternary viscosities are obtained from the binary mixtures water – ethanol, water – [emim][Cl] and ethanol – [emim][Cl] with a total of 139 experimental data points. For the ternary mixture containing EG, no binary data was measured and only the ternary data is regressed. This is because the range of measured compositions is wider than the viscosity of the ionic liquid in ternary mixtures and more ternary viscosities were

measured. Table 3.11 shows the regressed binary parameters for every mixing rule and Table 3.12 shows the regressed temperature-dependent binary parameters.

The lowest overall average deviation is observed for the ternary mixture containing EG. Therefore, the application of temperature-dependent interaction parameters to this mixture in the mixing rules presented here is unnecessary. For the case of ionic liquids, large overall deviations are observed for all the mixing rules. However, when viscosity is relatively low like [emim][DCA], the mixing rules perform better since the decreases in viscosity with temperature are not marked. This indicates that, temperature dependent interaction parameters are necessary to represent the marked decrease in viscosity with temperature in highly viscous ionic liquids like [emim][OAc] or [emim][Cl]. To calculate these last parameters the redlish-kister mixing rule is taken.

The lowest overall average deviation is observed for the ternary mixture containing EG. Therefore, the application of temperature-dependent interaction parameters to this mixture in the mixing rules presented here is unnecessary. For the case of ionic liquids, large overall deviations are observed for all the mixing rules. However, when viscosity is relatively low like [emim][DCA], the mixing rules perform better since the decreases in viscosity with temperature are not marked. This indicates that, temperature dependent interaction parameters are necessary to represent the marked decrease in viscosity with temperature in highly viscous ionic liquids like [emim][OAc] or [emim][Cl]. To calculate these last parameters the redlish-kister mixing rule is taken.

Table 3.11. Interaction parameters l_{ij} of the mixing rules for the Eyring-Patel-Teja model.

	EG			[emim][OAc]		
	RK	GMR1	GMR2	RK	GMR1	GMR2
l_{12}	-0.0026	0.1367	0.1659	0	0.1486	0.1132
l_{21}	0.1118	0.0086	-0.0852	0.1055	0.0000	0.0000
l_{13}	0.0095	0.0998	0.0549	0.3082	0.3132	0.2053
l_{31}	0.1055	0.0705	0.0864	0.3202	0.3381	0.2318
l_{23}	0.0753	-0.1199	-0.0085	0.1582	0.4524	0.0528
l_{32}	-0.1056	0.0499	-0.0159	0.0552	0.0717	0.1020
%ADD	**2.83**	**2.81**	**2.31**	**9.31**	**9.67**	**8.83**
	[emim][DCA]			[emim][Cl]		
	RK	GMR1	GMR2	RK	GMR1	GMR2
l_{12}	0	0.1484	0.1130	0	0.1548	0.1154
l_{21}	0.1062	0.0000	0.0000	0.1119	0	0
l_{13}	0.2160	0.1636	0.0943	0.0787	0.1862	0.1409
l_{31}	0.1757	0.2196	0.1654	0.1745	0.1212	0.0651
l_{23}	-0.0112	0.0073	0.0176	-0.3614	0.2467	0.1913
l_{32}	0.0043	-0.0166	-0.0232	0.3438	-0.3406	-0.2716
%ADD	**7.65**	**6.83**	**7.04**	**11.71**	**10.72**	**12.05**

Table 3.12. Temperature-dependent interaction parameters.

Water(1) + ethanol(2) + [emim][OAc](3)				
Binary parameter	$l_{ij}^{(1)}$	$l_{ij}^{(2)}$	$l_{ji}^{(1)}$	$l_{ji}^{(2)}$
l_{12}	0	0	-0.2722	119.1585
l_{13}	1.3438	-322.1689	0.7932	-148.6543
l_{23}	0.5802	-138.5173	0.8340	-234.9450
%ADD	**4.29**			
Water(1) + ethanol(2) + [emim][DCA](3)				
Binary parameter	$l_{ij}^{(1)}$	$l_{ij}^{(2)}$	$l_{ji}^{(1)}$	$l_{ji}^{(2)}$
l_{12}	0	0	-0.2668	117.6482
l_{13}	0.7341	-163.4698	0.6435	-146.4092
l_{23}	0.0313	-13.9840	0.2957	-91.0635
%ADD	**4.99**			
Water(1) + ethanol(2) + [emim][Cl](3)				
Binary parameter	$l_{ij}^{(1)}$	$l_{ij}^{(2)}$	$l_{ji}^{(1)}$	$l_{ji}^{(2)}$
l_{12}	0	0	-0.2565	116.09
l_{13}	2.4909	-803.94	1.3671	-398.59
l_{23}	4.389	-1569	-1.7407	687.86
%ADD	**6.18**			

As observed in Table 3.12, when applying the temperature – dependent interaction parameters, the overall average deviations decrease especially for [emim][OAc] and [emim][Cl]. However, the use of these new parameters are not advantageous when it comes to [emim][DCA]. Figures 3.2 to 3.4 show the experimental ternary viscosities (points) and results of the regression (lines). Good agreement is observed between the experimental points and the Eyring-Patel-Teja model which is able to represent changes in viscosity with temperature and composition of these highly polar and aqueous systems. Therefore, this model can be used for the rate-based simulations.

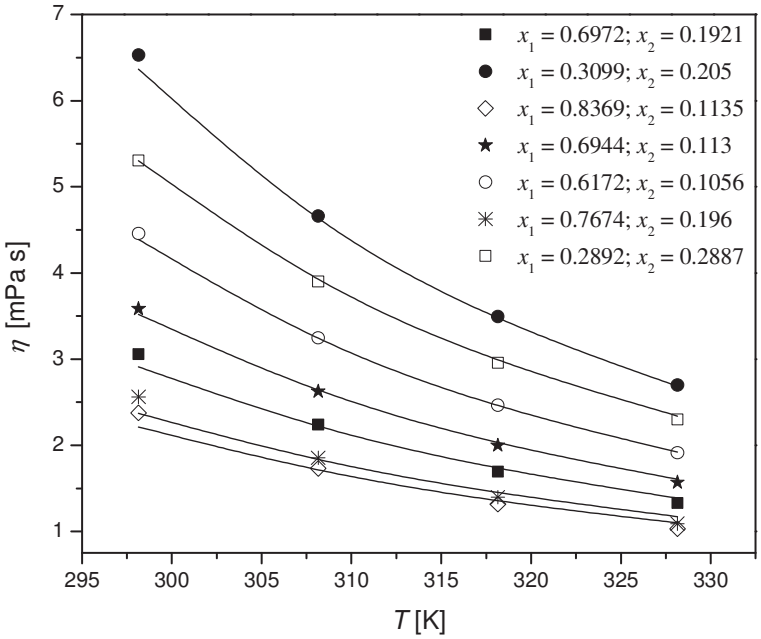

Figure 3.2. Correlation of the experimental ternary dynamic viscosities (symbols) with the Eyring-Patel-Teja model using the GM2 mixing rule (line) for the system (x_1 water + x_2 ethanol + 1-($x_1 + x_2$) EG).

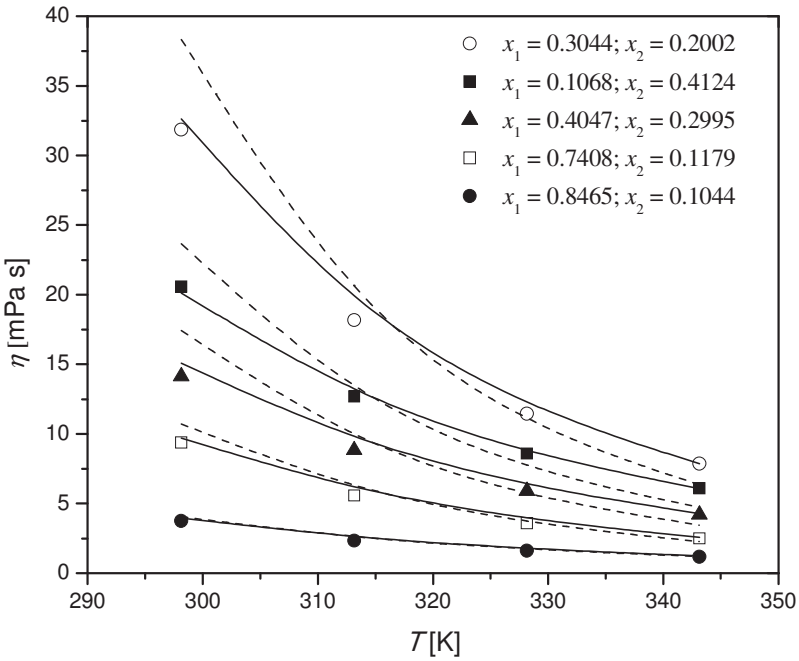

Figure 3.3. Correlation of the experimental ternary dynamic viscosities (symbols) with the Eyring-Patel-Teja model using the redlish-kister mixing rule and interaction parameters: (continuous line) temperature-dependent and (dashed line) temperature-independent, for the system (x_1 water + x_2 ethanol + 1-($x_1 + x_2$) [emim][OAc]).

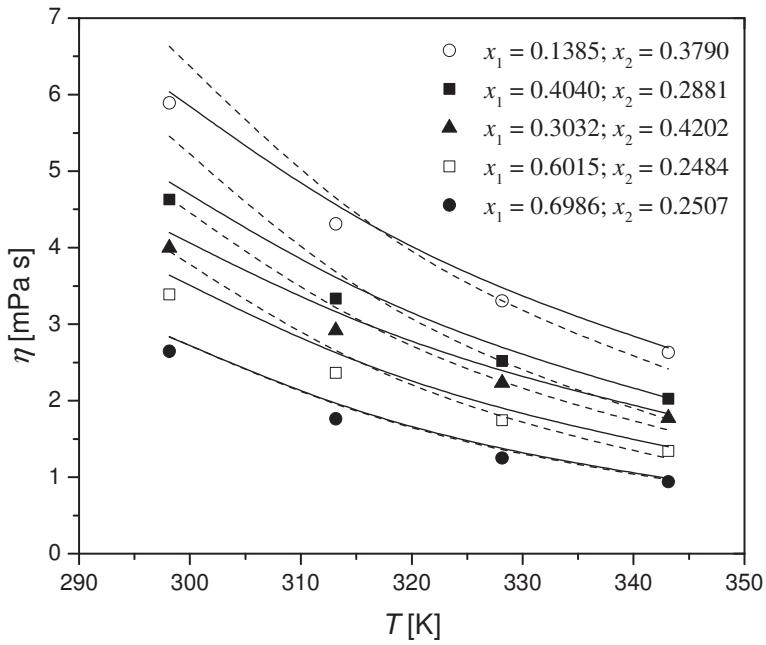

Figure 3.4. Correlation of the experimental ternary dynamic viscosities (symbols) with the Eyring-Patel-Teja model using the redlish-kister mixing rule and interaction parameters: (continuous line) temperature-dependent and (dashed line) temperature-independent, for the system (x_1 water + x_2 ethanol + 1-($x_1 + x_2$) [emim][DCA]).

3.3.4.3 Surface tension

The experimental surface tension data for the ternary system water – ethanol – solvent was correlated using the Fu-Li-Wang mixing rule [3] depicted in Chapter 2. Table 3.13 shows the obtained parameters and the overall average deviation from the experimental data that were found with the help of non-linear square method. In general, the regression of the ternary surface tension for the system water – ethanol – solvent shows excellent results considering that these are hydrogen-bonding systems. A larger average deviation is observed for the case of EG. Less experimental points were taken in this case due to the availability in literature of binary experimental data for the systems water – EG [12] and ethanol – EG [28] which were regressed along with these binary data. This is a source of

deviations. Therefore, The Li-Wang-Fu mixing rule can be used in the rate-based simulations to represent the changes in surface tension with composition in an extractive distillation column. And more importantly, the changes in interfacial area for mass transfer with surface tension.

Table 3.13. Binary parameters l_{ij} of the Fu-Li-Wang mixing rule .

	EG	[emim][OAc]	[emim][DCA]	[emim][Cl]
Binary parameter	value	value	value	value
l_{12}	22.84	29.0231	10.06	52.3295
l_{21}	0.04	0.0626	0.16	-2.4858
l_{13}	3.51	8.4685	20.43	8.6310
l_{31}	0.42	1.0605	0.13	0.0838
l_{23}	0.44	-0.2066	3.00	22.1832
l_{32}	2.81	2.4044	0.83	0.2095
%ADD	**6.91**	**3.27**	**2.87**	**3.51**

3.4 Conclusions

An experimental work was carried out in order to meet the requirements of the rate-based model to simulate the extractive distillation for water – ethanol separation with the ionic liquids 1-ethyl-3-methylimidazolium acetate [emim][Oac], 1-ethyl-3-methylimidazolium dicyanamide [emim][DCA] and 1-ethyl-3-methylimidazolium chloride [emim][Cl] and the reference solvent ethylene glycol EG.

The measured properties were liquid viscosity, infinite dilution diffusion coefficients and surface tension. Additionally, liquid density was measured to obtain dynamic viscosities instead of kinematics. All the measured data covers a wide range of temperature and concentration of binary and ternary mixtures. Surface tension was only measured at temperatures around $T = 298.15$ K.

Apart from that, all the pure and mixture data and the mixture data were correlated with available models from literature. Polynomials correlated pure densities and infinite dilution diffusion coefficients. The Vogel [1] equation described very well the viscosity of

all the solvents with temperature. In mixtures, a quadratic mixing rule [38] correlated very well liquid densities; liquid dynamic viscosities were correlated successfully with the Eyring-Patel-Teja [2] model using three different mixing rules with temperature-dependent interaction parameters. For for non-viscous solvent, temperature-independent parameters were enough. An finally, the mixture surface tensions was correlated very well using the Fu-Li-Wang mixing rule[3]. All this information can be used to develop a rate-based model to study the possible decrease in mass transfer efficiency with solvent viscosity.

Nomenclature

a, b	Constants
$Đ^{0}_{i,j}$	Infinite Dilution diffusion coefficient, m s^{-1}
C	Molar concentration, mol m^{-3}
K_{ij}	Interaction parameter in quadratic mixing rule
l	Binary parameter in mixing rules
$\bar{l}$	Averaged binary parameter, $\bar{l} = \left(l_{i,k} + l_{k,i}\right)/2$
T	Temperature, K
V^{l}	Liquid molar volume, cm^{3} mol^{-1}
x	Molar fraction of the liquid

Greek letters

γ	Any property in equation 3.6 and 3.7
η	Liquid viscosity, mPa s

Λ^0	Infinite dilution molar conductivity, m^2 S mol^{-1}
ρ	Mass density, g cm^{-3}
σ	Surface tension, nN m^{-1}
σ_{EC}	Electrical conductivity, S m^{-1}

Subscripts

i, j, k	Component indices
lit	Data obtained from literature
pred	predicted

Reference List

[1] D.S.Viswanath, N.V.K.Dutt, and K.R.Rani, Viscosity of liquids: theory, estimation, experiment, and data, Springer, Drodrecht, 2007.

[2] M.Lee, J.Chiu, S.Hwang, and H.Lin, Viscosity Calculations with Eyring-Patel-Teja Model for Liquid Mixtures, Ind. Eng. Chem. Res., 38 (1999) 2867-2876.

[3] J.Fu, B.Li, and Z.Wang, Estimation of Fluid-Fluid Interfacial Tensions of Multicomponent Mixtures, Chem. Eng. Sci., 41 (1986) 2673-2679.

[4] S.Fendt, S.Padmanabhan, H.W.Blanch, and J.M.Prausnitz, Viscosities of Acetate or Chloride-Based Ionic Liquids and Some of Their Mixtures with Water or Other Common Solvents, J. Chem. Eng. Data, 56 (2011) 31-34.

[5] M.G.Freire, A.R.R.Teles, M.A.A.Rocha, B.Schröder, C.M.S.S.Neves, P.J.Carvalho, D.V.Evtuguin, L.M.N.B.F.Santos, and J.A.P.Coutinho, Thermophysical Characterization of Ionic Liquids Able To Dissolve Biomass, J. Chem. Eng. Data, 56 (2011) 4813-4822.

[6] P.Benhôte, A.Dias, and N.Papageorgiou, Hydrophobic, Highly Conductive Ambient-Temperature Molten Salts, Inorg. Chem, 35 (1996) 1168-1178.

[7] C.Schreiner, S.Zugmann, R.Hartl, and H.J.Gores, Fractional Walden Rule for Ionic Liquids: Examples from Recent Measurements and a Critique of the So-Called Ideal KCl Line for the Walden Plot, J. Chem. Eng. Data, 55 (2010) 1784-1788.

[8] S.I.Fletcher, F.B.Sillars, N.E.Hudson, and P.J.Hall, Physical Properties of Selected Ionic Liquids for Use as Electrolytes and Other Industrial Applications, J. Chem. Eng. Data, 55 (2010) 778-782.

[9] A.P.Fröba, H.Kremer, and A.Leipertz, Density, Refractive Index, Interfacial Tension, and Viscosity of Ionic Liquids [EMIM][$EtSO_4$], [EMIM][NTf_2], [EMIM][$N(CN)_2$], and [OMA][NTf_2] in Dependence on Temperature at Atmospheric Pressure, J. Phys. Chem. B, 112 (2008) 12420-12430.

[10] T.Leong, I.Sun, M.Deng, and C.Wu, Electrochemical Study of Copper in the 1-Ethyl-3-Methylimidazolium Dicyanamide Room Temperature Ionic Liquid, J. Electrochem. Soc., 155 (2008) F55-F60.

[11] F.S.Jerome, J.T.Tseng, and L.T.Fan, Viscosities of Aqueous Glycol Solutions, J. Chem. Eng. Data, 13 (1968) 496.

[12] N.G.Tsierkesos and I.E.Molinou, Thermodynamic Properties of Water + Ethylene Glycol at 283.15, 293.15, 303.15 and 313.15 K, J. Chem. Eng. Data, 43 (1998) 989-993.

[13] C.Yang, P.Ma, F.Jing, and D.Tang, Excess Molar Volumes, Viscosities, and Heat Capacities for the Mixtures of Ethylene Glycol + Water from 273.15 K to 353.15 K, J. Chem. Eng. Data, 48 (2003) 836-840.

[14] T.Sun and A.S.Teja, Density, Viscosity, and Thermal Conductivity of Aqueous Ethylene, Diethylene, ans Triethylene Glycol Mixtures between 290 K and 450 K, J. Chem. Eng. Data, 48 (2003) 198-202.

[15] M.Dizechi and E.Marschall, Viscosity of Some Binary and Ternary Liquid Mixtures, J. Chem. Eng. Data, 27 (1982) 358-363.

[16] B.B.Gurung and M.N.Roy, Study of densities, viscosity deviations, and isentropic compressibilities of ternary liquid mixtures of water and ethane-1,2-diol with some monoalcohols at various temperatures, Phys. Chem. Liq., 45 (2007) 331-343.

[17] J.Klomfar, M.Soucková, and J.Pátek, Temperature Dependence of the Surface Tension and Density at 0.1 MPa for 1-Ethyl- and 1-Butyl-3-methylimidazolium Dicyanamide, J. Chem. Eng. Data, 56 (2011) 3454-3462.
[18] J.Jacquemin, P.Husson, A.A.H.Padua, and V.Majer, Density and viscosity of several pure and water-saturated ionic liquids, Green Chem., 8 (2006) 172-180.
[19] E.Gómez, B.González, N.Calvar, E.Tojo, and Á.Domínguez, Physical Properties of Pure 1-Ethyl-3-methylimidazolium Ethylsulfate and Its Binary Mixtures with Ethanol and Water at Several Temperatures, J. Chem. Eng. Data, 51 (2006) 2096-2102.
[20] M.B.Shiflett and A.Yokozeki, Phase Behavior of Carbon Dioxide in Ionic Liquids: [emim][Acetate], [emim][Trifluoroacetate], and [emim][Acetate] + [emim][Trifluoroacetate] Mixtures, J. Chem. Eng. Data, 54 (2009) 108-114.
[21] A.P.Fröba, M.H.Rausch, K.Krzeminski, D.Assenbaum, P.Wasserscheid, and A.Leipertz, Thermal Conductivity of Ionic liquids: Measurement and Prediction, Int. J. Thermophys., 31 (2010) 2059-2077.
[22] C.Wong, A.N.Soriano, and M.Li, Diffusion coefficients and molar conductivities in aqueous solutions of 1-ethyl-3-methylimidazolium-based ionic liquids, Fluid Phase Equilibr., 271 (2008) 43-52.
[23] B.González, N.Calvar, E.Gómez, and Á.Domínguez, Density, dynamic viscosity, and derived properties of binary mixtures of methanol or ethanol with water, ethyl acetate, and methyl acetate at T = (293.15, 298.15, and 303.15) K, J. Chem. Thermodyn., 39 (2007) 1578-1588.
[24] T.Singh, A.Kumar, M.Kaur, G.Kaur, and H.Kumar, Non-ideal behaviour of imidazolium based room temperature ionic liquids in ethylene glycol at T = (298.15 to 318.15) K, J. Chem. Thermodyn., 41 (2009) 717-723.
[25] L.Albuquerque, C.Ventura, and R.Gonçalves, Refractive Indices, Densities, and Excess Properties for Binary Mixtures Containing Methanol, Ethanol, 1,2 ethanediol and 2-Methoxyethanol, J. Chem. Eng. Data, 41 (1996) 685-688.
[26] E.Rilo, J.Pico, S.García-Garabal, L.M.Varela, and O.Cabeza, Density and surface tension in binary mixtures of CnMIM-BF_4 ionic liquids with water and ethanol, Fluid Phase Equilibr., 285 (2009) 83-89.
[27] G.Vázquez, E.Alvarez, and J.M.Navaza, Surface Tension of Alcohol + Water from 20 to 50 ºC, J. Chem. Eng. Data, 40 (1995) 614.
[28] S.Azizian and M.Hemmati, Surface Tension of binary Mixtures of Ethanol + Ethylene Glycol from 20 to 50 °C, J. Chem. Eng. Data, 48 (2003) 662-663.
[29] E.Andrade, Theory of Viscosity of Liquids, Philos. Mag., 17 (1934) 698-732.
[30] C.Wong, A.N.Soriano, and M.Li, Infinite dilution diffusion coefficients of [Bmim]-based ionic liquids in water and its molar conductivities, J. Taiwan Inst. Chem. E., 40 (2009) 77-83.
[31] W.Li, Z.Zhang, B.Han, S.Hu, Y.Xie, and G.Yang, Effect of Water and Organic Solvents on the Ionic Dissociation of Ionic Liquids, J. Phys. Chem. B, 111 (2007) 6452-6456.
[32] E.V.Anslyn and D.A.Dougherty, Modern Physical Organic Chemistry, University Science Books, Sausalito, California, 2005.
[33] A.K.Covington and T.Dickinson, Physical chemistry of organic solvent systems, Plenum Press, London, 1973.

[34] K.C.Pratt and W.A.Wakeham, The mutual diffusion coefficient of ethanol-water mixtures: determination by a rapid, new method, Proc. R. Soc. Lon. Ser-A, 336 (1974) 393-406.
[35] M.T.Tyn and W.F.Calus, Temperature and Concentration Dependence of Mutual diffusion Coefficients of Some Binary Liquids Systems, J. Chem. Eng. Data, 20 (1975) 310-316.
[36] C.H.Byers and C.J.King, Liuqid Diffusivities in the Glycol-Water System, J. Phys. Chem., 70 (1966) 2499-2503.
[37] T.Tominaga and S.Matsumoto, Diffusion of Polar and Nonpolar Molecules in Water and Ethanol, B. Chem. Soc. Jpn., 63 (1990) 533-537.
[38] B.E.Poling, J.M.Prausnitz, and J.P.O'Connell, The Properties of Gases and Liquids, McGraw-Hill, London, 2001.
[39] R.Belda, J.V.Herraez, and O.Diez, Rheological study and thermodynamic analysis of the binary system (water/ethanol): Influence of concentration, Phys. Chem. Liq., 42 (2004) 467-479.

4

Pilot plant validation of a rate-based extractive distillation model for water-ethanol separation with the ionic liquid [emim][DCA] as solvent

Abstract

With the objective of validating a developed rate-based model for the separation of water – ethanol mixtures by using 1-ethyl-3-methylimidazolium dicyanamide and ethylene glycol as solvents and investigating the effect of the solvent physical properties on mass transfer efficiency, an extractive distillation pilot-plant equipped with Mellapak® 750Y was constructed and operated in continuous mode. It was found that the rate-based model predicts the performance of this pilot plan very well for all the studied conditions within a 10% relative error. More optimistic water contents of the distillate stream were predicted and experimentally the ionic liquid produced lower water contents than ethylene glycol. The use of this ionic liquid provides higher mass transfer efficiencies for all the studied solvent-to-feed ratios. Finally, increasing the solvent-to-feed ratio enhances the mass transfer efficiencies for both solvents and effects of liquid viscosity decreasing the mass transfer efficiency are observed in the rectifying section of the extractive distillation column.

4.1 Introduction

The performance of an extractive distillation (ED) column can be predicted and the mass transfer efficiency calculated by the use of rate-based models [1,2]. For instance, the rate based model could evaluate the decrease in efficiency caused by the viscosity of ionic liquids by only knowing the physical and transport properties of the system studied. However, the predictive capabilities of this model depend on both the accuracy offered by the used mass transfer and interfacial area correlations and the accuracy of the provided physical properties. Since, ionic liquids exhibit higher viscosities than the normal organic solvents (typically up to 40 times higher at 298.15 K), the liquid side mass transfer resistance could become significant and the existing mass transfer correlations could fail in describing the performance of the ED column.

The aim of this work is to establish and validate a rate-based model that describes the separation of water – ethanol mixtures by means of ED using an ionic liquid as solvent and a common organic solvent with experimental data from a pilot scale ED column equipped with Mellapak® 750Y structured packing. Furthermore, the mass transfer efficiency of this ED column is studied by comparing the use of both solvents. The mass transfer is described by the Rocha et al. (1993,1996) [3,4] mass transfer correlation for a metal sheet structured packing. Among others, the ionic liquid 1-ethyl-3-methylimidazolium dicyanamide ([emim][DCA]) has been previously proposed as a promising solvent for this separation [5,6] and demonstrated to be thermally stable in pilot plant tests [7]. This ionic liquid is compared with the benchmark solvent ethylene glycol (EG) in terms of Height Equivalent to a Theoretical Plate (*HETP*). Other ionic liquids have been also proposed in literature [5,8] to separate this mixture. In these studies, 1-ethyl-3-methylimidazolium acetate ([emim][OAc]) appears as the most suitable. However, this ionic liquid is not thermally stable and thus not appropriate for this application.

Studies on extractive distillation in pilot plants are rather scarce [9-11] and mostly limited to the use of common organic solvents. To our knowledge, an industrial-scale study on an extractive distillation column to separate difluoromethane and pentafluoroethane operated with ionic liquids can be found in the open literature [12] where only the equilibrium stage model was used. Also, BASF is currently conducting research at pilot plant scale extractive distillation to separate azeotropes (water + tetrahydrofuran) using

ionic liquids [13]. Although, the separation of the water – ethanol mixture with ionic liquids have been already extensively studied and promoted at laboratory scale by means of VLE experiments [5,6,14,15], the performance of the reported ionic liquids in real distillation columns remains unknown. By carrying out experiments in a pilot plant it is possible to know to what extent the mass transfer correlations and thus the rate-based model are able to predict the performance of ionic liquids in the extractive distillation process. This is of great importance at high solvent-to-feed ratios where liquid viscosities increase and can become a limiting factor for mass transfer [9].

4.2 Pilot-scale extractive distillation column

4.2.1 Experimental features and dimensions

Figure 4.1 illustrates the extractive distillation column at Eindhoven University of Technology in The Netherlands. This column is equipped with Mellapak® 750Y structured packing provided by Sulzer® (Figure 4.2) and designed to operate in continuous mode. To prevent maldistribution, the column contains three liquid distributors. They were designed at the University of Dortmund [16]. These distributors uniformly spread the liquid over the packing segments and divide the column into three equal sections. An electrical thermosyphon reboiler provides energy for boiling up. During the experiments, the liquid level of this reboiler was controlled visually. At the top of the column, a vertical condenser with an internal funnel provides reflux, which is controlled by adjusting the distillate rate. Cooling water was used to condense the vapor. The cooling water flow rate was adjusted by a rotameter. Heat losses are prevented as to the maximum extend by a double layer of Armaflex HT® insulating material and an electrical tracing system. Four coriolis-type flow-meters are installed to ensure accurate flow measurements at the feed, solvent, bottoms and distillate streams. Secondly, to validate the model, six liquid circular collector basins are installed inside the packing segments to collect liquid samples. Along with this, the liquid temperature of the collected liquid is also measured at these points. Finally, a pressure drop sensor was installed to monitor the hydraulics. Figure 4.2 shows a packing segment containing a collector basin. Liquid samples can also be withdrawn at the distillate stream

and at the reboiler. A summary of the column dimensions is given in Table 4.1. All operating conditions were controlled and monitored by means of InTouch from Wundeware® control software. The graphic interface of the ED pilot plant was developed at the Eindhoven University of Technology.

Table 4.1. Column dimensions

Feature	Value
Packing type	Sulzer Mellapak® 750Y
Packing height [m]	3.120
Packing material	Stainless steel 316L
Column diameter [m]	0.049

4.2.2 Operating conditions

The pilot plant was operated in continuous supply of feed and solvent and continuous withdrawal of distillate and bottom product. Around 60 min were needed to achieve a constant temperature profile over the column that is considered the steady state. The pilot plant was operated at around 60-70% flooding, which was determined from Sulzer Sulcol® and ASPEN® Radfrac calculations. The F-Factor has a value of approximately 1. Two solvent-to-feed ratios, low and high, were used to demonstrate the ability of the rate-based model and therefore the mass transfer correlations to predict the performances of the ED pilot-plant for both solvents. Table 4.2 summarizes the main operating conditions that are kept fixed and the corresponding operating variables. Additionally, two distillate rates are used in these experiments to modify the compositions profiles

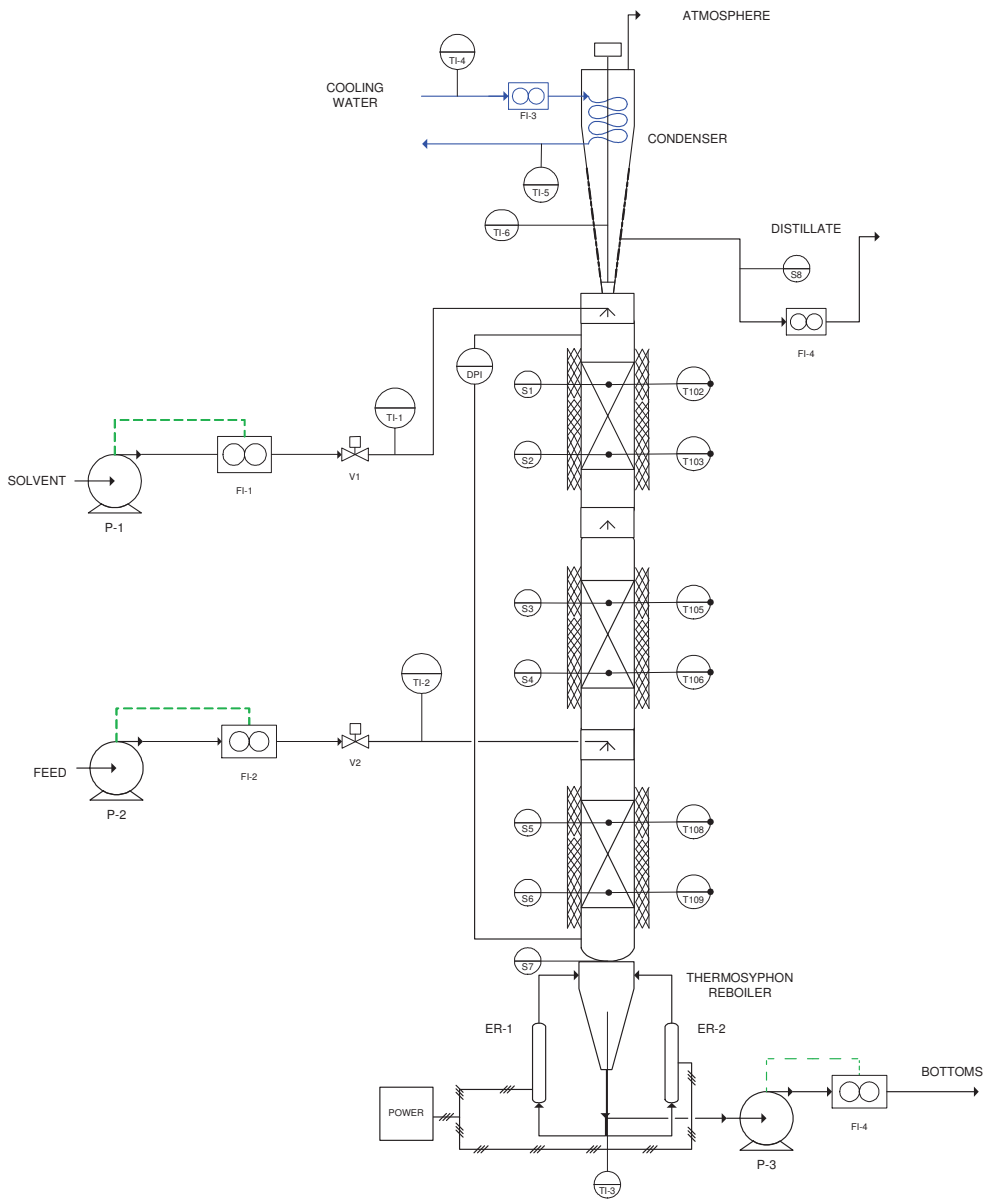

Figure 4.1. Simplified P&ID of the extractive distillation pilot plant located at Eindhoven University of Technology.

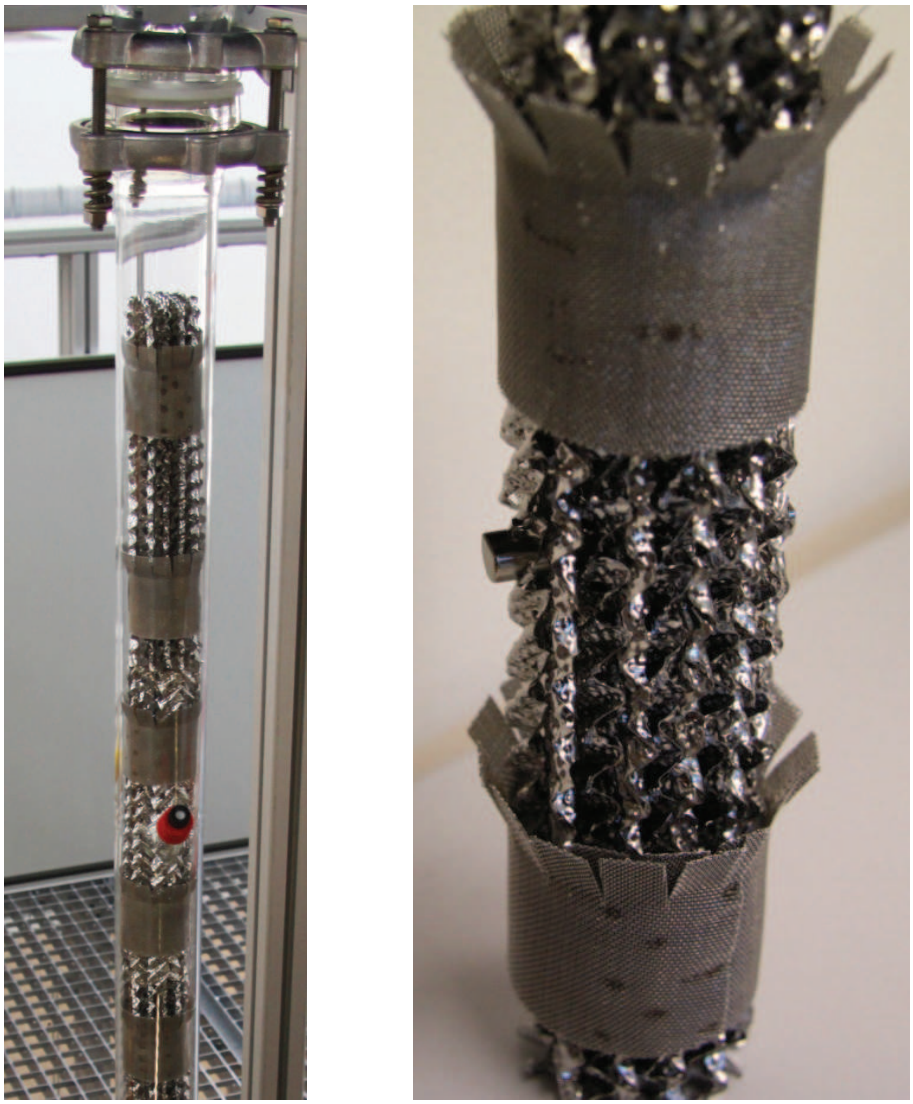

Figure 4.2. Mellapak® 750Y containing a liquid collector basin. Left: a view of a column section. Right: a packing segment with a collector basin.

.

Table 4.2. Operating conditions

Variable		Value
Feed flow rate [kg h^{-1}]		3
Ethanol concentration at feed [wt%]		30
Feed temperature [ºC]		50
Solvent temperature [ºC]		70
Reboiler duty [kW]		2.04
Condensor pressure		atmospheric
	S/F	*D* [kg h^{-1}]
Run 1	0.5	0.7
Run 2	2	0.7
Run 3	2	0.9

4.3 Experimental section

4.3.1 Materials

For the pilot plant tests, a purchased water – ethanol mixture at its azeotropic point (96% v/v) and deionized water were used to prepare the feed concentration. 1-ethyl-3-methylimidazolium dicyanamide was purchased at Ionic Liquid Technologies, Iolitec GmbH (≥ 98 %). The water content was 0.08 %. Ethylene glycol was purchased from Merck (≥ 99.5 %) with a water content of 0.04 %. 746 Karl Fisher analysis was used to determine water content. For the analysis of the liquid samples taken from the pilot plant, analytical grade chemicals were used. Ethanol was purchased from Merck (≥ 99.5 %) with a water content of 0.04 %. This ethanol was used without further purification. Ethylene glycol was purchased at Merck (≥ 99.8%) and a water content of 0.02 %. For the Gas Chromatography analysis analytical grade acetone (99.9 %.) as diluent and *n*-butanol (99.9 %) as internal standard were used.

4.3.2 Analysis of the samples taken from the pilot plant

After reaching steady state a small volume (~ 0.5 ml) of liquid sample was taken out of the collector basins with a syringe in order to not disturb the compositions profiles inside the column. Additionally, liquid samples were taken from the reboiler and condenser. These liquid samples were stored in GC vials and analyzed after allowing them to cool down to room temperature. To determine the ethanol content in the sample, Gas Chromatography analysis was used. 0.1 ml of sample was used. 0.1 ml of *n*-butanol was used as an internal standard and 1 ml of acetone as a diluent. The analyses of the samples were carried out with a Varian 430 gas chromatograph equipped with a Supelco Nukol® Fused silica capillary column (15 m x 0.53 mm x 0.5 µm). After sample injection, the ionic liquid is collected in a cup-liner in order to no disrupt the analysis [17,18]. The GC analyses were carried out in triplicate. A 746 Karl Fisher analysis was used to determine the water content of the liquid samples.

The reproducibility of the GC analysis is less than 2% and the accuracy is less than 5%. The reproducibility of the Karl Fisher analysis is less than 1% and the accuracy is less than 2%. The mass fraction of the ionic liquid was determined by a mass balance.

4.4 Set-up of the rate-based model

4.4.1 Property methods

The rate based model was firstly proposed by Krishnamurphy and Taylor [19,20]. Since then, it has been extensively studied due to the fact that it gives great accuracy in predicting performances. The rate-based model is available in ASPEN® Plus radfrac. This package is used to solve this case. Furthermore, this model needs the knowledge of physical and transport properties of both individual components and mixtures to accurately predict the separation process. The necessary physical and transport properties to accurately predict the performance of the pilot plant were studied extensively in chapters 2 and 3. Table 4.3 summarizes the property method used in these simulations.

Table 4.3. Property method in the liquid phase

Property	Method	Ref.
VLE	NRTL	[6]
Component and ternary liquid viscosities	Vogel, Eyring-Patel-Teja	[21,22]
Maxwell-Stefan Liquid binary diffusion coefficients	Nerst-Haskell, Wilke-Chang, Kooijmann-Taylor mixing rule	[23,24]
Component and mixture surface tensions	Polynomial[a], Fu-Li-Wang mixing rule	[21,25]
Component and mixture liquid densities	Polynomial[a], Quadratic mixing rule	[21]
Component and mixture liquid thermal conductivity	Polynomial[a], Li mixing rule	[26,27]
Component heat capacity	Polynomial[a,b]	[28]

[a] The polynomial and the corresponding parameters for EG obtained from Apen® Plus.
[b] Component heat capacity polynomial for [emim][DCA]: $Cp = 199743.8 + 427.5T$

4.4.2 Mass transfer and interfacial area correlations

Nowadays, mass transfer and interfacial area correlations to calculate binary mass transfer coefficients in either random or structured packings are widely available [29] even though they are still a matter of research due to the great variety of new structured packings. For metallic corrugated sheet packings like Mellapak® 750Y, Rocha et al [3,4] describes the mass transfer performance under distillation conditions. This correlation uses the previously developed interfacial area correlation of Shi and Mersmann [30] and contains the concepts of liquid holdup, liquid spreading and film thickness. Other correlations are available to describe metal sheet structured packing. The Rocha et al. mass transfer correlation is an improvement of the former Bravo et al. correlation [31] developed for gauze structured packings. Billet and Schultes [32,33] also developed a correlation that takes into consideration liquid holdup. However, this correlation requires packing related parameters that, to our knowledge, are not available for Mellapak® 750Y.

4.5 Results and Discussion

4.5.1 Experimental versus simulated composition and temperature profiles

Figures 4.3 and 4.4 show the experimental and predicted composition profiles for the separation of water – ethanol mixture with EG and [emim][DCA] as solvent respectively. Before going into the analysis, it is worth noting that these profiles are excluding the condenser and reboiler as these two stages are assumed to be in equilibrium because the ED pilot-plant provides vapor in equilibrium with the liquid at the reboiler and liquid in equilibrium with the vapor at the condenser. A discussion on reboiler efficiencies can be found elsewhere [34]. A visual observation of these figures indicates that the rigorous rate-based model with the Rocha et al. mass transfer correlation predicts the performance of the ED pilot plant with both [emim][DCA] and EG as solvents. Furthermore, the model is able to correctly represent the changes in solvent-to-feed ratio, which is the most important characteristic of the extractive distillation process. Some small deviations are observed in the stripping section when increasing the distillate rate. In this water-solvent rich zone the surface tension increases and the wetting of the packing surface becomes poorer resulting in less interfacial area for mass transfer. The use of accurate surface tensions allows both representing very well the changes in surface wetting and markedly improving the predictions of the experimental concentration and temperature profiles. For instance, a molar average can be used to predict the mixture surface tension instead in absence of experimental data. However, this was found to lead to large errors especially in the water rich zone. Figures 4.3 and 4.4 also show no large differences between the concentration profiles created by both solvents for both solvent-to-feed ratios and distillate rates. This is because of the differences in vapor-liquid equilibrium are not large as well.

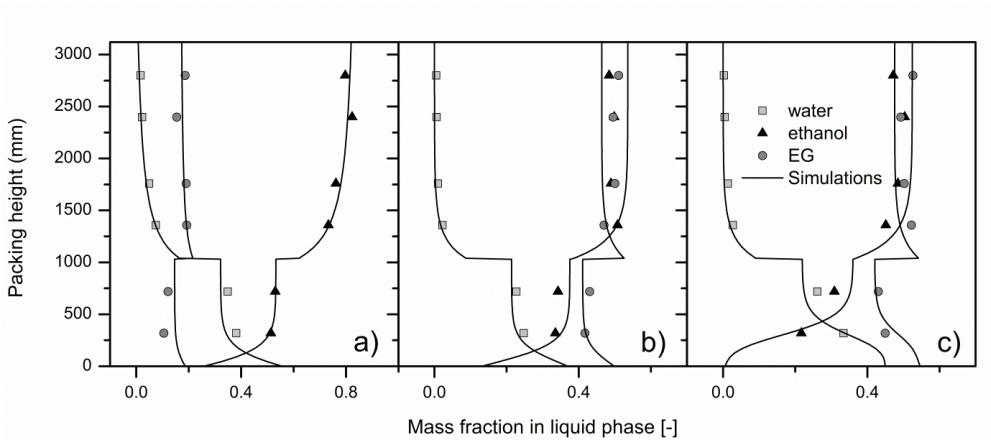

Figure 4.3. Experimental (points) and simulated (lines) composition profiles for a) *S/F* = 0.5 and *D* = 0.7 kg h^{-1}; b) *S/F* = 2 and *D* = 0.7 kg h^{-1} and c) *S/F* = 2 and *D* = 0.9 kg h^{-1} for the separation the water – ethanol mixture using EG as solvent.

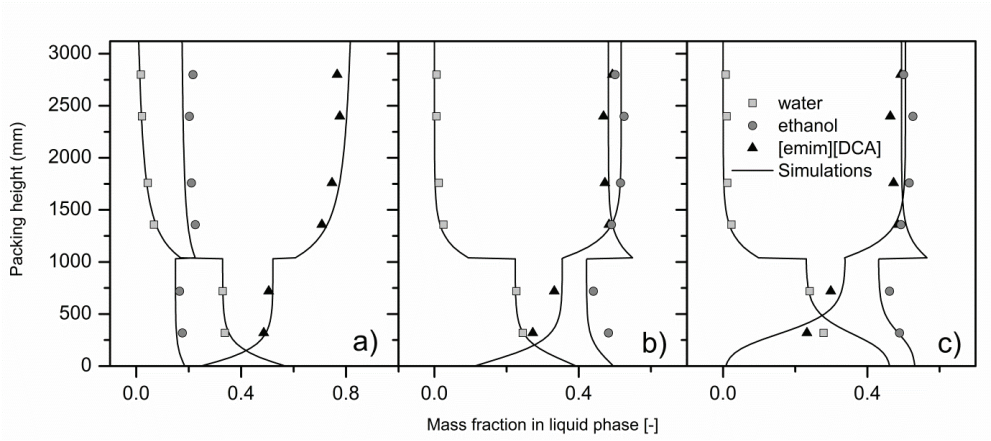

Figure 4.4. Experimental (points) and simulated (lines) composition profiles for a) *S/F* = 0.5 and *D* = 0.7 kg h^{-1}; b) *S/F* = 2 and *D* = 0.7 kg h^{-1} and c) *S/F* = 2 and *D* = 0.9 kg h^{-1} for the separation the water – ethanol mixture using [emim][DCA] as solvent.

Figures 4.5 and 4.6 depict the experimental and simulated temperature profiles generated when using EG and [emim][DCA] as solvent respectively. The rate-based model with the Rocha et al. mass transfer correlation shows very good predictions of these temperature profiles as well. This means that the model is able to predict both profiles at

low and high solvent-to-feed ratios for both solvents. When increasing the solvent-to-feed ratio (Figures 4.5.b and 4.6.b) the boiling temperature increases as well. Besides that, the separation of the water – ethanol mixture with EG produces higher temperatures due to the vaporization of this solvent. These facts are well predicted by the model. Secondly, although the rectifying section of the ED pilot plant does not have much variations and the model predicts this zone adequately, the stripping section does show large variations and is better to validate the ability of the rate-based model to predict performances (Figures 4.5.c and 4.6.c). The changes in temperature nearby the reboiler due to the increase in solvent concentration in all the studied cases are well predicted by the rate-based model, even when increasing the distillate rate. Here, the concentration of solvent increases at the reboiler leading to an increase in the liquid boiling point. For example, Figure 4.5.c shows a drastic step of 10 ºC in this section between the two experimental points that are well anticipated by the model.

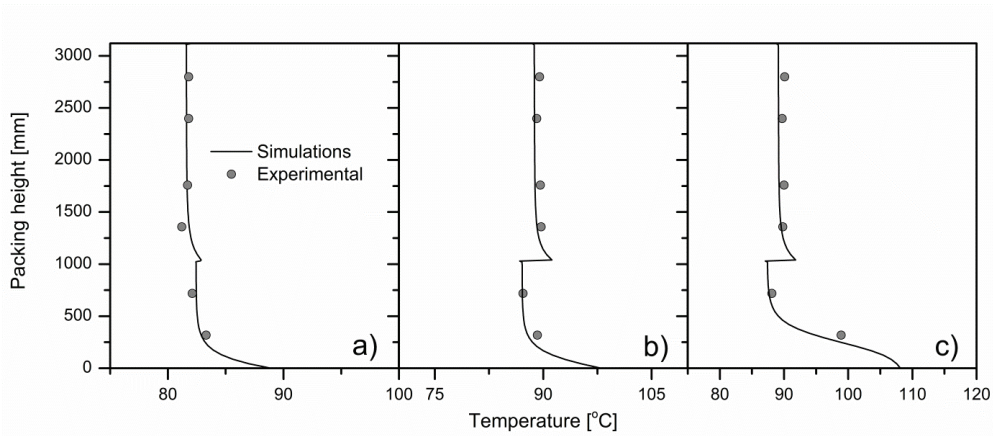

Figure 4.5. Experimental (points) and simulated (lines) temperature profiles of the liquid phase for a) *S/F* = 0.5 and *D* = 0.7 kg h^{-1}; b) *S/F* = 2 and *D* = 0.7 kg h^{-1} and c) *S/F* = 2 and *D* = 0.9 kg h^{-1} for the separation the water – ethanol mixture using EG as solvent.

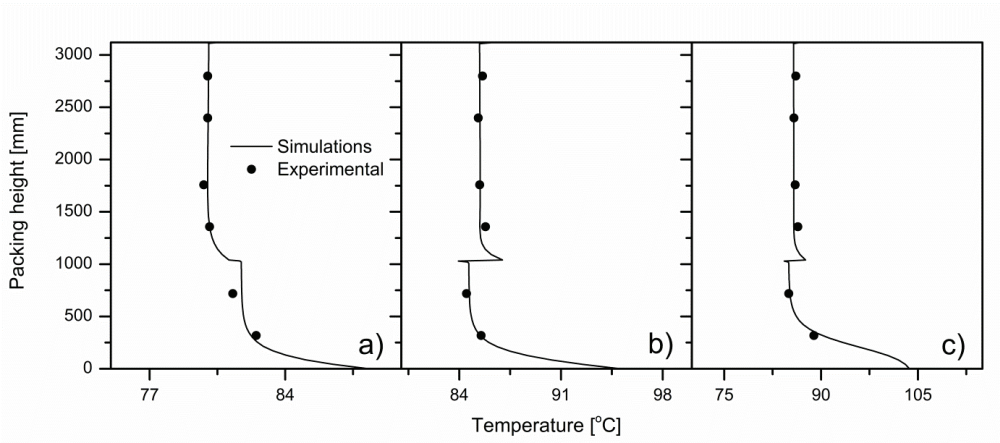

Figure 4.6. Experimental (points) and simulated (lines) temperature profiles of the liquid phase for a) *S/F* = 0.5 and *D* = 0.7 kg h^{-1}; b) *S/F* = 2 and *D* = 0.7 kg h^{-1} and c) *S/F* = 2 and *D* = 0.9 kg h^{-1} for the separation the water – ethanol mixture using [emim][DCA] as solvent.

To evaluate the quality of the predictions, Figure 4.7 shows parity plots of the simulated and experimentally obtained composition profiles with an arbitrary red dashed line that delimits a 10% relative error from the experimental data. These parity plots show that all the points fall around the diagonal line and they are randomly located over the diagonal. Tables 4.4.a and 4.4.b show the absolute deviations between experimental point and simulations for both mass fractions and temperatures respectively. It is important to say that the established rate-based model does not use simplifications such as those applied in equilibrium models and is therefore able to predict the performance of the pilot plant by only knowing the physical properties of the system in study.

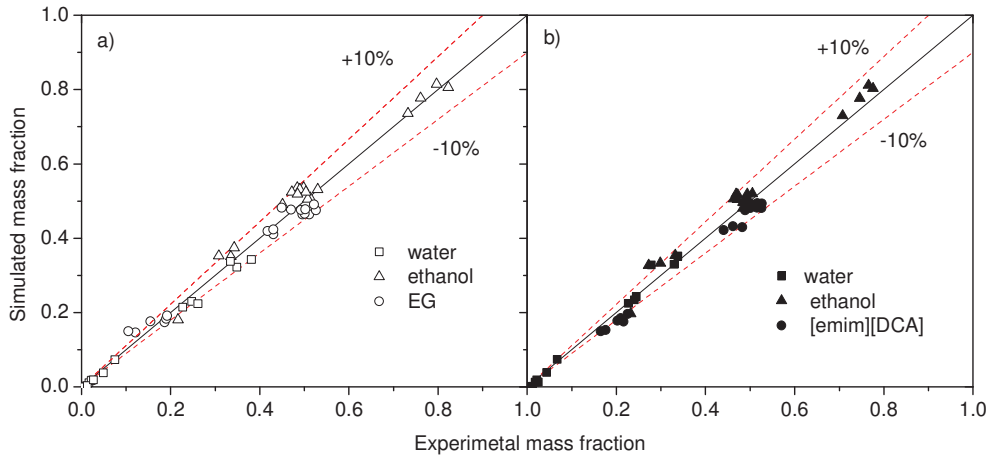

Figure 4.7. Comparison between experimental and predicted mass fractions for the system: a) water – ethanol – EG and b) water – ethanol – [emim][DCA].

Table 4.4.a. Maximum and minimum absolute deviations in composition between simulations and experimental data from the pilot plant.

EG		Maximum			Minimum		
S/F	*D* [kg h^{-1}]	water	ethanol	solvent	water	ethanol	solvent
0.5	0.7	0.0392	-0.0177	-0.0447	0.0019	-0.0015	0.0009
2	0.7	0.0181	-0.0520	0.0470	0.0050	0.0021	-0.0022
2	0.9	0.0373	-0.0525	0.0506	0.0019	-0.0206	0.0072
[emim][DCA]		Maximum			Minimum		
S/F	*D*[kg h^{-1}]	water	ethanol	solvent	water	ethanol	solvent
0.5	0.7	0.0153	0.0448	-0.0402	0.0002	0.0074	-0.0152
2	0.7	0.0103	-0.0491	0.0507	-0.0015	-0.0067	-0.0029
2	0.9	-0.0746	0.0710	0.0319	0.0025	0.0085	0.0036

Table 4.4.b. Maximum and minimum absolute deviations in temperature between simulations and experimental data from the pilot plant.

EG		Maximum	Minimum
S/F	*D* [kg h^{-1}]	*T* [ºC]	*T* [ºC]
0.5	0.7	1.458	0.043
2	0.7	1.331	0.088
2	0.9	4.019	0.256
[emim][DCA]		Maximum	Minimum
S/F	*D*[kg h^{-1}]	*T* [ºC]	*T* [ºC]
0.5	0.7	0.723	0.002
2	0.7	0.382	-0.039
2	0.9	-1.344	0.031

4.6 Experimental top purities

The most important variable to achieve in a distillation column is the top purity of the desired component. These experimental top purities are compared to the simulations in terms of the water content of the sample. Figure 4.8 shows the measured and predicted water contents in the distillate stream for all of the experimental runs. First of all, by using [emim][DCA] as solvent, the ED pilot plant is able to reduce the water content to lower levels than using EG as solvent. This is shown by the experimental data as well as simulations. Next, the simulations are able to predict well the water content of the distillate stream for each experimental run. The maximum absolute deviation between experiments and simulations are 0.0016 in the ED with EG as solvent and 0.0015 in the ED with [emim][DCA] as solvent. Furthermore, all the predictions are slightly more optimistic than the measured concentrations. Since the condenser is assumed to be in equilibrium, the accuracy of the model only depends on the vapor-liquid equilibrium model in this stage (NRTL). It means that, to obtain a better prediction in this zone, the VLE model should consider more experimental points to regress the binary parameters.

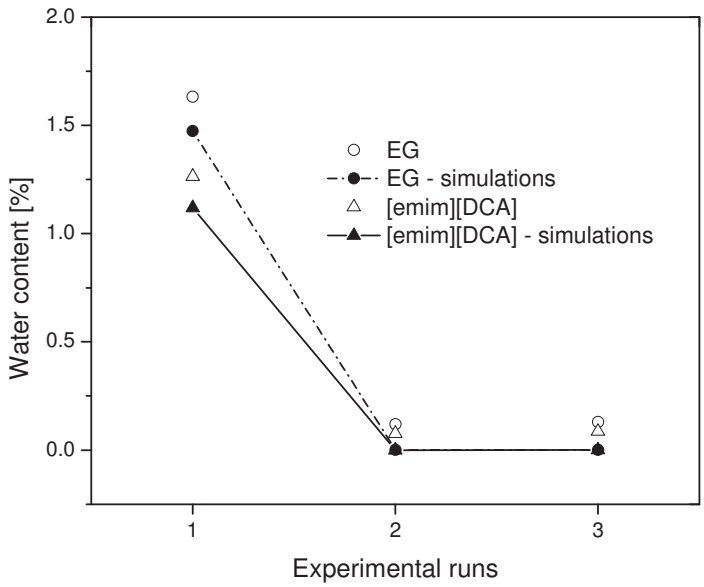

Figure 4.8. Experimental and predicted water content of the distillate rate for 1) *S/F* = 0.5, *D* = 0.7; 2) *S/F* = 2, *D* = 0.7 and 3) *S/F* = 2, *D* = 0.9.

4.7 Mass transfer efficiencies

The most important design parameter in distillation systems is the mass transfer efficiency. An erroneous prediction of this value brings problems like over or under design of distillation equipment or not meeting the desired top purity. In structured packing the mass transfer efficiency is quantified through the Height Equivalent to a Theoretical Plate, *HETP*. This value is calculated by the following set of equations:

$$HETP = H_{OV} \frac{\ln \Lambda}{\Lambda - 1} \qquad 4.1$$

$$H_{OV} = H_V + \Lambda H_L \qquad 4.2$$

$$\Lambda = \frac{KV}{L} \qquad 4.3$$

H_V and H_L are directly calculated by means of the Rocha et al. [3,4] mass transfer correlation. For a ternary system three values of H_{OV} are obtained since three Maxwell-Stefan binary diffusion coefficients are calculated. Besides that, three stripping factors Λ are obtained. This means that three values of *HETP* are calculated for a ternary mixture. In order to compare only one mass transfer efficiency value when using different solvents, the number of transfer units can be averaged, and:

$$H_{OV} = \frac{H}{N_{OV}} \qquad 4.4$$

$$\frac{1}{N_{OV}} = \frac{1}{N_V} + \frac{\Lambda}{N_L^{'}} \qquad 4.5$$

The mass transfer efficiency depends basically upon physical and transport properties, the distribution of the components between the two phases and packing features which do not change in this work. In this particular case, two solvents were used for the validation of the developed rate-based model: [emim][DCA] and benchmark solvent EG.

Figure 4.9 shows the *HETP* profiles over the column for both solvents at two different solvent-to-feed ratios. It can be clearly observed that these profiles are divided into two zones: the rectifying section where the solvent concentration is higher and therefore its effect on separation is stronger, and the stripping section where the solvent is diluted by the feed stream. For all the solvent-to-feed ratios and in the rectifying section the use of [emim][DCA] produces higher mass transfer efficiencies as compared to EG. These two solvents do not show large differences in transport properties, especially their viscosities are very similar (see Table 4.5). So, under these conditions, the observed differences in efficiency are caused by the differences in the vapor-liquid equilibrium. Table 4.5 depicts the relative volatilities of the water – ethanol mixture at different solvent-to-feed ratios. An obvious fact is that the more solvent is added the higher the relative volatilities. However, the largest differences are seen at high solvent-to-feed ratios where [emim][DCA] is a more advantageous solvent. This is observed at solvent-to-feed ratio 3 in Figure 4.9.

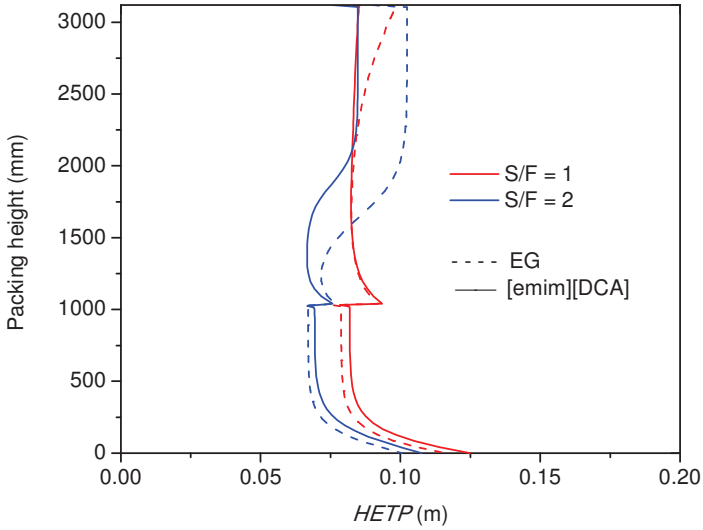

Figure 4.9. Efficiency profiles along the extractive distillation pilot plant containing both solvents.

Table 4.5. Pure viscosities of the used solvents and solvent-free-basis relative volatilities for the system water(1) – ethanol(2) – solvent(3) calculated at the water– ethanol azeotropic point.

Solvent	η [mPa s] (T = 298.15 K)		References
[emim][DCA]	14.90		[21]
EG	16.61		[22]
S/F	0	1	3
	α_{12}		
EG	1	1.835	2.727
[emim][DCA]	1	1.995	3.952

It is known that the solvent in extractive distillation interacts in the mixture by means of forming hydrogen bond networks mainly [35]. The ionic liquid strongly interacts with water and in a less extent with ethanol. This results in low distribution ratio values for water, K, increasing the relative volatility of the system along the column. EG also interacts with the mixture by hydrogen bonding. However, this interaction is weaker than using ionic liquid resulting in lower relative volatilities than those produced by [emim][DCA] in the rectifying section. In the stripping section EG produces slightly higher mass transfer efficiencies than those produced by [emim][DCA]. Due to this weak

interactions produced by EG in the mixture and the proximity to the reboiler, the ethanol concentration in the vapor phase is higher than the produced by the use of [emim][DCA] resulting in better relative volatilities and thus better mass transfer efficiencies.

On the other hands, since the viscosities of both systems are very similar, the effect of this property on mass transfer efficiency can be studied by increasing the solvent-to-feed ratio. Fig. 10 shows the *HETP* profiles along the column for solvent-to-feed ratios 1 and 3. Higher solvent-to-feed ratios are not possible to study since the experimental vapor-liquid equilibrium data is limited to a small range of solvent concentration [6] and a further increase could produce an erroneous prediction of the column performance due to the poor predictive capability of the NRTL model outside the experimental region. It is observed that, in general an increase in solvent-to-feed ratio lowers the *HETP* values for both solvents. Nevertheless, at the top of the column there is a decrease of mass transfer efficiency with increasing the solvent-to-feed ratio. This is more marked when using EG as solvent. This fact shows that at high solvent-to-feed ratios the resistance to mass transfer efficiency becomes more important. The rate-based model, without the help of previously defined efficiencies or methods to estimate these values is capable to predict a decrease in mass transfer efficiency with the solvent viscosity and could eventually predict any decrease of this important value when using a different potential ionic liquid to separate the water – ethanol mixture.

4.8 Conclusions

An extractive distillation pilot plant equipped with Mellapak® 750Y was constructed to validate a developed rate-based model for studying the performance of ethylene glycol and the 1-ethyl-3-methylimidazolium dicyanamide as solvents. The Rocha et al. [3,4] mass transfer correlation was implemented to describe the mass transfer performance in this structured packing.

When comparing the concentration profiles for both solvents and both distillate rates, no significant differences are observed. Differences are found in the temperature profiles over the column where the use of ethylene glycol as solvent produces higher liquid phase temperatures.

The rate-based model predicted the performance of the pilot plant for both solvent-to-feed ratios and distillate rates very well when only knowing the physical properties of the system under study, within a 10% deviation from the experimental data.

The water content of the distillate stream was measured. Lower water contents were obtained when 1-ethy-3-metyhylimidazolium was used as solvent for all the experimental conditions. More optimistic water contents were predicted by the developed model.

When predicting the mass transfer efficiency of the extractive distillation pilot plant for both solvents (EG and [emim][DCA]), the latter produces better mass transfer efficiencies for the studied range of solvent-to-feed ratios (S/F=1-3). In the rectifying section of the column and at high solvent-to-feed ratios, there is a slight effect of viscosity on mass transfer efficiency.

Nomenclature

C_P	Component heat capacity, J kmol^{-1} K^{-1}
D	Distillate rate, kg h^{-1}
$HETP$	Height equivalent to a theoretical plate, m
H_L	Height of transfer units in the liquid phase, m
H_V	Height of transfer units in the vapor phase, m
H_{OV}	Overall Height of transfer units, m
K	Distribution ratio
L	Liquid molar flow rate, kmol s^{-1}
$N_L^{'}$	Number of transfer units in the liquid phase
N_V	Number of transfer units in the vapor phase
N_{OV}	Overall number of transfer units

S/F	Solvent-to-feed ratio in mass basis
T	Temperature (K)

Greek letters

α_{12}	Relative volatility
η	Liquid dynamic viscosity (mPa s)
Λ	Stripping factor

Reference List

[1] R.Taylor and R.Krishna, Multicomponent Mass Transfer, Wiley, New York, 1993.
[2] H.A.Kooijman and R.Taylor, Modelling mass transfer in multicomponent distillation, Chem. Eng. J., 57 (1995) 177-188.
[3] J.A.Rocha, J.L.Bravo, and J.R.Fair, Distillation Columns Containing Strictured Packings: A Comprehensive Model for Their Performance. 2. Mass-Tranfer Model, Ind. Eng. Chem. Res., 35 (1996) 1660-1667.
[4] J.A.Rocha, J.L.Bravo, and J.R.Fair, Distillation Columns Containing Structured Packings: A Comprehensive Model for Their Performance. 1. Hydraulic Models, Ind. Eng. Chem. Res., 1993 (1993) 641-651.
[5] Y.Ge, L.Zhang, X.Yuan, W.Geng, and J.Ji, Selection of ionic liquids as entrainers for separation of (water + ethanol), J. Chem. Thermodyn., 40 (2008) 1248-1252.
[6] A.V.Orchillés, P.J.Miguel, F.J.Llopis, E.Vercher, and A.Martínez-Andreu, Isobaric Vapor-Liquid Equilibria for the Extractive Distillation of Ethanol + Water Mixtures Using 1-Ethyl-3-methylimidazolium Dicyanamide, J. Chem. Eng. Data, 56 (2011) 4875-4880.
[7] G.W.Meindersma, E.Quijada-Maldonado, T.A.M.Aelmans, J.P.Gutierrez, and A.B.de Haan, Ionic Liquids in Extractive Distillation of Ethanol/Water: From Laboratory to Pilot Plant, in: A.E.Visser, N.J.Bridges, and R.D.Rogers (Eds.), Ionic liquids: Science and Applications, ACS Symposium Series, 2012, pp. 239-257.
[8] Z.Lei, B.Chen, and C.Li, COSMO-RS modeling on the extraction of stimulant drugs from urine sample by the double actions of supercritical carbon dioxide and ionic liquid, Chem. Eng. Sci., 62 (2007) 3940-3950.
[9] S.Weiss and R.Arlt, On the Modelling of Mass Transfer in Extractive Distillation, Chem. Eng. Process., 21 (1987) 107-113.
[10] S.Kumar, J.D.Wright, and P.A.Taylor, Modelling and Dynamics of an Extractive Distillation column, Can. J. Chem. Eng., 62 (1984) 780-789.
[11] J.M.Resa, C.González, and A.Ruiz, Experiments of extractive distillation at laboratory scale for the rupture of the azeotropic mixture acetone + isopropyl ether, Sep. Purif. Technol., 18 (2000) 103-110.
[12] M.B.Shiflett and A.Yokozeki, Separation of difluoromethane and pentafluoroethane by extractive distillation using ionic liquid, Chemistry Today, 24 (2006) 28-30.
[13] K.Massonne, Ionic Liquids at BASF SE, (2010), http://wet.kuleuven.be/english/summerschools/ionicliquids/lectures/massonne.pdf.
[14] J.Zhao, C.Dong, C.Li, H.Meng, and Z.Wang, Isobaric vapor-liquid equilibria for ethanol-water system containing different ionic liquids at atmospheric pressure, Fluid Phase Equilibr., 242 (2006) 147-153.
[15] N.Calvar, B.González, E.Gómez, and .Domínguez, Vapor-Liquid Equilibria for Ternary System ethanol + Water + 1-Ethyl-3-methylimidazolium Ethylsulfate and the Corresponding binary System Containing the Ionic Liquid at 101.3 kPa, J. Chem. Eng. Data, 2008 (2008) 820-825.
[16] T.Keller, J.Holtbruegge, and A.Górak, Transesterification of dimethyl carbonate with ethanol in a pilot-scale reactive distillation column, Chem. Eng. J., 180 (2012) 309-322.
[17] M.T.G.Jongmans, B.Schuur, and A.B.de Haan, Binary and ternary LLE data of the system (ethylbenzene + styrene + 1-ethyl-3-methylimidazolium thyocyanate) and

binary VLE data of the system (styrene + 1-ethyl-3-methylimidazolium thiocyanate), J. Chem. Thermodyn., 47 (2012) 234-240.
[18] J.P.Gutierrez, W.Meindersma, and A.B.de Haan, Binary and ternary (liquid + liquid) equlibrium for {methylcyclohexane (1) + toluene (2) + 1-1hexyl-3-3methylimidazolium tetracyanoborate (3)/1-butyl-3-methilimidazolium tetracyanoborate (3)}, J. Chem. Thermodyn., 43 (2011) 1672-1677.
[19] R.Krishnamurthy and R.Taylor, A Nonequilibrium Stage Model of Multicomponent Separation Processes Part I: Model Description and Method of Solution, AIChE J., 31 (1985) 449-456.
[20] R.Krishnamurthy and R.Taylor, A Nonequlibrium Stage Model of Multicomponent Separation Processes Part II: Comparison with Experiment, AIChE J., 31 (1985) 456-465.
[21] E.Quijada-Maldonado, S.van der Boogaart, J.H.Lijbers, G.W.Meindersma, and A.B.de Haan, Experimental densities, dynamic viscosities and surface tensions of the ionic liquids series 1-ethyl-3-methylimidazolium acetate and dicyabamide and their binary and ternary mixtures with water and ethanol at T = (298.15 to 343.15) K, J. Chem. Thermodyn., 51 (2012) 51-58.
[22] E.Quijada-Maldonado, G.W.Meindersma, and A.B.de Haan, Viscosity and density data for the ternary system water(1) - ethanol(2) - ethylene glycol(3) between 298.15 and 328.15K, J. Chem. Thermodyn., 57 (2013) 500-505.
[23] C.Wong, A.N.Soriano, and M.Li, Diffusion coefficients and molar conductivities in aqueous solutions of 1-ethyl-3-methylimidazolium-based ionic liquids, Fluid Phase Equilibr., 271 (2008) 43-52.
[24] H.A.Kooijman and R.Taylor, Estimation of diffusion coefficients in multicomponent liquid system, Ind. Eng. Chem. Res., 30 (1991) 1217-1222.
[25] J.Fu, B.Li, and Z.Wang, Estimation of Fluid-Fluid Interfacial Tensions of Multicomponent Mixtures, Chem. Eng. Sci., 41 (1986) 2673-2679.
[26] A.P.Fröba, M.H.Rausch, K.Krzeminski, D.Assenbaum, P.Wasserscheid, and A.Leipertz, Thermal Conductivity of Ionic liquids: Measurement and Prediction, Int. J. Thermophys., 31 (2010) 2059-2077.
[27] C.C.Li, Thermal Conductivity of Liquid Mixtures, AIChE J., 22 (1976) 927-930.
[28] J.P.Gutierrez, Extractive distillation with ionic liquids as solvents: Selection and conceptual process design, Thesis/Dissertation, Eindhoven University of Technology, (2013).
[29] G.Q.Wang, X.G.Yuan, and T.Yu, Review of Mass-Tranfer Correlations for Packed Columns, Ind. Eng. Chem. Res., 44 (2005) 8715-8729.
[30] H.G.Shi and A.Mersmann, Effective Interfacial Area in Packed Columns, Ger. Chem. Eng., 8 (1985) 87-96.
[31] J.L.Bravo, J.A.Rocha, and J.R.Fair, Mass Tranfer in Gauze Packings, Hydrocarbon Process., 64 (1985) 91-95.
[32] R.Billet and M.Schultes, Predicting Mass Transfer in Packed Columns, Chem. Eng. Technol., 16 (1993) 1-9.
[33] R.Billet and M.Schultes, Prediction of Mass Tranfer Columns with Dumped and Arranged Packings: Updated Summary of the Calculations Method of Billet and Schultes, Chem. Eng. Res. Des., 77 (1999) 498-504.
[34] B.M.Jacimovic, S.B.Genic, and N.B.Jacimovic, Reboiler Separation Efficiencies for Binary Systems, Ind. Eng. Chem. Res., 51 (2012) 5793-5804.

[35] R.F.Strigle Jr., Packed Tower Design and Applications. Random and Structured Packings, Gulf, Houston, Texas., 1994.

5

Systematic analysis of ionic liquid effects on mass transfer efficiency in extractive distillation of water – ethanol mixtures

Abstract

The relatively high viscosities of ionic liquids used in extractive distillation could reduce the mass transfer efficiency of the separation process. To analyse this fact, the rate-based model is adopted since it was demonstrated that it can predict the performance of a pilot plant scale extractive distillation column using ionic liquids as solvent. Three ionic liquids with a wide range of dynamic viscosities and a commonly used organic solvent were used to study the effect of this property on mass transfer efficiency. The results were discussed using sieve trays and Mellapak® 250Y structured packing whose mass transfer characteristics are well described by known mass transfer correlations. Results indicate that high viscosities affect the mass transfer efficiency of the extractive distillation column. However, the remarkable improvements in relative volatilities shown by ionic liquids help to overcome this decrease in mass transfer efficiency. These effects are more pronounced in Mellapak® 250Y. However, very high solvent viscosities (>65[mPa s] at T = 353.15K) produce mass transfer limitations that cannot be overcome by high relative volatilities. Additionally, at higher distillate rates high relative volatilities can yield negative effects in mass transfer efficiency.

5.1 Introduction

It is recognized that increased viscosity of a solvent in ED lowers the mass transfer efficiency of the process. This is a very important parameter in the design of the a ED column because a lower efficiency leads to a higher number of separation stages in tray columns and larger *HETP* values in packed columns to achieve a required separation. This problem becomes more important when applying ionic liquids as solvents in ED whose viscosities can range from 2 up to 20 times higher compared to common organic solvents. Several studies have pointed out the high viscosity of ionic liquids as a reason to discard promising ionic liquids in spite of their excellent vapor – liquid equilibrium performance [1]. Two phenomena could reduce this "fear":

1. The solvent is dissolved in the mixture to be separated, which strongly decreases the solvent viscosity [2-4].
2. The high temperatures inside the ED column considerably lower the viscosity of ionic liquids [2].

However, the knowledge about effect of the solvent viscosity on mass transfer efficiency in distillation is fairly limited [5] and it is not studied yet for extractive distillation with ionic liquids. Even for regular solvents, only a few studies have related the effect of viscosity on mass transfer efficiency in distillation columns [6,7].

The objective of this chapter is to study the effect of the solvent viscosity on the mass transfer efficiency of the ED process for the water – ethanol mixture using several ionic liquids and the commonly used organic solvent ethylene glycol (EG) by means of a rigorous rate-based mass transfer model. In the previous chapter it was demonstrated that the developed rated-based model to describe this separation using 1-ethyl-3-methylimidazolium dicyanamide, [emim][DCA] was able to predict the performance of an extractive distillation pilot plant while only knowing the physical, transport and vapor-liquid equilibrium (VLE) properties of the system. Therefore, this model allows the analysis of a possible decrease in mass transfer efficiency with solvent viscosity. On the other hand, the use of various ionic liquid allows to study a wide range of solvent viscosities and relative volatilities. Therefore, the combined effect of viscosity and relative

volatility on mass transfer efficiency is studied. Additionally, the mass transfer efficiency of sieve trays and Mellapak® 250Y structured packing are compared and two solvent-to-feed ratios evaluated to increase the liquid phase viscosities inside the ED column as this is the most important operating variable when higher purities are desired.

5.2 Case study

Table 5.1 shows the change in relative volatility of the water – ethanol mixture at two different solvent-to-feed ratios (S/F) calculated at the azeotropic point with the NRTL model. From this table it is observed that at both S/F ratios the order is [emim][Cl] > [emim][OAc] > [emim][DCA] > [EG]. Eventually, the best candidate to be chosen as a solvent would be [emim][Cl] due to the highest achieved relative volatilities followed by [emim][OAc]. Table 5.1 also lists the viscosities of the solvent at T = 298.15 K and 353 K. Especially for [emim][Cl] relatively high values are observed that could limit the mass transport. However, a second important characteristic mentioned in the introduction, is that at higher temperatures a drastic viscosity decrease is observed. For these conditions the real decrease in mass transfer efficiency needs to be analyzed.

Table 5.1. Relative volatilities at different S/F ratios (mass basis) for different solvents calculated at the water - ethanol azeotropic point and pure solvent viscosities at T = 298.15 and 353.15 K

	α			η [mPa s]		
Solvent	S/F =1	S/F = 2	Ref.	T = 298.15 K	T = 353.15 K	Ref.
[emim][Cl]	2.62	3.98	[1]	2597.69[a]	65.18	[8]
[emim][OAc]	2.24	2.92	[1]	132.91	13.60	[2]
[emim][DCA]	1.89	2.58	[1]	14.90	4.66	[2]
EG	1.83	2.41	Aspen®	16.61	3.14	[9]

[a] Extrapolated viscosity from three experimental data points.

The study of mass transfer efficiency comprises the analysis of the overall number of transfer units for trays and the overall height of transfer units for packing:

$$E_{OV} = \exp(-N_{OV}) \quad 5.1$$

$$HETP = H_{OV}\frac{\ln(\Lambda)}{\Lambda - 1} \quad 5.2$$

$$\frac{1}{N_{OV}} = \frac{1}{N_V} + \frac{\Lambda}{N_L^{'}} \quad 5.3$$

$$H_{OV} = H_V + \Lambda H_L \quad 5.4$$

Equations 5.1 to 5.4 describe the change in efficiency with physical properties, vapor-liquid equilibrium and the column internals. These equations are used to compare the mass transfer efficiency performance of the different solvents studied in this work. The number of transfer units and the height of transfer units preset in equation 5.1 to 5.4 are calculated using the mass transfer correlation presented in chapter 2. The distribution ratio is calculated using the NRTL model [1]. In a ternary system, three mass transfer efficiencies are obtained since there are three Maxwell-Stefan binary diffusion coefficients. To compare the effect of the solvents on the separation it is necessary to use only an efficiency. This is obtained by averaging the mass transfer efficiencies as follows:

$$E_{OV} = \left(E_{OV1} \times E_{OV2} \times E_{OV3}\right)^{1/n} \quad 5.5$$

and for the packed column:

$$N_{OV} = \frac{\left(N_{OV1} + N_{OV2} + N_{OV3}\right)}{n} \quad 5.6$$

where

$$H_{OV} = \frac{H_P}{N_{OV}} \quad 5.7$$

5.3 Simulation setup

ASPEN Plus® radfrac with the rate-sep package enables the use of the rate-based model to evaluate the effect of the solvent on the mass transfer efficiency in the ED process. This model needs physical and transport properties of both pure components and the ternary mixture water – ethanol – solvent. The physical and transport properties and the used models to correlate these data for the four systems in this study were presented in chapter 2 and 3. To select the process parameters some simple criteria have been taken into account. In order to compare solvents the process parameters are the same for all the solvents and internals.

The most important process parameter to study a possible decrease in mass transfer efficiency by the effect of liquid phase viscosity is the S/F ratio. Two S/F ratios are used to increase the liquid phase viscosity in the column and also to increase the effect of the solvent on the separation [1]. Additionally, the effect of the vapor-liquid ratio on mass transfer efficiency is analyzed since this property strongly depends on the vapor-liquid equilibrium performance provided by the solvent. Ionic liquids show improvements in relative volatility with regard to the common organic solvents as it was observed in Table 5.1. These improvements lead to a different vapor-liquid ratio inside the ED column. This could have an impact on mass transfer efficiency. Therefore, two distillate-to-feed ratios (D/F) are selected.

The other process parameters are the feed flow rate, feed concentration, feed temperature and the reflux ratio. The first of these parameters is the feed flow rate which should allow to use a relatively small diameter to assume that the liquid on the tray is completely mixed in the horizontal direction and thus tray efficiency is the same as point efficiency [10,11]. The feed concentration also plays an important role in this study: the ethanol concentration was set at 50% (w/w). A lower concentration of ethanol would produce entrainment of the liquid from a tray to an upper one [12]. Entrainment decreases the mass transfer efficiency of a distillation column [10]. Next, the feed and solvent temperatures are not important parameters in mass transfer efficiency. However, not any temperature can be used and they should be close to the temperatures inside the ED

column. Finally the reflux ratio was set at a fix number. Table 5.2 resumes the process parameters.

Sieve trays and Mellapak® 250Y are the selected internals for this study. The chosen flow models for them are plug flow and countercurrent respectively. Table 5.3 summarizes the features of these internals that were taken on the basis to decrease to the maximum extent the effect of other variables on mass transfer efficiency. In trays, the tray spacing is high enough to avoid liquid entrainment and the tray layout (weir height, hole diameter) avoids the possibility of having weeping. These two phenomena: liquid entrainment and weeping are well documented elsewhere [10] to decrease the mass transfer efficiency. The rest of the parameters like deck thickness, number of liquid passes and the hole area-to-active area ratio were default values in ASPEN® Plus.

The feed stage was put in the middle. To set the packing height in the packed column which is related somehow to the number of stages in the tray column we appeal to the following relationship [13]:

$$H_P = (HETP) N_{real} E_O \qquad 5.5$$

Equation 5.5 relates the number of real stages in a tray column with the height of a packed column through the *HETP* and the section efficiency, E_O. To our knowledge, values of section efficiency or murphree tray efficiency for ED of water – ethanol mixtures with EG or another organic solvent cannot be found in open literature. However, section efficiency values can be found in the literature for the distillation of water – ethanol mixtures in a plate column [12] where the value of section efficiency is approximately 70%. Next, the *HETP* number can also be obtained from a Sulzer® brochure [14]. Thus, the *HETP* for Mellapak® 250Y is approximately 0.4 m. Therefore, the packing height used in this work is 5.6 m that will be approximated to 6 m. Finally, the flow rates in the sieve tray column and packed column were set at 70% of the flooding flow rates for all the solvents. A summary is given in Table 5.3.

Table 5.2. Operating conditions

Variable	Value
Feed flow rate [kg h^{-1}]	100
Ethanol concentration at feed [wt%]	50
Feed temperature [ºC]	70
Solvent temperature [ºC]	70
Distillate-to-feed ratio (mass)	0.4 and 0.5
Solvent-to-feed ratio (mass)	1 and 2
Reflux ratio	2
Condenser pressure	Atmospheric

Table 5.3. Used column internal characteristics in the simulations for 100 kg/h of mixture and 50% wt ethanol as a base flow and feeding concentration respectively

Sieve Tray	
Parameter	**Value**
Tray spacing (m)	0.5
Number of stages (real stages including reboiler and condenser)	22
Feed tray	12
Weir heights (m)	0.05
Hole diameter (m)	0.005
Deck thickness	10 gauge
Number of passes	1
Pitch	Triangular
Hole area/active area	0.12
Flooding	70%
Mellapak® 205Y structured packing	
Parameter	**Value**
Packing height (m)	6
Feed point (m)	3
Packing material	Stainless steal
Flooding	70%

5.4 Results

5.4.1 Sieve tray column

First of all, the viscosity profiles for all the solvents over the column height are shown in Figure 5.1 at two S/F ratios. The region above tray 12 is the rectifying section (left side), and below it is the stripping section (right side). In the rectifying section the solvent concentration is higher than in the stripping section. Therefore, higher liquid phase viscosities are encountered. However, a higher concentration of the solvent allows a better separation effect as well. Figure 5.1.a clearly shows the effect of the pure solvent viscosity (see table 5.1) on the resulting liquid phase viscosities inside the column. The viscosity order in this zone being: [emim][Cl] > [emim][OAc] > [emim][DCA] > EG. In the stripping section the liquid viscosity drops for all four solvents as the solvent concentration is reduced by dilution with the feed stream. All the liquid phase viscosities in this zone are comparable with each other having a value around 1 [mPa s]. When increasing the S/F ratio to 2, (figure 5.1.b) the profiles show an obvious rise in liquid phase viscosity again following the order of the pure solvent viscosities. In Figures 5.1a and 5.1b it is observed that at these S/F ratios the liquid phase viscosities are not as high as could be expected because of the high temperatures inside the ED column and the dilution of the solvent in the water – ethanol mixture.

The effect of the liquid phase viscosities on the mass transfer coefficients is shown in figure 5.2 for both S/F ratios. In Figure 5.2.a it is observed that the value of these coefficients follow the same order as the liquid phase viscosity inside the column indicating that there is an effect of the solvent viscosity on mass transfer. In the stripping section EG shows significantly higher mass transfer efficiency values than the ionic liquids who show similar values to each other. This is due to the higher temperatures nearby the reboiler produced by the evaporation of EG. These higher temperatures are because of the lower water content when using EG than the column containing an ionic liquid increasing the boiling temperature. When using ionic liquids as solvent more water is extracted due to the hydrophilic behavior of the presented ionic liquids. To show more clearly the effect of viscosity on mass transfer, the S/F ratio is increased. Figure 5.2.b confirms an overall decrease of all the mass transfer coefficient profiles by the increased liquid phase

viscosities. However, the differences between the two S/F ratios are limited because an increase in the solvent concentration leads to an increase in the boiling point of the mixture and thus the temperature profiles. The higher the temperature the lower the liquid phase viscosity and the less resistance to mass transfer.

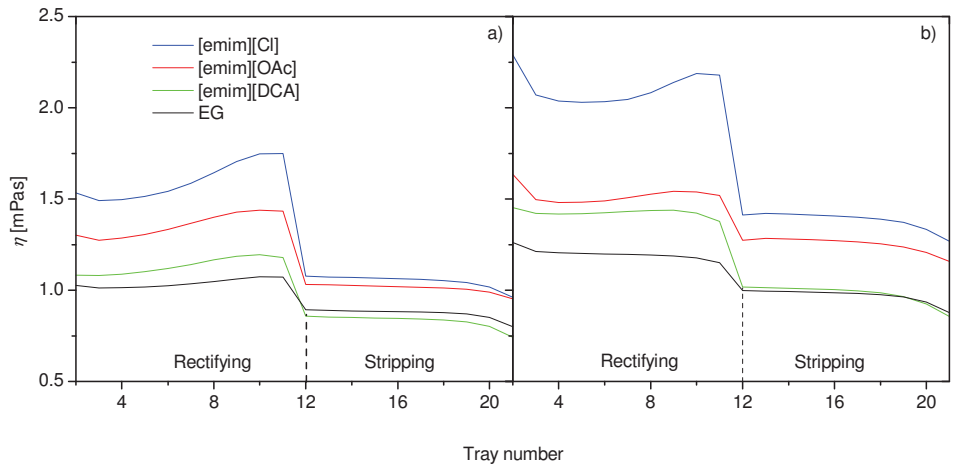

Figure 5.1. Viscosity profiles along the column for a) S/F = 1 and b) S/F = 2 (mass basis) formed when the different solvents are added to the column and D/F = 0.4 (mass basis).

Figure 5.3 shows the tray efficiency profiles over the ED column calculated using Equation. 5.1. The rectifying section shows lower mass transfer efficiencies than the stripping section due to the effect of solvent viscosity. At S/F = 1 (Figure 5.3.a) the differences between solvents are relatively small, and the mass transfer efficiency order is [emim][OAc] > [emim][DCA] > EG > [emim][Cl]. This order does not exactly follow the viscosity order shown in figure 5.1. Therefore, the viscosity is not the only important effect in calculating the mass transfer efficiency as observed in equation 5.1. Table 5.1 gives the relative volatility values at two S/F ratios. Ionic liquids are able to outperform the relative

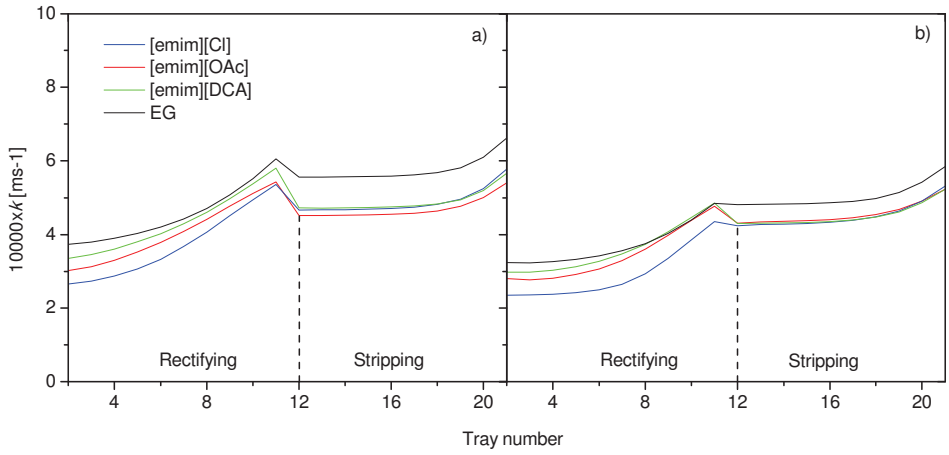

Figure 5.2. Averaged-liquid-side mass transfer coefficient profiles over the column for a) S/F = 1 and b) S/F = 2 (mass basis) calculated for the different solvents added to the column and D/F = 0.4 (mass basis). The column is numbered from the top to the bottom.

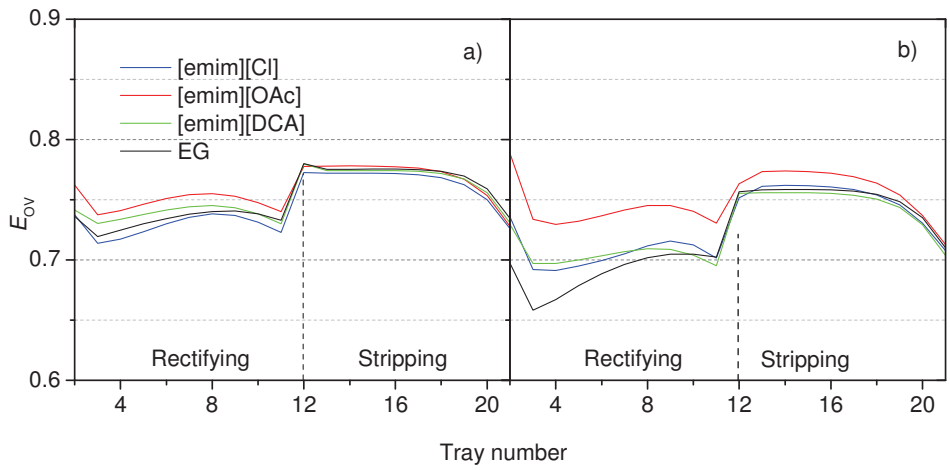

Figure 5.3. Tray efficiency profiles along the column for a) S/F = 1 and b) S/F = 2 (mass basis) calculated when the different solvents are added to the column and D/F = 0.4 (mass basis). The column is numbered from the top to the bottom.

volatilities of the common organic solvents as it has previously found in literature [15]. In this table it is observed that very good relative volatilities are produced by [emim][OAc]. This property enhances the mass transfer efficiency even though having relatively high viscosity. However, [emim][Cl] shows the highest relative volatility (see table 5.1) and also very high liquid phase viscosities (see figure 5.1.a). Here, due to the high viscosities this property becomes the predominant factor in mass transfer efficiency. Therefore, moderately high viscosities are not an important factor in mass transfer efficiency when combined with high values of relative volatility. However, the relative volatility does not enhance mass transfer efficiency sufficiently in the presence of a very viscous ionic liquid.

To support these observations the S/F ratio is increased (Figure 5.3.b). In the rectifying section, the tray efficiency order is [emim][OAc] > [emim][DCA] ≈ [emim][Cl] > EG. Although, there is an increase in liquid phase viscosity for this S/F ratio (see Figure 5.1b), [emim][OAc] does not show a significant decrease in the tray efficiency profiles between S/F ratios because the increase of it also produces an increase in relative volatility and this last property is predominant in calculating the mass transfer efficiency. This is not seen for the rest of the solvents where the increase in liquid phase viscosity does have an important impact on mass transfer efficiency. For example, EG exhibits a drastic decrease in tray efficiency when increasing the S/F ratio. As observed in table 5.1 EG has a minor impact on the relative volatility when compared to the rest of the solvents. Therefore, the changes in tray efficiency correspond directly with changes in the liquid phase viscosity. A very interesting case is [emim][Cl]. The decrease in mass transfer efficiency is not as drastic as would be expected from the viscosity increase alone. This is due to the large increase in relative volatility at this S/F ratio (see table 5.1) compensating the effect of viscosity to some extent.

In the stripping section and for S/F = 1, there is an increase in mass transfer efficiency for all the solvents since the solvent concentration is reduced by dilution with the feed stream and viscosity is a less important issue. Indeed, there are no significant differences in mass transfer efficiency between solvents. For S/F = 2, [emim][OAc] shows the highest tray efficiency values and the rest of the solvents show a slight decrease with regard to S/F = 1.

The effect of the solvent on mass transfer efficiency in the stripping section could become more important at different operating conditions. One example is the use of a higher D/F ratio to withdraw more vapor from the condenser. This is depicted in Figure 5.4 that shows the tray efficiency profiles for both S/F ratios at an increased D/F ratio of 0.5 instead of 0.4.

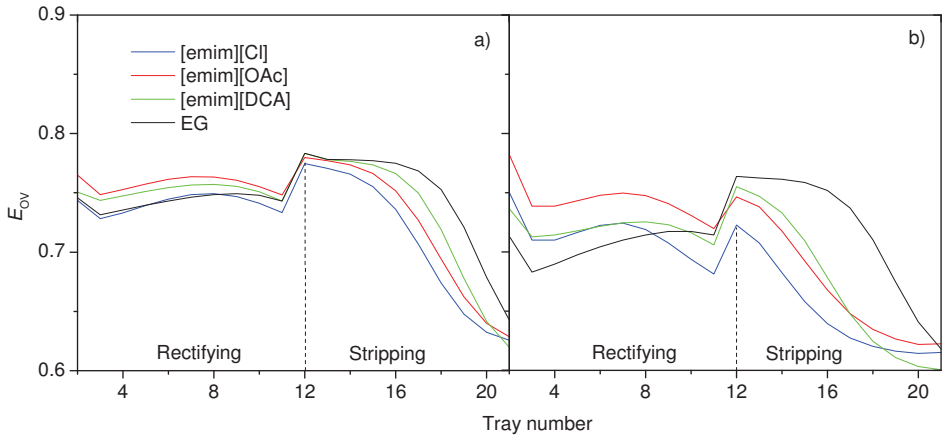

Figure 5.4. Tray efficiency profiles along the column for a) S/F = 1 and b) S/F = 2 (mass basis) calculated when the different solvents are added to the column and D/F = 0.5 (mass basis).

From figure 5.4 it is clear that the rectyfing section exhibits the same trend as the previuos operating conditions (D/F = 0.4). However, large differences in mass transfer efficiency between D/F ratios are observed in the stripping section especially at S/F = 2 (Figures 5.3b and 5.4b). At S/F = 1 (Figures 5.3a and 5.4a) the differences are less noticeable. Let us focus on why these differences are produced. When increasing the D/F ratio more vapor is withdrawn from the condenser, mainly ethanol, increasing the less volatile components at the bottom of the column: water and solvent. The water – solvent concentration in this zone depends on the relative volatility of the system. Then, the explanation is that the higher the relative volatility, the lower the ethanol concentration at the bottom. Since water requires more energy to be evaporated, the mass transfer efficiency

drops due to the decrease in the vapor velocity. Indeed, the drop in the mass transfer efficiency profiles follow the inverse order of those relative volatility values in table 5.1. These decreases in mass transfer effciency are more noticeable at S/F = 2 since the concentration of the solvent is higher than at S/F = 1. At S/F = 2 the separation effect of the solvent on the mixture becomes stronger and this decreases more the concentration of ethanol at the bottom of the column and this produces even less vaporizable ethanol and thus vapor velocity. This is observed in all the profiles generated when using ILs but more pronounced for the case of [emim][Cl] with a drastic mass transfer efficiency decrease at S/F = 2. To show the decrease in vapor velocity and therefore the decrease in mass transfer eficiency, figure 5.5 shows the ratio of vapor velocity/vapor velocity at flooding ($u_{VS} / u_{VS,flooding}$) for both S/F ratios and both D/F ratios. Marked decreases in vapor velocity are observed for both D/F ratios and when using the ionic liquids. These decreases are more marked at S/F = 2 for both D/F ratios. However, at D/F = 0.5 drastic drops in vapor velocity are observed for both S/F ratios. These drops are even found in the rectifying section at S/F = 2. The lower production of vapor decreases the mass transfer efficiency. Therefore, the viscosity is not the only property that lowers the mass transfer efficiency in the rectifying section.

In conclusion the distribution ratios can play either a positive or negative role in the separation of water – ethanol mixtures. For D/F = 0.4 the distribution ratios can overcome mass transfer limitations caused by moderately high liquid phase viscosities. However, for D/F = 0.5, adverse mass transfer efficiencies are obtained when using ionic liquids in the stripping section.

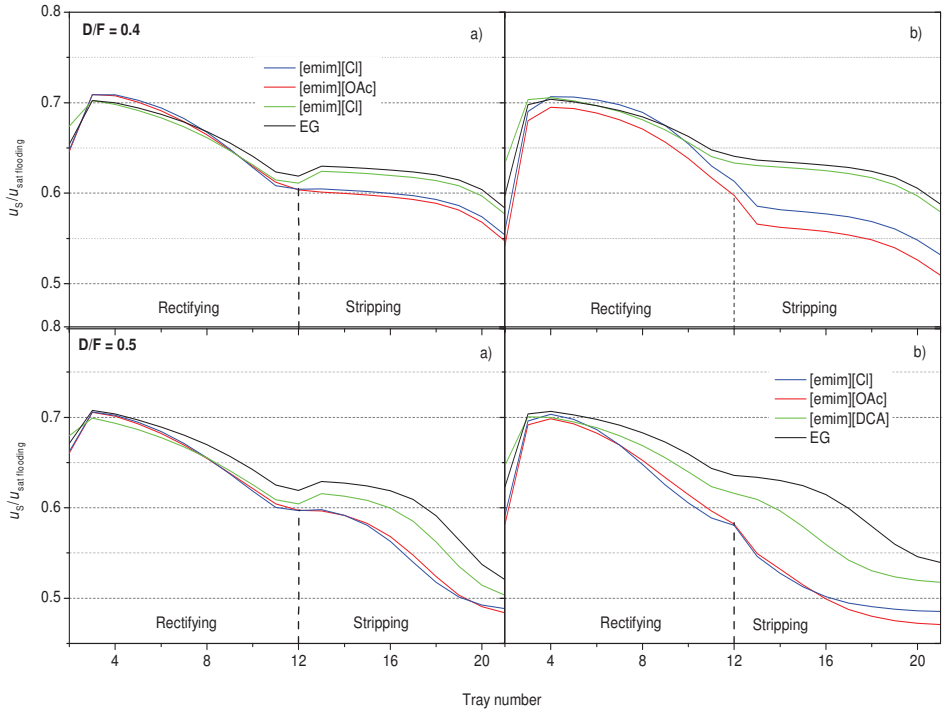

Figure 5.5. Ratio vapor velocity-vapor velocity at flooding profiles for a) S/F = 1 and b) S/F = 2 (mass basis).

5.5 Mellapak® 250Y structured packing.

The mass transfer efficiency of the water – ethanol separation is studied for the same operating conditions as the sieve tray column but now using Mellapak® 250Y structured packing. The analysis will follow the same structure, meaning that, from the liquid phase viscosity profile we analyze the posible decrease in mass transfer efficiency for D/F = 0.4. Figure 5.6 depicts the liquid phase viscosity profiles over the column. The same trends and viscosity values as with the column containing sieve trays are observed because this property does not depend upon the internals. Next, Figure 5.7 shows the average mass transfer coefficient profiles over the column. These coefficients drop in the rectifying

section as compared to the stripping section by the effect of liquid phase viscosity. The effect is clearly observed with [emim][Cl] that shows the lowest values and EG that shows the highest ones. This trend is the same as sieve trays. Additionally, two important facts are observed. First, similar to sieve trays, the increase in S/F ratio does not produce a significant decrease in the mass transfer coefficient profiles because of a rise in the temperature profiles (boiling points) that moderates the increase in liquid phase viscosities. A small decrease is observed for [emim][Cl]. Additionally, when increasing the S/F ratio, the superficial liquid velocities on the packing increase. This improves mass transfer. Secondly, the mass transfer coefficients in packing are lower than in sieve trays. This is because in sieve trays the vapor flows upward and vigorously bubbles through the liquid on the tray forming a turbulent vapor-liquid dispersion. Additionally, a liquid holdup is maintained on the tray. These characteristics create a large vapor-liquid contact area and high mass transfer coefficients. In a packed colum instead, a continuous vapor-liquid contact is promoted by the interfacial area. However, a lower liquid holdup and therefore lower contact time between phases are achieved. As a result lower mass transfer coefficients than in trays are obtained [16].

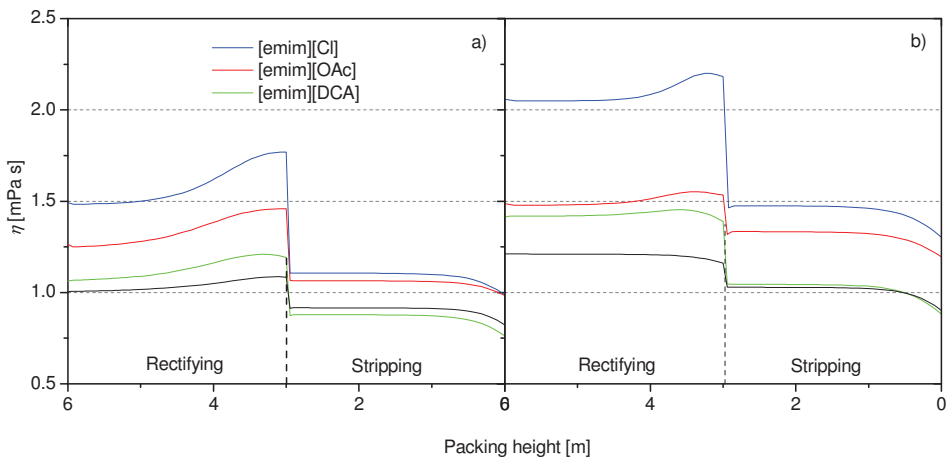

Figure 5.6. Liquid phase viscosity profiles along the column for a) S/F = 1 and b) S/F = 2 (mass basis) calculated when the different solvents are added to the column and D/F = 0.4 (mass basis).

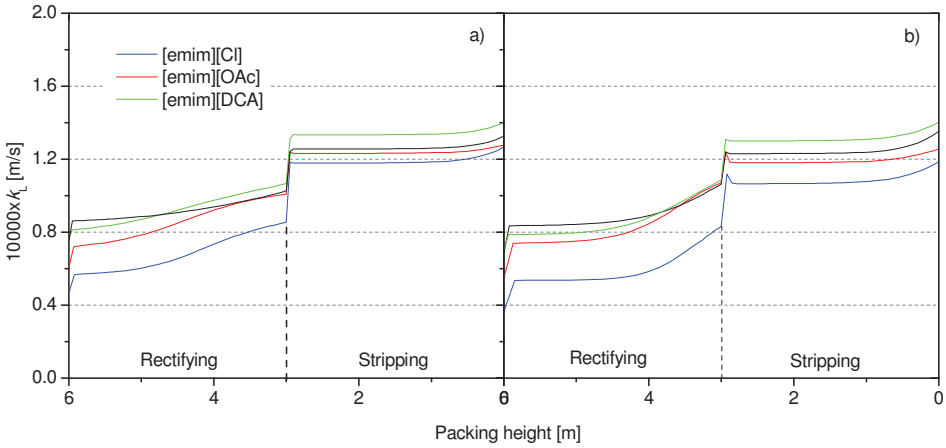

Figure 5.7. Averaged mass transfer coefficient profiles along the column for a) S/F = 1 and b) S/F = 2 (mass basis) calculated when the different solvents are added to the column and D/F = 0.4 (mass basis).

Figure 5.8 shows the *HETP* profiles over the column. The mass transfer efficiency order is [emim][OAc] > [emim][DCA] > [emim][Cl] > EG in the rectifying section for both S/F ratios. The observation of these profiles does not produce different conclusions from sieve trays. However, two important points are noticed. Firstly, in contrast to sieve trays, improvements in mass transfer efficiency when using ILs are obtained when increasing the S/F ratio. This is explained by the fact that in packed columns the liquid and vapor flow are in countercurrent and the packing surface allows an intimate vapor-liquid contact. As a result, the packed distillation column operates closer to equilibrium than sieve trays, and thereby the effect of the relative volatility predominates over the increase in liquid phase viscosity. Secondly, and continuing with this observation, EG presents the lowest mass transfer efficiency (highest *HETP*) for both S/F ratios due to the low increment in relative volatility and the increase of liquid phase viscosity.

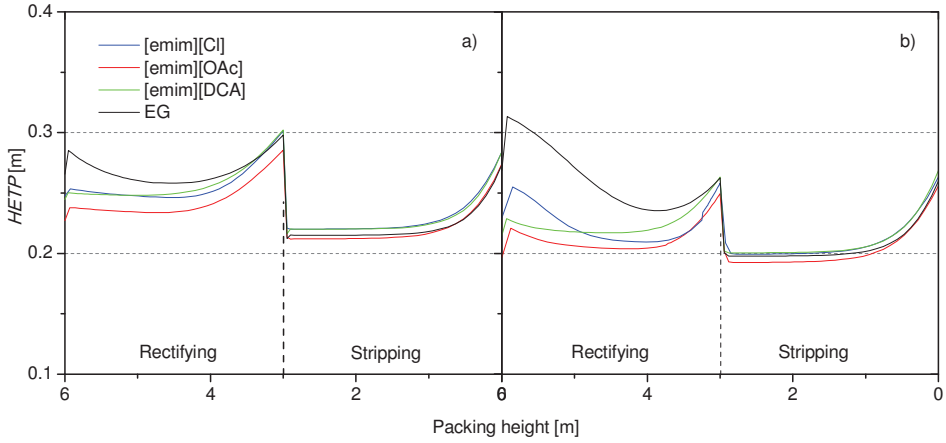

Figure 5.8. *HETP* profiles along the column for a) S/F = 1 and b) S/F = 2 (mass basis) calculated when the different solvents are added to the column and D/F = 0.4 (mass basis).

5.6 Conclusions

The mass transfer efficiency in extractive distillation for the separation of water – ethanol mixtures using ionic liquids and the reference organic solvent ethylene glycol (EG) was analyzed for two solvent-to-feed ratios and two internals: Sieve trays and Mellapak® 250Y.

With both internals, the liquid phase viscosity inside the colum has a limited impact on mass transfer coefficients. When increasing the solvent-to-feed ratio, there is a slight decrease in all the mass transfer coefficient profiles in sieve trays. In Mellapak® 250Y, this decrease is less pronounced.

In sieve trays, relatively high viscosities affect the mass transfer efficiency. However, the improvements in relative volatilities shown by ionic liquids allow to overcome this effect. Very viscous ionic liquids (> 65[mPa s] at T = 353.15K) lower the mass transfer efficiency no matter how high relative volatility.

Increased distillate-to-feed ratios produce drastic mass transfer efficiency drops in the stripping section when using ionic liquids as solvent.

In Mellapak® 250Y, also the relatively high viscosities does not decrease the mass transfer efficiency due to improved relative volatilities. Also here, the increase in solvent-to-feed ratio enhances mass transfer efficiency when using ionic liquids.

Nomenclature

E_{OV}	Point efficiency, Tray Efficiency
E_O	Section efficiency
$HETP$	Height equivalent to a theoretical plate, m
H_L	Height of transfer units in the liquid phase, m
H_V	Height of transfer units in the vapour phase, m
H_{OV}	Overall height of transfer units, m
H_P	Actual height of the packing, m
k_L	Liquid phase mass transfer coefficient, m s^{-1}
$N_L^{'}$	Number of transfer units in the liquid phase
N_{real}	Actual number of stages
N_V	Number of transfer units in the vapor phase
N_{OV}	Overall number of transfer units
T	Temperature, K
u_{VS}	Vapor velocity, m s^{-1}
$u_{VS,flooding}$	Vapor velocity at flooding, m s^{-1}

Greek letters

α	Relative volatility
Λ	Stripping factor
η	Dynamic viscosity, mPa s

References

[1] Y.Ge, L.Zhang, X.Yuan, W.Geng, and J.Ji, Selection of ionic liquids as entrainers for separation of (water + ethanol), *J.Chem.Thermodyn.*, 40, 2008, 1248 - 1252.
[2] E.Quijada-Maldonado, S.van der Boogaart, J.H.Lijbers, G.W.Meindersma, and A.B.de Haan, Experimental densities, dynamic viscosities and surface tensions of the ionic liquids series 1-ethyl-3-methylimidazolium acetate and dicyabamide and their binary and ternary mixtures with water and ethanol at T = (298.15 to 343.15) K, *J.Chem.Thermodyn.*, 51, 2012, 51 - 58.
[3] E.Gómez, B.González, Á.Domínguez, E.Tojo, and J.Tojo, Dynamic Viscosities of a Series of 1-Alkyl-3-methylimidazolium Chloride ionic Liquids and Their Binary Mixtures with Water at Several Temperatures, *J.Chem.Eng.Data*, 51, 2006, 696 - 701.
[4] E.Gómez, B.González, N.Calvar, E.Tojo, and Á.Domínguez, Physical Properties of Pure 1-Ethyl-3-methylimidazolium Ethylsulfate and Its Binary Mixtures with Ethanol and Water at Several Temperatures, *J.Chem.Eng.Data*, 51, 2006, 2096 - 2102.
[5] S.Weiss and R.Arlt, On the Modelling of Mass Tranfer in Extractive Distillation, *Chem.Eng.Process*, 21, 1987, 107 - 113.
[6] H.E.O'Connell, Plate efficiency of fractionating columns and absorbers, *Trans.AIChE.*, 42, 1946, 741 -
[7] S.Böcker and G.Ronge, Distillation of Viscous Systems, *Chem.Eng.Technol.*, 28, 2005, 25 - 28.
[8] S.Fendt, S.Padmanabhan, H.W.Blanch, and J.M.Prausnitz, Viscosities of Acetate and Chloride-Based Ionic Liquids and Some of Their Mixtures with Water or Other Common Solvents, *J.Chem.Eng.Data*, 56, 2011, 31 - 34.
[9] E.Quijada-Maldonado, G.W.Meindersma, and A.B.de Haan, Viscosity and density data for the ternary system water(1) - ethanol(2) - ethylene glycol(3) between 298.15 and 328.15K, *J.Chem.Thermodyn.*, (2012),
[10] M.J.Lockett, *Distillation Tray Fundamentals*, Cambridge University Press, New York, 1986.
[11] R.Taylor and R.Krishna, *Multicomponent Mass Transfer*, Wiley, New York, 1993.
[12] F.H.Rhodes and P.G.Slachman, Plate Efficiency and Entrainment in Distillation, *Ind.Eng.Chem.*, 29, 1937, 51 - 54.
[13] H.Z.Kister, P.M.Mathias, D.E.Steinmeyer, W.R.Penney, B.B.Crocker, and J.R.Fair, Equipment for Distillation, Gas Absorption, Phase Dispersion, and Phase Separation, 8th, (2007),
[14] Sulzer Chemtech, Structured Packings for Distillation, Absorption and Reactive Distillation, (2006),
[15] Z.Lei, C. Li and B.Chen, Extractive Distillation: A Review, *Sep.Purif.Rev.*, 32, 2003, 121 - 213.
[16] B.K.Dutta, *Principles of Mass Tranfer and Separation Processes*, Prentice-Hall of India, New Delhi, 2007.

6

Pilot plant study on the separation of Toluene-Methylcyclohexane mixtures using NMP and the ionic liquid [HMIM][TCB] as solvents.

Abstract

The separation of the close-boiling point mixture: toluene – methylcyclohexane can be carried out by extractive distillation using the ionic liquid [hmim][TCB]. However, high solvent-to-feed ratios are needed to separate this mixture. Therefore, higher liquid phase viscosities are expected than for ethanol-water separation with [emim][DCA] in the previous chapters with the corresponding mass transfer limitations. Experiments in an extractive distillation pilot plant were carried out with the objective of first exploring different operating conditions and second to compare the mass transfer efficiencies produced by [hmim][TCB] and the reference solvent NMP. From two distillate rates and two reboiler duties, it was found that all the studied operating conditions were in the one-liquid-phase region. As expected the high solvent-to-feed ratios created high liquid phase viscosities and consequently the use of this ionic liquid produces HETPs twice as high as the reference solvent.

6.1 Introduction

In the previous chapters the decrease in mass transfer efficiency with solvent viscosity has been study for the water – ethanol mixture. This study can be perfectly extended to any kind of mixture where an ionic liquid is thought to replace a conventional organic solvent. The separation of aromatic – aliphatic mixtures is a good example. The separation of toluene and methylcyclohexane is difficult due to their proximity of their boiling points. This separation is possible by extractive distillation (ED) using N-methyl-2-pyrrolidone (NMP) as solvent [1]. Recently, the ionic liquid 1-hexyl-3-methylimidazolium tetracyanoborate ([HMIM][TCB]) has been proposed as a promising replacement of conventional organic solvents [2] as the produced relative volatilities outperform by far that of the currently used polar organic solvents. To our knowledge, no other ionic liquid has been proposed to separate this mixture.

When using this new separating agent, challenging process conditions are required to utilize the solvent potential. Due to the high polarity of this ionic liquid and the low polarity of toluene and methylcylcohexane, the solubility of the solvent in the mixture is very limited [2] and the formation of two liquid phases becomes an issue. The two liquid phases inside the ED column do not allow achieving a proper separation. The limited solubility is causing high S/F ratios even at the very low reflux ratios required due to the strongly increased relative volatility. This represents challenging operating parameters since high S/F ratios bring an increase in liquid phase viscosities and thus mass transfer limitations that could result in a longer column required to achieve a desired purity. This fact was studied in detail in the previous chapter for the water – ethanol separation using 1-ethyl-3-methylimidazolium dicyanamide [emim][DCA]. In that chapter rate-based simulations were validated using pilot plant experiments. So then, the rate-based model should be the tool to study the proper operating parameters for the toluene – methylcyclohexane separation with [HMIM][TCB] and the decrease in mass transfer efficiency due to the high S/f ratios. However, to carry out such simulations, accurate VLE data are essential along with the rest of the physical and transport properties. Only liquid-liquid equilibrium data (LLE) of the ternary mixture toluene – methylcyclohexane – [hmim][TCB] at low temperatures (from 20 to 60ºC) is available in literature [2] and could be used to obtain the binary parameters of a model to predict VLE such as Wilson, NRTL or UNIQUAC. However, the parameters were

not regressed from VLE data and the rate-based simulation could lead to erroneous results from using LLE to predict VLE. Furthermore, determination of these VLE data and physical properties, would be highly time consuming. For these reasons, pilot plant experiments to compare solvent performances has been used as an alternative to the rate-based simulations. It is worth nothing that the ED column was already built and used in Chapter 4.

Therefore, the objective of this chapter is to compare the performance of two solvents: NMP and [HMIM][TCB] in an ED pilot plant equipped with Mellapak® 750Y structured packing at several operating conditions that allow to have one liquid phase. Additionally, the liquid phase resistances and the mass transfer efficiency quantified through the Height Equivalent to a Theoretical Plate (*HETP*) obtained under these challenging operating conditions are studied in this work. To our knowledge, this is the first study where the performance of this new promising ionic liquid is studied in a pilot plant.

6.2 Operating parameters

As explained in the introduction, the limited solubility of the ternary system toluene – methylcyclohexane – [HMIM][TCB] represents the most challenging issue in this separation because it requires operating parameters that avoid the two-phase region. Figure 6.1 depicts the solubility region for this system in a ternary diagram. This diagram corresponds to a vapor-liquid-liquid diagram.

The phase diagram was constructed using the UNIQUAC model with parameters obtained from the literature [2]. It is observed that the solubility of methylcyclohexane in [hmim][TCB] is limited to a mole fraction of 0.16 while the toluene solubility in [hmim][TCB] is 0.82 at the indicated temperature in Figure 6.1. The temperature does not have a significant influence on the solubility for this system [2]. In the ED column the solvent is added at the top of the column where methylcylcohexane is obtained in the condenser. To maintain operation in the one-phase region, a low reflux ratio and high S/F ratios are required. By doing this, the methylcyclohexane is mainly removed from the condenser and not recycled back to the column. Knowing these two facts and using the UNIQUAC model, equilibrium calculations in ASPEN® Plus Radfrac can be carried out to estimate the process parameters. Table 6.1 lists the obtained process parameters.

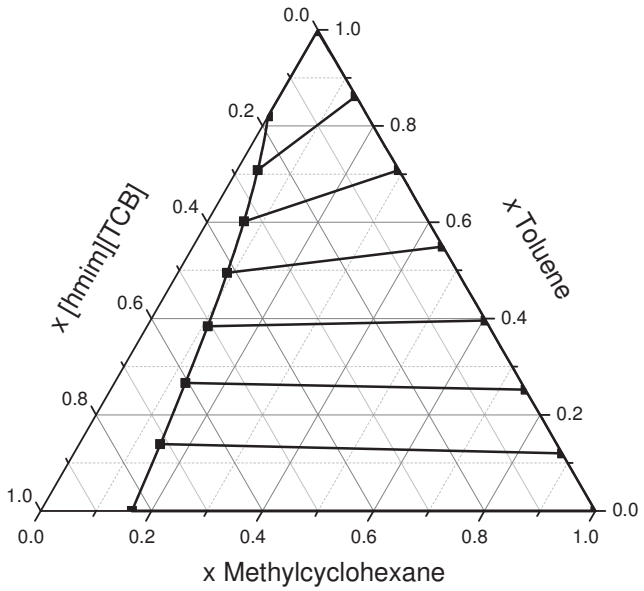

Figure 6.1. Ternary diagram for the system Toluene – Methylcyclcohexane – [hmim][TCB] at the equilibrium temperature.

However, the equilibrium calculations are insufficient to represent the real process of this pilot plant since they do not take into account the heat and mass transfer limitations. For this reason, several operating conditions are tested in the ED pilot plant of which the main features were already presented in chapter 4.

As observed from Table 6.1 only one S/F ratio is studied because a further increase of this parameter made the pilot plant very difficult to operate and by reducing S/F the liquid-liquid immiscibility region would be entered.

Table 6.1. Operating conditions

Variable		Value	
Feed flow rate [kg h^{-1}]		2	
Toluene concentration at feed [wt%]		70	
Feed temperature [ºC]		90	
Solvent temperature [ºC]		100	
Solvent-to-feed ratio (mass)		5	
Case studies	Solvent	Reboiler duty [kW][a]	Distillate rate [kg h^{-1}]
Case I.a	NMP	50%	0.3
Case I.b	[hmim][TCB]	50%	0.3
Case II	[hmim][TCB]	50%	0.6
Case III	[hmim][TCB]	30%	0.3

[a] 100% = 2.04 [kW]

6.3 Physical properties of the solvents

To calculate the mass transfer coefficients and determine the liquid phase resistances, physical and transport properties are needed. The most relevant to this work is the viscosity and its change with concentration and temperature in the ternary mixture along with the vapor-liquid equilibrium information. The relative volatilities and the viscosities of [hmim][TCB] and NMP are depicted in tables 6.2 and 6.3 respectively. Liquid dynamic viscosities in the ternary mixture toluene – methylcyclohexane – [hmim][TCB] are presented in Appendix A.6. The experimental procedure to determine this property is explained in detail in chapter 3. In chapter 5 we have concluded that the viscosity of the solvents does not affect the mass transfer efficiency of the extractive distillation process as long as the solvent produces high relative volatilities.

Table 6.2. Relative volatilities at a SFR in mass basis obtained by the use of different solvent and calculated at 70% w/w toluene[a].

	α		
Solvent	S/F = 5	Model	Source of binary parameters
NMP	2.83	NRTL	ASPEN® Plus
[hmim][TCB]	9.42	UNIQUAC	[2]

[a] This concentration falls into the one-phase region in figure 6.1

Table 6.3. Pure solvent viscosities as function of temperature.

T [K]	η [mPa s]	
	NMP[a]	[hmim][TCB][b]
298.15	1.89	47.83
303.15	1.72	37.42
308.15	1.58	29.89
313.15	1.45	24.33
318.15	1.34	20.11
323.15	1.24	16.89
328.15	1.15	14.28
333.15	1.07	12.30
338.15	0.99	10.68
343.15	0.93	9.34

[a] Values obtained from Aspen® Plus.
[b] Measured in this work.

Table 6.2 confirms the significant increase in relative volatility when using [hmim][TCB] instead of NMP. As discussed in Chapter 4, this variable contributes to an increase in mass transfer efficiency. Furthermore, in table 6.3 the viscosities of both solvents are compared at different temperatures. It is observed that the viscosity of the ionic liquid is around 25 times higher than the organic solvent at T = 298.15 K. However, this ionic liquid is not as viscous as other ionic liquids [3]. Therefore, the reduction in mass transfer is expected to be limited. Nevertheless, the high S/F ratio could have an effect.

6.4 Liquid phase resistance

The mass transfer efficiency in a packed column is expressed by the Height Equivalent to a Theoretical Plate:

$$HETP = H_{OV} \frac{\ln(\Lambda)}{\Lambda - 1} \qquad 6.1$$

and the overall height of transfer units is calculated as:

$$H_{OV} = H_V + \Lambda H_L \qquad 6.2$$

which is composed of the height of transfer unit in the vapor phase, H_V and the height of transfer unit in the vapor phase by the stripping factor, ΛH_L. Both originate from the resistance. The height of transfer units is calculated using a mass transfer correlation along with the rate-based model. A rate-based model was built to predict the performance of the pilot plant and to compare the performance of both solvent NMP and [hmim][TCB] in terms of the height of transfer units in the liquid phase and the mass transfer efficiency or *HETP* value. To carry out these rate-based simulations physical and transport properties were defined. In chapter 2 it was established that liquid viscosities, surface tension and infinite dilution diffusion coefficients have to be accurately provided. In the appendix section (table A.6.1) experimental ternary viscosities for the ternary system toluene – methylcyclohexane – [hmim][TCB] are presented. Additionally, the surface tension of the pure ionic liquid was experimentally determined. Table 6.4 shows the experimental value. Minimal differences in surface tension is observed between NMP and [hmim][TCB]. Infinite dilution diffusion coefficients were calculated using the Wilke&Chang equation. Although, all the requirements to run the rate-based simulations were complete, it appeared impossible obtain convergence. The thermodynamic parameters used in this work were determined from experimental liquid – liquid data at low temperatures (T = 293.15 to 333.15 K) [2]. This last point could be the source of instability when running simulations. Therefore, it was finally decide to calculate the liquid side height of transfer units and the *HETP* number manually.

In this work the Rocha et al. mass transfer correlation [4,5] was previously chosen to successfully predict the performance of the ED pilot plant using ionic liquid as solvent. Nevertheless, for simplicity in calculating mass transfer coefficients the Bravo et al. [6] mass transfer correlation has been chosen. The main assumption in this correlation is that the surface provided by the packing is completely wetted and the change of interfacial area for mass transfer as function of surface tension is not considered. Furthermore, the effect of surface tension on interfacial area will especially be stronger in high surface area packing like Mellapak® 750Y. For aqueous systems, this assumption brings large deviations as

demonstrated previously in Chapter 4. However, in this work, the components of the ternary mixture have relatively low surface tensions that would enhance the degree of wetting of the packing surface approaching to the complete wetting. Several studies confirm this fact. For instance Tsai et al. [7] measured the changes in effective area with surface tension in chemical absorption using Mellapak® 250Y and 500Y. Reductions in surface tension of the system enhance the effective area for mass transfer. Additionally, Ataki and Bart [8] determined that viscosity exhibits an effect on degree of wetting of Rombopak® structured packing. Highly viscous forces increase the degree of wetting of the packing surface. For these reasons it is considered a valid approach to estimate the mass transfer in this low surface tension and viscous system by the Bravo et al. [6] mass transfer correlation.

Table 6.4. Pure component surface tension at T = 298.15 K

Component	σ [mN m]
Toluene	27.92[a]
Methylcyclohexane	23.31[a]
NMP	42.2[a]
[hmim][TCB]	40.3[b] ± 0.1[c]

[a] Values obtained from Aspen® Plus.
[b] Measured in this work. Measuring temperature T = 296.12 ± 0.25[c]
[c] Standard deviation.

Finally, the relation between the height of transfer units and the mass transfer coefficient is:

$$H_L = \frac{u_L}{k_L a'} \qquad 6.3$$

$$H_V = \frac{u_V}{k_V a'} \qquad 6.4$$

Equations 6.1 and 6.3 are the basis for the comparisons between solvents. However, the Height Equivalent of a Theoretical Plate could be calculated under several assumptions. In equations 6.1 and 6.2 the stripping factor Λ is required which is obtained from vapor-liquid equilibrium calculations. In this work, the stripping factor is obtained from the

experimental liquid phase compositions from the pilot plant and using the UNIQUAC model parameters [2]. By doing this, it is assumed that those compositions in the liquid phase are in equilibrium with the calculated compositions in the vapor phase. Hereafter, the obtained vapor compositions are used to calculate the mass transfer coefficients in the vapor phase. Next, the liquid and vapor molar flow rates are calculated using ASPEN® Plus in equilibrium mode and taking into account the operating conditions from every experiment. Finally, the superficial velocities in the vapor and liquid phases are calculated based on the molar vapor and liquid flow rates respectively.

6.5 Results

6.5.1 Experimental profiles

Figures 6.2 to 6.5 show the experimentally obtained concentration and temperature profiles over the column at the respective operating conditions shown in Table 6.1. First, NMP and [hmim][TCB] are compared (cases I.a and I.b respectively). Figure 6.2 and 6.3 show the concentration and temperature profiles respectively.

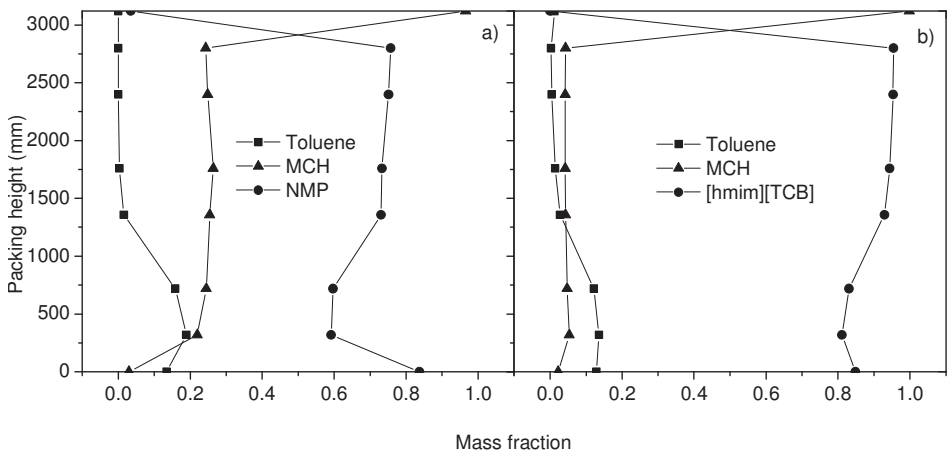

Figure 6.2. Concentration profiles (mass fractions) for the ED of toluene – MCH using a) NMP (case I.a) and b) [hmim][TCB] (case I.b) as solvents. The operating conditions are detailed in Table 6.1.

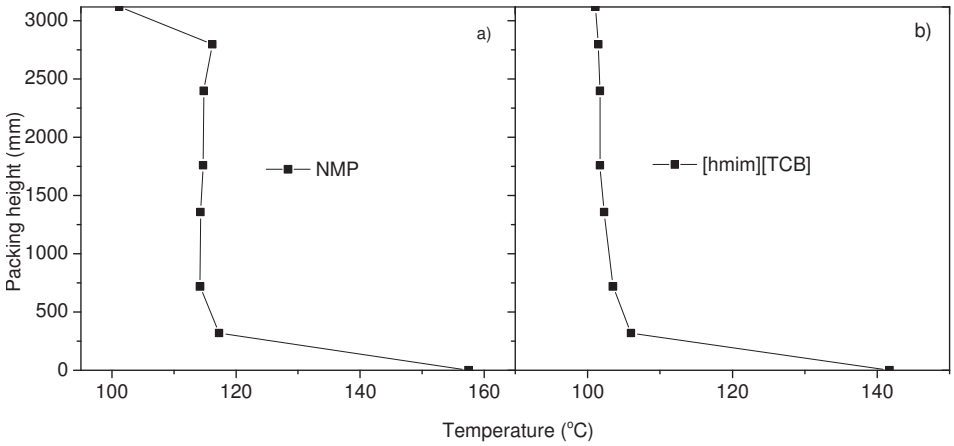

Figure 6.3. Experimental temperature profiles obtained from the pilot plant for the ED of toluene – MCH using a) NMP (case I.a) and b) [hmim][TCB] (case I.b) as solvents.

As a consequence of S/F = 5, high (60-90 wt%) solvent concentrations are observed in Figure 6.2 for both cases I.a and I.b. This produces a viscous liquid phase inside the column and may thus yield mass transfer limitations especially when using the ionic liquid. Differences between solvents are observed in the solvent concentration where [hmim][TCB] is present in even higher concentrations than NMP due to its negligible vapor pressure. As NMP has a vapor pressure, part of it is vaporized and the liquid concentration reduced, while the ionic liquid remains in the liquid phase. For both cases, the toluene concentration is very low in the two concentration points below the condenser. It is worth noting that the concentration points when using [hmim][TCB] as solvent are within the one-phase region in the ternary diagram. (see Figure 6.6)

Figure 6.3 shows the temperature profiles over the column for both solvents. As expected, higher temperatures are obtained when applying NMP. This is because NMP is partially vaporized and its boiling point influences the temperature profiles. This phenomenon is also observed in chapter 4 where the profiles containing the ionic liquids showed lower temperatures than those of the conventional solvent ethylene glycol for the separation of ethanol/water.

After these runs, two additional cases are studied to decrease the reflux ratio and test operating conditions that fall into the one-phase region in the ternary diagram. In case II the distillate rate is increased keeping the rest of the operating variables constant. In case III the reboiler duty is reduced to decrease the reflux ratio. However, in both cases the *L/V* ratio is modified influencing the mass transfer efficiency of the process. Figure 6.4 shows the concentration profiles of a) case II and b) case III.

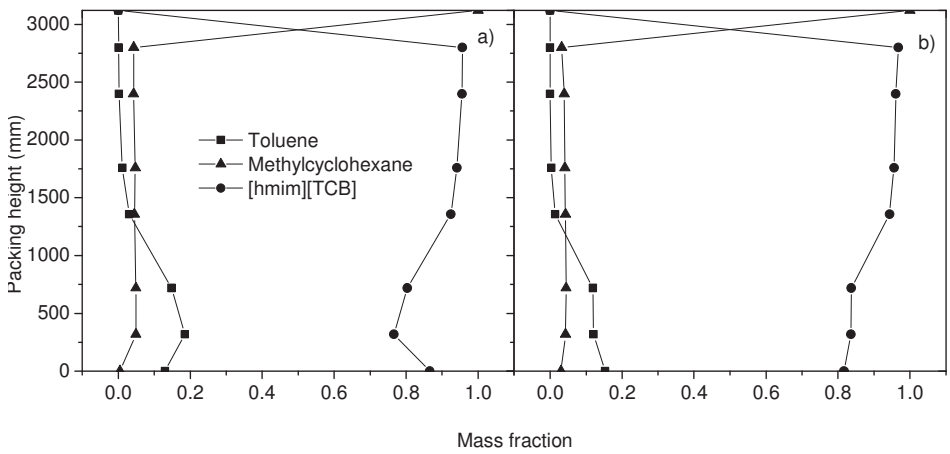

Figure 6.4. Experimental concentration profiles for the ED of toluene – MCH obtained from the pilot plant for a) case II and b) case III. The operating conditions are detailed in Table 6.1.

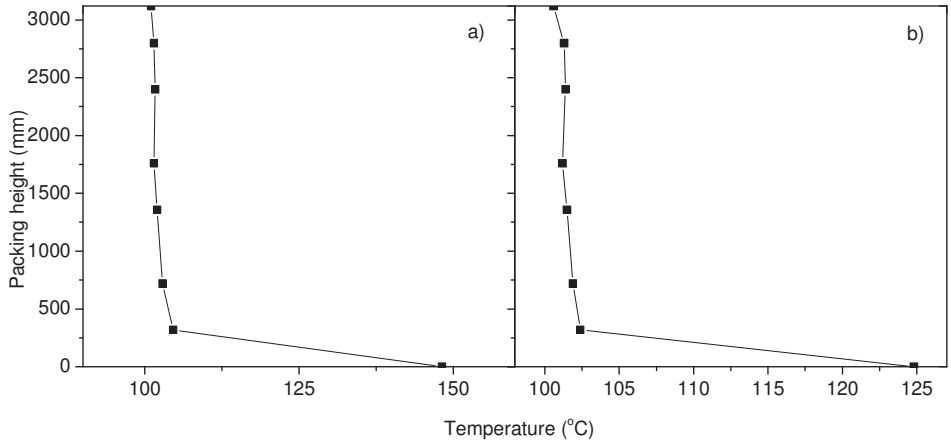

Figure 6.5. Experimental temperature profiles from the pilot plant for the ED of toluene – MCH for a) case II and b) case III. The operating conditions are detailed in table 6.2.

Basically, no significant differences are observed in figure 6.4 when compared to figure 6.2b. The concentrations profiles are very similar to Case I because the S/F ratio is the predominant operating variable. However, the differences appear in the temperature profiles. As expected, lower temperatures are obtained when reducing the reboiler duty because less vaporizable liquid passes from the liquid to the vapor phase staying in the liquid phase. This decreases the boiling point of the mixture. Figure 6.6 shows the ternary diagram containing the experimental points for all three cases. It confirms that for all the cases the experimental compositions fall into the one phase region. Case II is operating the farthest away from the two phase boundary because more vapor of methylcyclohexane is withdrawn from the column when increasing the distillate rate decreasing the methylcyclohexane concentration over the column.

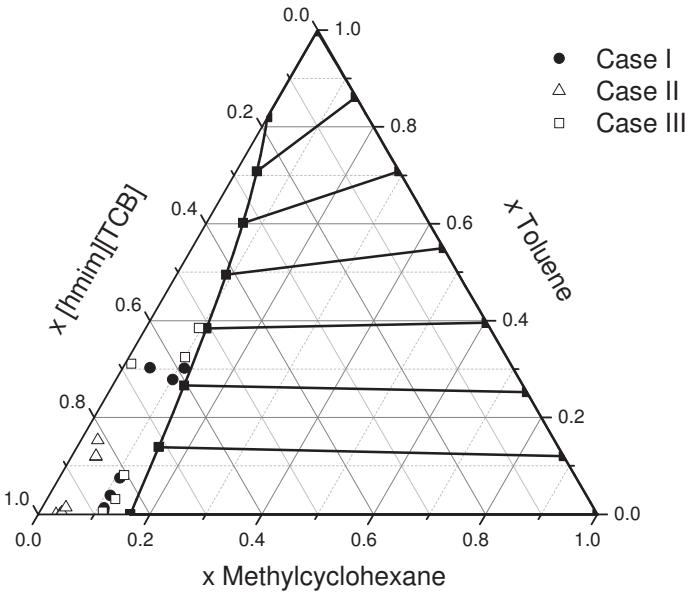

Figure 6.6. Experimental concentration profiles located inside the ternary diagram.

6.5.2 Mass transfer

A high S/F ratio is needed when using this ionic liquid to avoid forming two-liquid phases. As mentioned above, and studied in the two previous chapters, this could bring mass transfer limitations. Figure 6.7.a and 6.7.b show the viscosity profiles and the liquid phase height of transfer unit profiles respectively for all the experimental cases (I.a, I.b, II and III). The liquid phase viscosities were obtained experimentally (the experimental procedure is explained in chapter 3) and subsequently correlated using the Eyring-Patel-Teja model [9]. This information is given in appendix A.6. Finally, the model is used to calculate viscosities with the experimental compositions from the pilot plant.

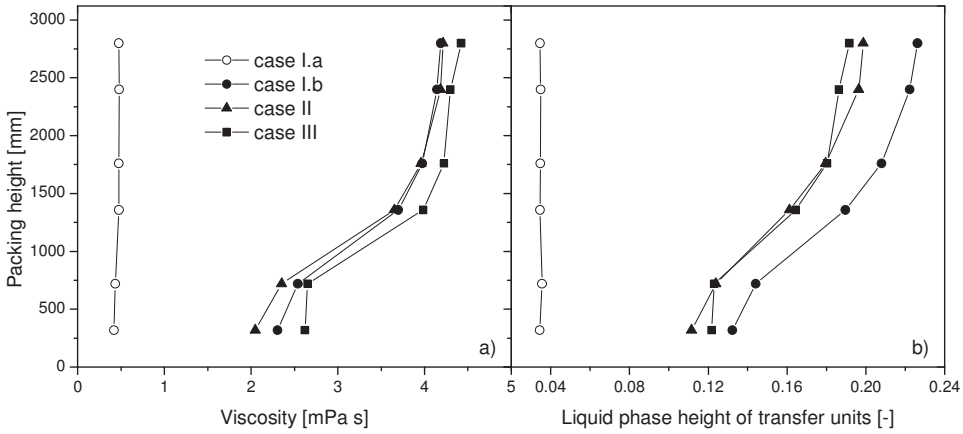

Figure 6.7. Calculated liquid phase viscosity and liquid phase height of transfer unit profiles for the ED of toluene – MCH for all the studied cases.

In Figure 6.7.a the influence of [hmim][TCB] on the liquid viscosity can be clearly observed. While the separation of the toluene – methylcyclohexane mixture with NMP (Case 1.a) shows low viscosities, [hmim][TCB] exhibits high values reaching 4 [mPa s] in the rectifying section. This behavior is observed for all the cases where the IL is involved with small differences between them. Next, the liquid phase height of transfer unit profiles for all the cases are presented in figure 6.7.b. The effect of viscosity on these profiles is clearly noticed since they follow the same trend. Case I.b shows the highest values because of the differences in vapor-liquid ratios. In distillation processes it is well recognized that the main resistance to mass transfer is in the vapor phase. The large differences between NMP and the IL in figure 6.7.b illustrate the need to study the mass transfer efficiency profiles in more detail.

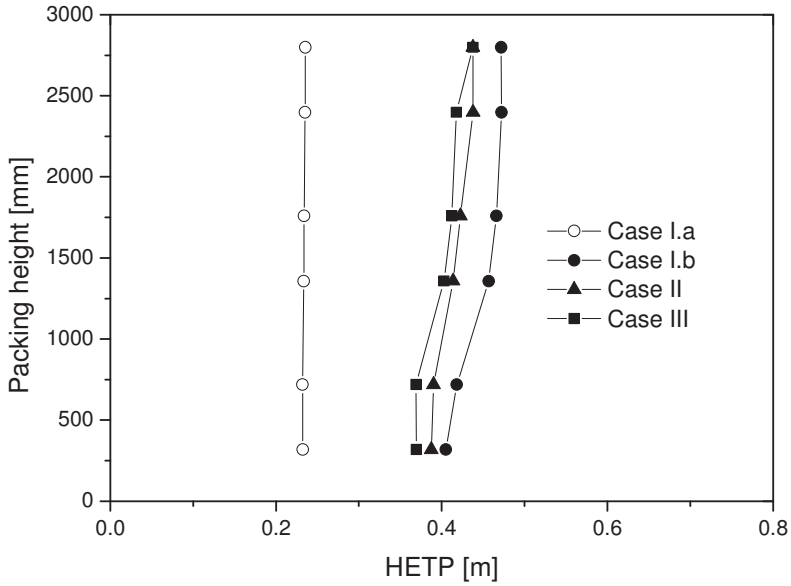

Figure 6.8. Calculated *HETP* profiles for the ED of toluene – methylcyclohexane for all studied cases.

Figure 6.8 shows the calculated *HETP* profiles over the ED pilot plant for all the cases. It can be observed that the impact of the liquid phase resistance on the mass transfer efficiency is significant. As previously noticed, the high viscosities produced inside the pilot plant by the high *S/F* ratios when using [hmim][TCB], resulted in a decrease of mass transfer efficiency with regard to the reference solvent NMP even though the use of the IL solvent produces much higher relative volatilities. As a result the HETP when using [hmim][TCB] is about twice as high as the HETP when using NMP.

6.6 Conclusions

The operation and the mass transfer efficiency for the separation of toluene – methylcyclohexane mixtures using the ionic liquid 1-hexyl-3-methylimidazolium tetracyanoborate and the reference solvent *N*-methyl-2-pyrrolidone were compared in an extractive distillation pilot plant equipped with Mellapak® 750Y structured packing.

In general, all the proposed operating conditions were favorable for the separation of this mixture. High solvent-to-feed ratios were required because this avoided the formation of two liquid phases.

The liquid phase viscosity profiles over the column were estimated using the Eyring-Patel-Teja model using the experimental compositions from the pilot plant. High viscosities were observed as a consequence of the high solvent-to-feed ratios and the viscosity of the ionic liquid.

The liquid side height of transfer unit and the mass transfer efficiency of the process (*HETP*) were estimated. The use of the IL as solvent exhibited lower mass transfer efficiencies for all the studied cases. The *HETP*s when using [hmim][TCB] were almost as twice as high as with NMP.

In this case, high solvent-to-feed ratios were required to avoid forming two liquid phases leading to attractive relative volatilities (α = 9.42 at S/F ratio 5) and high liquid phase viscosities. However, the first could not overcome the effect of liquid phase viscosity. Therefore, during the solvent screening for this separation it would be crucial to select a less viscous ionic liquid (<< 47.83 [mPa s] at 298.15 K) with high relative volatilities.

Nomenclature

E_{OV}	Tray efficiency
$HETP$	Height equivalent to a theoretical plate, m
H_L	Height of transfer units in the liquid phase, m
H_V	Height of transfer units in the vapor phase, m
H_{OV}	Overall height of transfer units, m
k_L	Liquid side mass transfer coefficient, m s^{-1}
k_V	Vapor side mass transfer coefficient, m s^{-1}
$N_L^{'}$	Number of transfer units in the liquid phase
N_V	Number of transfer units in the 137apour phase
N_{OV}	Overall number of transfer units
T	Temperature, K
u_L	Superficial velocity of liquid, m s^{-1}
u_V	Superficial velocity of vapour, m s^{-1}

Greek letters

α	Relative volatility
Λ	Stripping factor
η	Dynamic viscosity, mPa s
σ	Surface tension, mN m^{-1}

Reference List

[1] Z.Lei, C. Li and B.Chen, Extractive Distillation: A Review, Sep.Purif.Rev., 32, 2003, 121 - 213.

[2] J.P.Gutierrez, W.Meindersma, and A.B.de Haan, Binary and ternary (liquid + liquid) equilibrium for {methylcyclohexane (1) + toluene (2) + 1-hexyl-3-methylimidazolium tetracyanoborate (3)/1-butyl-3-methylimidazolium tetracyanoborate (3)}, J.Chem.Thermodyn., 43, 2011, 1672 - 1677.

[3] E.Quijada-Maldonado, S.van der Boogaart, J.H.Lijbers, G.W.Meindersma, and A.B.de Haan, Experimental densities, dynamic viscosities and surface tensions of the ionic liquids series 1-ethyl-3-methylimidazolium acetate and dicyanamide and their binary and ternary mixtures with water and ethanol at T = (298.15 K to 343.15 K)., J.Chem.Thermodyn., 51, 2012, 51 - 58.

[4] J.A.Rocha, J.L.Bravo, and J.R.Fair, Distillation Columns Containing Structured Packings: A Comprehensive Model for Their Performance. 1. Hydraulic Models, Ind.Eng.Chem.Res., 1993, 1993, 641 - 651.

[5] J.A.Rocha, J.L.Bravo, and J.R.Fair, Distillation Columns Containing Strictured Packings: A Comprehensive Model for Their Performance. 2. Mass-Tranfer Model, Ind.Eng.Chem.Res., 35, 1996, 1660 - 1667.

[6] J.L.Bravo, J.A.Rocha, and J.R.Fair, Mass Tranfer in Gauze Packings, Hydrocarbon Process., 64, 1985, 91 - 95.

[7] R.R.Tsai, A.F.Seibert, R.B.Eldridge, and G.T.Rochelle, Influence of viscosity and surface tension on the effective mass transfer area of structured packing, Energy Procedia I, 1, 2009, 1197 - 1204.

[8] A.Ataki and H.-J.Bart, Experimental and CFD Simulation Study for the Wetting of a Structured Packing Element with Liquids, Chem.Eng.Technol., 29, 2006, 336 - 347.

[9] M.Lee, J.Chiu, S.Hwang, and H.Lin, Viscosity Calculations with Eyring-Patel-Teja Model for Liquid Mixtures, Ind.Eng.Chem.Res., 38, 1999, 2867 - 2876.

7

Conclusions and Outlook

In this work the mass transfer efficiency decrease with solvent viscosity was studied by using a rate-based model and a extractive distillation pilot plant for two separation cases: water - ethanol and toluene – methylcyclohexane. By using experimentally determined physical and transport properties of the ionic liquids a rate-based model was developed to predict the changes in mass transfer efficiency with viscosity. Later, this model was validated with a constructed pilot plant where the model appeared able to predict the performance of the pilot plant. By the use of the rate-based model it was demonstrated that the physical properties of ionic liquids and specifically the viscosity do affect the mass transfer efficiency of extractive distillation columns. However, when considerable improvements in relative volatilities are achieved, it is possible to overcome these reductions in mass transfer efficiency. To corroborate this conclusion, experiments in the pilot plant showed that for the separation of toluene – methylcyclohexane the reference solvent showed higher mass transfer efficiency because the use of 1-hexyl-3-methylimidazolium tetracyanoborate required high solvent-to-feed ratios and therefore yielded high liquid phase viscosities.

7.1 Conclusions

The main objective of this work was an

Investigation into the effects of physical properties of ionic liquids as solvents on the mass transfer efficiency in an extractive distillation column using the rate-based model.

To achieve the main objective, sub-objectives were defined as follows:

- Investigation of the relevant physical properties to study the decrease of the mass transfer efficiency by the use of ionic liquids as solvents
- Experimental determination of liquid viscosity, infinite dilution diffusion coefficients and surface tension of the selected ionic liquids for water – ethanol separation.
- Validation with experimental data from a pilot plant of a built rate-based model to predict the water – ethanol separation using ionic liquids as solvent.
- Investigation into the effect of liquid viscosity of ionic liquid on mass transfer efficiency.
- Experimental comparison an ionic liquid and an organic solvent on the performance of the toluene - methylcyclohexane separation in an extractive distillation pilot plant.

Sieve trays and Mellapak® 250Y were the selected internals to study the effect of physical properties on mass transfer efficiency. For the water – ethanol separation three ionic liquids were chosen: 1-ethyl-3-methyimidazolium chloride, [emim][Cl]; 1-ethyl-3-methyimidazolium acetate [emim][OAc]; and 1-ethyl-3-methyimidazolium dicyanamide, [emim][DCA]. Furthermore, ethylene glycol was selected as the reference solvent.

The rate-based model requires physical and transport properties to provide predictions. The required physical and transport properties to be experimentally determined and thus

accurately represent the changes in mass transfer efficiency with the use of ionic liquids were:

- dynamic viscosities as function of temperature and concentration in the ternary mixture water – ethanol – solvent;
- infinite dilution diffusion coefficients of ionic liquids in water or ethanol
- liquid surface tension as function of concentration at room temperature.

The experimental work to determine the above mentioned physical and transport properties as then carried out for the pure solvents and they in binary and ternary mixtures in a wide range of concentration and temperatures. Next, all the pure and mixture data were successfully correlated with available models from literature. With the correlation of all the measured properties, the rate-based model was developed.

An extractive distillation pilot plant equipped with Mellapak® 750Y was constructed to validate the built rate-based model. This pilot plant operated with ethylene glycol and the 1-ethyl-3-methylimidazolium dicyanamide as solvents. The comparisons between the experimental data and the simulations showed very good agreements confirming the predictive characteristic of the rate-based model.

The rate-based model stablished that in both studied column internals the relatively high viscosities of ionic liquids affected the mass tranfer efficiency. However, when considerable improvements in relative volatility were achieved it was possible to overcome the effect of viscosity on mass transfer limitations.

Finally, the constructed extractive distillation pilot plant was used to extend the mass transfer efficiency study to the separation of toluene – methylcyclohexane mixtures using the ionic liquid 1-hexyl-3-methylimidazolium tetracyanoborate and the reference solvent *N*-methyl-2-pyrrolidone. The high solvent-to-feed ratios during the operation of the pilot plant brought high liquids phase viscosities leading to decrease in mass transfer efficiency to the half of the separation with the organic solvent even though the high reported relative volatilities.

Concerning the above mentioned conclusions it is justified to conclude that although the relatively high viscosity of ionic liquids reported in this work and in literature, these novel solvents should not be discarded as solvent in extractive distillation. It is accepted in literature and academia that viscosity brings mass transfer limitations. However, the use of ionic liquids allows achieving increased relative volatilities and this property is often more important when calculating mass transfer efficiency. This new finding should be taken into account firstly in solvent screening and next in equipment design.

7.2 Outlook

In this study the effect of physical properties and especially dynamic viscosity of ionic liquids on mass transfer efficiency was evaluated using a predictive rate-based model. It was concluded that the increase in relative volatility can compensate for relatively high liquid phase viscosities. However, in the second case, the separation of toluene and methylcyclohexane showed that the high liquid phase viscosities produced by the high solvent-to-feed ratio reduced the mass transfer efficiency no matter how high the relative volatility was. This general conclusion leads to say that viscosity of ionic liquids has to be taken into account during a solvent screening.

Second, the rate-based model predicted these mass transfer efficiency changes. This model needed accurate physical and transport properties. In this sense, a more complete study on vapor – liquid equilibrium would enable the analysis of the mass transfer efficiency at any solvent-to-feed ratio. In the second separation case, the rate-based model did not produced result possibly because of the thermodynamic parameters regressed from liquid-liquid equilibrium experiments. Here, a complete vapor-liquid equilibrium is necessary to obtain predictions from the rate-based model.

Appendices

Appendix A: Data physical properties

Table A.3.1. Experimental densities, ρ, and dynamic viscosities, η, of the binary mixtures (x_1 water + $(1-x_1)$IL) at several temperatures.

x_1	ρ [g cm^{-3}]	η [mPa s]	x_1	ρ [g cm^{-3}]	η [mPa s]	x_1	ρ [g cm^{-3}]	η [mPa s]
[emim][OAc]			[emim][DCA]			[emim][Cl]		
T = 298.15 K						T = 323.15 K		
0	1.09778	132.91	0	1.10198	14.90	0.2963	1.12494	63.98
0.0992	1.09833	109.71	0.1299	1.09967	12.78	0.3946	1.12687	38.76
0.2220	1.09960	89.23	0.2248	1.09756	11.24	0.4933	1.12251	22.09
0.3233	1.10135	72.97	0.3042	1.09554	10.14	0.5818	1.11914	15.28
0.4207	1.10342	59.52	0.4308	1.09163	8.39	0.6211	1.11410	12.45
0.5408	1.10590	44.42	0.5429	1.08693	6.96	0.6715	1.10978	8.31
0.6135	1.10648	35.87	0.6534	1.08099	5.41	0.7407	1.09993	5.66
0.6805	1.10586	28.75	0.7355	1.07356	4.41	0.8002	1.08858	4.00
0.7482	1.10395	21.90	0.7944	1.06672	3.61	0.8665	1.06715	2.42
0.8134	1.09790	15.44	0.8803	1.05139	2.46	0.9344	1.02683	1.49
0.9067	1.07245	6.16	0.9530	1.02746	1.47			
1	0.99704	0.89	1	0.99704	0.89			
T = 313.15 K						T = 333.15 K		
0	1.08862	57.72	0	1.09209	10.07	0.2963	1.11939	41.04
0.0992	1.08918	49.47	0.1299	1.08976	8.71	0.3946	1.12355	28.51
0.2220	1.09043	42.26	0.2248	1.08759	7.79	0.4933	1.11693	15.95
0.3233	1.09226	35.96	0.3042	1.08552	7.04	0.5818	1.11351	11.47
0.4207	1.09404	30.19	0.4308	1.08152	5.80	0.6211	1.10836	9.41
0.5408	1.09647	23.49	0.5429	1.07671	4.81	0.6715	1.10396	6.51
0.6135	1.09710	19.09	0.6534	1.07067	3.81	0.7407	1.09439	4.42
0.6805	1.09611	15.63	0.7355	1.06316	3.11	0.8002	1.08249	3.18
0.7482	1.09400	11.99	0.7944	1.05634	2.56	0.8665	1.06107	2.10
0.8134	1.08770	8.51	0.8803	1.04142	1.73	0.9344	1.02031	1.01
0.9067	1.06285	3.74	0.9530	1.01908	1.08			
1	0.99221	0.65	1	0.99221	0.65			
T = 328.15 K						T = 343.15 K		
0	1.07953	30.31	0	1.08236	7.26	0.2963	1.11392	27.82
0.0992	1.08039	27.00	0.1299	1.07998	6.33	0.3946	1.11590	19.70
0.2220	1.08138	23.49	0.2248	1.07776	5.65	0.4933	1.11140	11.96
0.3233	1.08322	20.48	0.3042	1.07565	5.11	0.5818	1.10790	8.83
0.4207	1.08488	17.50	0.4308	1.07154	4.30	0.6211	1.10265	7.32
0.5408	1.08718	13.85	0.5429	1.06661	3.58	0.6715	1.09813	5.08
0.6135	1.08762	11.44	0.6534	1.06042	2.84	0.7407	1.08839	3.52
0.6805	1.08639	9.43	0.7355	1.05277	2.32	0.8002	1.07635	2.60
0.7482	1.08404	7.32	0.7944	1.04590	1.90	0.8665	1.05463	1.81
0.8134	1.07742	5.30	0.8803	1.03117	1.31	0.9344	1.01490	0.86

0.9067	1.05288	2.54	0.9530	1.00992	0.82			
1	0.98569	0.51	1	0.98569	0.51			
		T = 343.15 K					T = 358.15 K	
0	1.07054	18.10	0	1.07277	5.48	0.2963	1.10585	16.96
0.0992	1.07110	16.46	0.1299	1.07035	4.84	0.3946	1.10788	12.30
0.2220	1.07243	14.52	0.2248	1.06806	4.34	0.4933	1.10322	8.22
0.3233	1.07422	13.21	0.3042	1.06590	3.94	0.5818	1.09958	6.26
0.4207	1.07589	11.11	0.4308	1.06168	3.33	0.6211	1.09410	5.27
0.5408	1.07799	8.98	0.5429	1.05661	2.78	0.6715	1.08941	3.75
0.6135	1.07818	7.48	0.6534	1.05022	2.23	0.7407	1.07935	2.64
0.6805	1.07667	6.22	0.7355	1.04238	1.80	0.8002	1.06706	2.01
0.7482	1.07406	4.87	0.7944	1.03539	1.48	0.8665	1.04406	1.36
0.8134	1.06707	3.57	0.8803	1.02065	1.04	0.9344	0.99934	0.68
0.9067	1.04251	1.81	0.9530	1.00007	0.66			
1	0.97777	0.41	1	0.97777	0.41			

[a] Standard uncertainties u are $u(T)$ = 0.003, $u(x)$ = 5E-05, $u(\rho)$ = 1E-05 and the relative standard uncertainty u_r in $u_r(\eta)$ = 0.0038.

Table A.3.2. Experimental densities, ρ, and dynamic viscosities, η, of the binary mixtures (x_2 ethanol + $(1-x_2)$IL) at several temperatures[a].

x_2	ρ [g cm^{-3}]	η [mPa s]	x_2	ρ [g cm^{-3}]	η [mPa s]	x_2	ρ [g cm^{-3}]	η [mPa s]
	[emim][OAc]			[emim][DCA]			[emim][Cl]	
		T = 298.15 K					T = 323.15 K	
0	1.09778	132.91	0	1.10198	14.90	0.1306	1.10890	76.15
0.1059	1.08681	92.32	0.1020	1.09128	12.69	0.1997	1.10005	53.58
0.1638	1.07968	75.01	0.1981	1.07970	10.80	0.2652	1.08923	37.70
0.2471	1.06814	54.23	0.2790	1.06926	9.27	0.3356	1.07200	25.70
0.3504	1.05116	35.17	0.3596	1.05570	7.85	0.4001	1.05301	18.61
0.4165	1.03874	26.52	0.4741	1.03392	6.04	0.4769	1.03429	12.48
0.4824	1.02487	19.82	0.6028	1.00180	4.42	0.5335	1.01479	9.39
0.5572	1.00685	14.11	0.6867	0.97518	3.47	0.6000	0.99543	6.53
0.6646	0.97514	8.27	0.7678	0.94285	2.72	0.6683	0.96865	4.58
0.7494	0.94523	5.35	0.8503	0.90143	2.08	0.7336	0.94036	3.20
0.8666	0.87790	2.67	0.9327	0.84639	1.53	0.8012	0.91146	2.26
1	0.78507	1.09	1	0.78507	1.09	0.8670	0.86755	1.60
						0.9333	0.82059	1.10
		T = 313.15 K					T = 333.15 K	
0	1.08862	57.72	0	1.09209	10.07	0.1306	1.11994	58.76
0.1059	1.07754	43.53	0.1020	1.08134	8.69	0.1997	1.10437	41.89
0.1638	1.07035	36.91	0.1981	1.06970	7.53	0.2652	1.08559	29.86
0.2471	1.05871	28.48	0.2790	1.05921	6.58	0.3356	1.06568	20.42
0.3504	1.04158	20.30	0.3596	1.04558	5.68	0.4001	1.04692	15.01
0.4165	1.02905	16.06	0.4741	1.02367	4.45	0.4769	1.02815	10.30

0.4824	1.01506	12.48	0.6028	0.99143	3.31	0.5335	1.00861	7.88
0.5572	0.99689	9.24	0.6867	0.96448	2.65	0.6000	0.98906	5.56
0.6646	0.96488	5.79	0.7678	0.93185	2.10	0.6683	0.96216	3.98
0.7494	0.93468	3.89	0.8503	0.88997	1.63	0.7336	0.93329	2.81
0.8666	0.86640	2.02	0.9327	0.83424	1.19	0.8012	0.89754	2.00
1	0.77202	0.83	1	0.77202	0.83	0.8670	0.85976	1.42
						0.9333	0.81210	0.97
		T = 328.15 K					T = 343.15 K	
0	1.07953	30.31	0	1.08236	7.26	0.1306	1.09119	41.93
0.1059	1.06836	24.14	0.1020	1.07156	6.32	0.1997	1.08296	30.46
0.1638	1.06111	21.14	0.1981	1.05986	5.50	0.2652	1.07192	22.13
0.2471	1.04938	17.22	0.2790	1.04932	4.86	0.3356	1.05940	15.14
0.3504	1.03210	12.77	0.3596	1.03561	4.29	0.4001	1.04083	11.42
0.4165	1.01947	10.47	0.4741	1.01356	3.47	0.4769	1.02226	8.13
0.4824	1.00537	8.44	0.6028	0.98105	2.59	0.5335	1.00252	6.37
0.5572	0.98703	6.48	0.6867	0.95388	2.09	0.6000	0.98278	4.60
0.6646	0.95472	4.27	0.7678	0.92088	1.67	0.6683	0.95567	3.37
0.7494	0.92420	2.96	0.8503	0.87848	1.30	0.7336	0.92633	2.42
0.8666	0.85480	1.59	0.9327	0.82195	0.93	0.8012	0.88352	1.75
1	0.75858	0.64	1	0.75858	0.64	0.8670	0.85214	1.24
						0.9333	0.80388	0.85
		T = 343.15 K						
0	1.07054	18.10	0	1.07277	5.48			
0.1059	1.05928	14.96	0.1020	1.06192	4.85			
0.1638	1.05198	13.51	0.1981	1.05017	4.25			
0.2471	1.04014	11.24	0.2790	1.03956	3.81			
0.3504	1.02274	8.69	0.3596	1.02577	3.37			
0.4165	1.01000	7.31	0.4741	1.00356	2.76			
0.4824	0.99577	6.05	0.6028	0.97068	2.13			
0.5572	0.97726	4.76	0.6867	0.94333	1.70			
0.6646	0.94462	3.27	0.7678	0.90993	1.37			
0.7494	0.91374	2.33	0.8503	0.86693	1.10			
0.8666	0.84320	1.28	0.9327	0.80940	0.75			
1	0.74453	0.50	1	0.74453	0.50			

[a] Standard uncertainties u are $u(T)$ = 0.003, $u(x)$ = 5E-05, $u(\rho)$ = 1E-05 and the relative standard uncertainty u_r in $u_r(\eta)$ = 0.0036.

Table A.3.3. Experimental densities, ρ, and dynamic viscosities, η, of the ternary mixtures (x_1 water + x_2 ethanol + 1-(x_1 + x_2) IL) at several temperatures[a].

x_1	x_2	ρ [g cm^{-3}]	η [mPa s]	x_1	x_2	ρ [g cm^{-3}]	η [mPa s]
[emim][OAc]				[emim][DCA]			
T = 298.15 K							
0.4047	0.2995	1.03263	14.14	0.4040	0.2881	1.02854	4.63
0.3101	0.2242	1.06176	28.03	0.3032	0.4202	1.00280	4.00
0.7408	0.1179	1.05000	9.38	0.7083	0.2007	0.99042	2.87
0.3044	0.2002	1.06707	31.85	0.6015	0.2484	1.00117	3.39
0.1068	0.4124	1.03228	20.57	0.6986	0.2507	0.95781	2.65
0.6879	0.2635	0.95983	3.80	0.3486	0.1191	1.06403	6.67
0.8465	0.1044	1.01034	3.75	0.1385	0.3790	1.03972	5.89
0.2523	0.4630	0.99872	10.07	0.7595	0.0957	1.03309	3.15
0.4053	0.4916	0.93642	4.47	0.4093	0.4889	0.93514	2.77
0.6021	0.2489	1.01417	8.23	0.8359	0.1156	0.99282	2.25
0.1068	0.5914	0.98010	8.43	0.2046	0.6949	0.89979	2.27
0.1967	0.7052	0.89436	3.19				
T = 313.15 K							
0.4047	0.2995	1.02274	8.83	0.4040	0.2881	1.01807	3.33
0.3101	0.2242	1.05232	16.28	0.3032	0.4202	0.99219	2.92
0.7408	0.1179	1.03944	5.57	0.7083	0.2007	0.97958	2.00
0.3044	0.2002	1.05768	18.16	0.6015	0.2484	0.99034	2.36
0.1068	0.4124	1.02256	12.70	0.6986	0.2507	0.94642	1.76
0.6879	0.2635	0.94817	2.41	0.3486	0.1191	1.05384	4.77
0.8465	0.1044	0.99995	2.34	0.1385	0.3790	1.02947	4.31
0.2523	0.4630	0.98861	6.66	0.7595	0.0957	1.02266	2.21
0.4053	0.4916	0.92508	2.99	0.4093	0.4889	0.92354	1.95
0.6021	0.2489	1.00350	5.06	0.8359	0.1156	0.98293	1.52
T = 328.15 K							
0.4047	0.2995	1.01279	5.91	0.4040	0.2881	1.00765	2.52
0.3101	0.2242	1.04289	10.41	0.3032	0.4202	0.98161	2.23
0.7408	0.1179	1.02863	3.58	0.7083	0.2007	0.96843	1.42
0.3044	0.2002	1.04831	11.45	0.6015	0.2484	0.97936	1.74
0.1068	0.4124	1.01294	8.57	0.6986	0.2507	0.93461	1.25
0.6879	0.2635	0.93613	1.64	0.3486	0.1191	1.04378	3.64
0.8465	0.1044	0.98908	1.60	0.1385	0.3790	1.01934	3.30
T = 343.15 K							
0.4047	0.2995	1.00275	4.20	0.4040	0.2881	0.99726	2.02
0.3101	0.2242	1.03347	7.22	0.3032	0.4202	0.97104	1.77
0.7408	0.1179	1.01758	2.49	0.7083	0.2007	0.95695	1.08
0.3044	0.2002	1.03896	7.86	0.6015	0.2484	0.96821	1.34
0.1068	0.4124	1.00337	6.09	0.6986	0.2507	0.92234	0.94
0.6879	0.2635	0.92367	1.19	0.3486	0.1191	1.03382	2.85
0.8465	0.1044	0.97774	1.15	0.1385	0.3790	1.00932	2.63

[a] Standard uncertainties u are $u(T)$ = 0.003, $u(x)$ = 5E-05, $u(\rho)$ = 1E-05 and the relative standard uncertainty u_r in $u_r(\eta)$ = 0.0035.

Table A.3.4. Experimental densities ρ and dynamic viscosities η of the ternary system (x_1 water + x_2 ethanol + 1-($x_1 + x_2$)EG) at several temperatures[a].

		ρ [g cm^{-3}]				η [mPa s]			
		T [K]				T [K]			
x_1	x_2	298.15	308.15	318.15	328.15	298.15	308.15	318.15	328.15
0.4024	0.2725	0.98438	0.97668	0.96882	0.96078	4.578	3.383	2.566	2.005
0.8369	0.1135	0.97758	0.97123	0.96445	0.95729	2.375	1.731	1.317	1.030
0.7015	0.2350	0.94283	0.93501	0.92695	0.91861	2.755	2.006	1.514	1.192
0.7496	0.0969	1.01146	1.00478	0.99779	0.99051	3.165	2.322	1.769	1.387
0.6972	0.1921	0.96895	0.96144	0.95368	0.94565	3.056	2.239	1.690	1.324
0.6064	0.2391	0.96407	0.95631	0.94834	0.94014	3.334	2.464	1.872	1.472
0.3099	0.2050	1.02378	1.01634	1.00876	1.00104	6.530	4.662	3.495	2.700
0.5988	0.2058	0.98327	0.97570	0.96791	0.95990	3.691	2.708	2.058	1.612
0.5101	0.2408	0.98186	0.97418	0.96632	0.95825	4.055	2.987	2.273	1.779
0.6944	0.1130	1.01822	1.01133	1.00419	0.99679	3.584	2.627	1.999	1.565
0.6172	0.1056	1.03042	1.02334	1.01605	1.00854	4.458	3.247	2.463	1.913
0.7674	0.1960	0.94708	0.93955	0.93173	0.92362	2.562	1.854	1.398	1.090
0.2892	0.2887	0.99282	0.98518	0.97739	0.96945	5.307	3.902	2.956	2.299
0.8011	0.1000	0.99703	0.99059	0.98379	0.97664	2.688	1.974	1.504	1.184
0.1074	0.4050	0.97171	0.96396	0.95610		5.121	3.778	2.892	
0.2766	0.4220	0.94218				3.726			
0.1097	0.5862	0.90768				3.033			
0.4213	0.4769	0.89154				2.460			
0.2107	0.6868	0.85146				1.945			
0.3126	0.4726	0.91549				3.035			
0.5023	0.2981	0.95601				3.533			
0.5076	0.3919	0.90958				2.659			
0.1130	0.6858	0.87165				2.257			
0.7919	0.0490	1.03009				2.897			
0.1998	0.5973	0.88887				2.553			
0.3940	0.4086	0.92694				3.166			
0.1025	0.4945	0.94117				3.925			
0.2997	0.5938	0.86859				2.196			
0.1177	0.7891	0.83374				1.677			
0.0010	0.9071	0.81674				1.432			
0.0010	0.7826	0.85881				2.017			
0.0009	0.6667	0.89753				2.789			
0.0009	0.5990	0.91981				3.333			
0.0009	0.4943	0.95424				4.471			

[a] Standard uncertainties u are $u(T)$ = 0.003, $u(x)$ = 5E-05, $u(\rho_m)$ = 1E-05 and the relative standard uncertainty u_r in $u_r(\eta_m)$ = 0.0044.

Table A.3.5. Infinite molar conductivities Λ^0 [m^2 S mol^{-1}] of ionic liquids in water or ethanol*

	IL in water			IL in ethanol		
T [K]	[emim][OAc]	a	b	[emim][OAc]	a	b
298.15	0.00789	0.3170	0.007649	0.00416	0.3175	0.009681
303.15	0.00883	0.3171	0.008599	0.00456	0.3177	0.010960
308.15	0.00978	0.3173	0.009556	0.00496	0.3179	0.012270
313.15	0.01073	0.3174	0.010520	0.00537	0.3181	0.013600
318.15	0.01168	0.3175	0.011500	0.00578	0.3183	0.014960
323.15	0.01265	0.3176	0.012480	0.00620	0.3185	0.016340
SSE	5.633E-08			1.662E-08		
T [K]	[emim][DCA]	a	b	[emim][DCA]	a	b
298.15	0.00956	0.3173	0.009579	0.00502	0.3178	0.011620
303.15	0.01064	0.3174	0.010680	0.00549	0.3180	0.013100
308.15	0.01172	0.3176	0.011780	0.00598	0.3183	0.014610
313.15	0.01282	0.3177	0.012900	0.00647	0.3185	0.016150
318.15	0.01392	0.3192	0.014030	0.00697	0.3187	0.017720
323.15	0.01502	0.3180	0.015170	0.00747	0.3190	0.019320
SSE	3.369E-08			2.528E-08		
T [K]	[emim][Cl]	a	b	[emim][Cl]	a	b
298.15	0.01193	0.3172	0.009756	0.00438	0.3178	0.011510
303.15	0.01326	0.3174	0.010990	0.00479	0.3180	0.012890
308.15	0.01460	0.3175	0.012240	0.00521	0.3182	0.014290
313.15	0.01595	0.3177	0.013500	0.00563	0.3185	0.015710
318.15	0.01730	0.3179	0.014770	0.00606	0.3187	0.017170
323.15	0.01867	0.3180	0.016050	0.00650	0.3189	0.018650
SSE	7.371E-08			2.941E-08		

* $\Lambda = \Lambda^0 - \left(a\Lambda^0 + b\right)\sqrt{C}$, where $\Lambda = 1000\left(\frac{\sigma_{EC}}{C}\right)$

Table A.3.6. Experimental surface tension for the system system (x_1 water + x_2 ethanol + 1-($x_1 + x_2$)EG) at around T = 298.15 [K].

T [K] ± st			x_1	x_2	σ [mN m^{-1}] ± st		
297.6	±	0.06	0.1120	0.4246	28.23	±	0.06
297.2	±	0.10	0.1853	0.6871	24.60	±	0
297.4	±	0.06	0.4957	0.1970	32.63	±	0.06
297.3	±	0.00	0.5773	0.3381	27.80	±	0
297.3	±	0.00	0.6116	0.1236	35.83	±	0.06
297.3	±	0.00	0.6508	0.2543	28.97	±	0.06
296.9	±	0.25	0.7139	0.0027	43.00	±	0.10
297.1	±	0.21	0.7154	0.0025	42.00	±	0
297.4	±	0.10	0.7176	0.1002	36.70	±	0
297.2	±	0.15	0.7574	0.0293	43.33	±	0.21

Table A.3.7. Experimental surface tension for the system system (x_1 water + x_2 ethanol + 1-($x_1 + x_2$)[emim][OAc]) at around T = 298.15 [K].

T [K] ± st			x_1	x_2	σ [mN m^{-1}] ± st		
298.2	±	0.06	0.8607	0.0671	32.23	±	0.35
298.9	±	0.36	0.6972	0.2312	29.10	±	0.00
298.7	±	0.25	0.8811	0.0350	40.60	±	0.30
298.8	±	0.43	0.9111	0.0035	44.85	±	0.97
298.5	±	0.17	0.7375	0.1646	31.50	±	0.00
298.8	±	0.15	0.8061	0.0454	40.37	±	0.21
298.3	±	0.06	0.7525	0.0942	36.37	±	0.06
298.5	±	0.43	0.8478	0.0046	35.77	±	0.31
298.6	±	0.15	0.6802	0.1552	33.50	±	0.00
298.2	±	0.15	0.7797	0.0302	41.30	±	0.20
297.0	±	0.15	0.1088	0.7030	27.50	±	0.00

Table A.3.8. Experimental surface tension for the system system (x_1 water + x_2 ethanol + 1-($x_1 + x_2$)[emim][DCA]) at around T = 298.15 [K].

T [K] ± st			x_1	x_2	σ [mN m^{-1}] ± st		
298.3	±	0.12	0.0023	0.8140	25.6	±	0.06
297.7	±	0.10	0.0024	0.7947	26.1	±	0
297.2	±	0.15	0.0026	0.7636	27.3	±	0.15
297.7	±	0.06	0.0028	0.7342	28.3	±	0.06
297.1	±	0.10	0.0202	0.7853	27.2	±	0.15
297.0	±	0.21	0.1249	0.7953	24.6	±	0
297.8	±	0.10	0.1328	0.7419	25.8	±	0.10
296.6	±	0.15	0.1395	0.8216	23.9	±	0.10
298.5	±	0.15	0.3418	0.6159	25.3	±	0.10
299.0	±	0.17	0.4859	0.3737	30.7	±	0.06
298.5	±	0.15	0.5391	0.3771	29.3	±	0
297.2	±	0.10	0.7776	0.1194	40.9	±	0.17
296.7	±	0	0.7866	0.1743	34.3	±	0.06
297.4	±	0.10	0.7984	0.0853	45.3	±	0.06
297.7	±	0.14	0.8211	0.0652	43.8	±	0.17
297.5	±	0.06	0.8324	0.0830	44.3	±	0.10
299.1	±	0.10	0.8335	0.1080	39.3	±	0.21
297.8	±	0.13	0.8576	0.0307	46.1	±	0.29
297.6	±	0.10	0.8611	0.1064	38.9	±	0.06
297.6	±	0.06	0.8675	0.0674	45.9	±	0
297.8	±	0.06	0.8722	0.0000	46.9	±	0.21
297.8	±	0.08	0.8857	0.0125	53.0	±	0.12
297.3	±	0.10	0.8912	0.0000	50.3	±	0.15
299.4	±	0.25	0.8917	0.0865	40.1	±	0.06
298.1	±	0.12	0.8944	0.0025	48.3	±	0.31
297.5	±	0.06	0.9081	0.0000	49.8	±	0.26
297.4	±	0	0.9215	0.0000	50.3	±	0.21
297.8	±	0.21	0.9405	0.0259	49.2	±	0.25

Table A.3.9. Experimental surface tension for the system system (x_1 water + x_2 ethanol + 1-($x_1 + x_2$)[emim][Cl]) at around T = 298.15 [K].

T [K] ± st			x_1	x_2	σ [mN m^{-1}] ± st		
298.0	±	0.17	0.8553	0.0343	42.40	±	0.36
298.7	±	0.26	0.8977	0.0037	50.73	±	0.06
296.8	±	0.20	0.6163	0.2845	28.47	±	0.06
297.1	±	0.15	0.8033	0.0968	36.77	±	0.15
297.4	±	0.10	0.8969	0.0033	51.67	±	0.21
297.5	±	0.15	0.7706	0.0535	38.17	±	0.12
297.1	±	0.20	0.7167	0.0984	37.53	±	0.06
297.6	±	0.06	0.8017	0.0081	54.97	±	0.15
297.4	±	0.17	0.6577	0.1510	34.07	±	0.06
297.7	±	0.17	0.7311	0.0475	45.83	±	0.30
296.6	±	0.35	0.0967	0.6870	27.43	±	0.06
297.3	±	0.20	0.1621	0.5689	29.13	±	0.06

Table A.6.1. Densities and dynamic viscosities of the ternary mixture toluene(1) – methylcyclohexane (2) - [hmim][TCB](3) at several temperatures.

x_1	x_2	ρ [g cm^{-3}]	η [mPa s]
		T = 298.15 K	
0.6042	0.0251	0.9497	7.317
0.4855	0.0439	0.9580	11.089
0.0392	0.1279	0.9759	36.245
0.2784	0.0859	0.9690	19.837
0.0000	0.1074	0.9818	41.252
		T = 308.15 K	
0.6042	0.0251	0.9424	5.590
0.4855	0.0439	0.9506	8.151
0.0392	0.1279	0.9688	23.506
0.2784	0.0859	0.9618	13.733
0.0000	0.1074	0.9746	26.395
		T = 318.15 K	
0.6042	0.0251	0.9348	4.411
0.4855	0.0439	0.9433	6.251
0.0392	0.1279	0.9617	16.290
0.2784	0.0859	0.9546	10.054
0.0000	0.1074	0.9676	18.053

T = 328.15 K			
0.6042	0.0251	0.9274	3.596
0.4855	0.0439	0.9359	4.953
0.0392	0.1279	0.9546	11.857
0.2784	0.0859	0.9475	7.698
0.0000	0.1074	0.9605	13.040

Parameter regression

The Eyring-Patel-Teja model was used to correlate the experimental data. The model needs of parameters that are obtained by regressing experimental data and minimizing the relative difference between the experimental data and the calculated value. A Margules type mixing rule (chapter 2) in combination with the mentioned model are used to correlate de experimental data. The obtained parameters are given in table A.6.2.

Table A.6.2. Interaction parameters $l_{i,j}$ of GM3 mixing rule in the Eyring-Patel-Teja model (Chapter 2).

Interaction parameter	GM2
l_{12}	0
l_{21}	0.8071
l_{13}	0.1462
l_{31}	0.0077
l_{23}	0.6531
l_{32}	-0.3519
$\%ADD$[a]	2.54

[a] $ADD\ [\%] = 100/n_{\exp} \sum_{i=1}^{n_{\exp}} \left| \eta_{mix,exp} - \eta_{mix,calc} \right| / \eta_{mix,exp}$

Figure A.6.1 shows the experimental and regressed ternary dynamic viscosities as function of temperature.

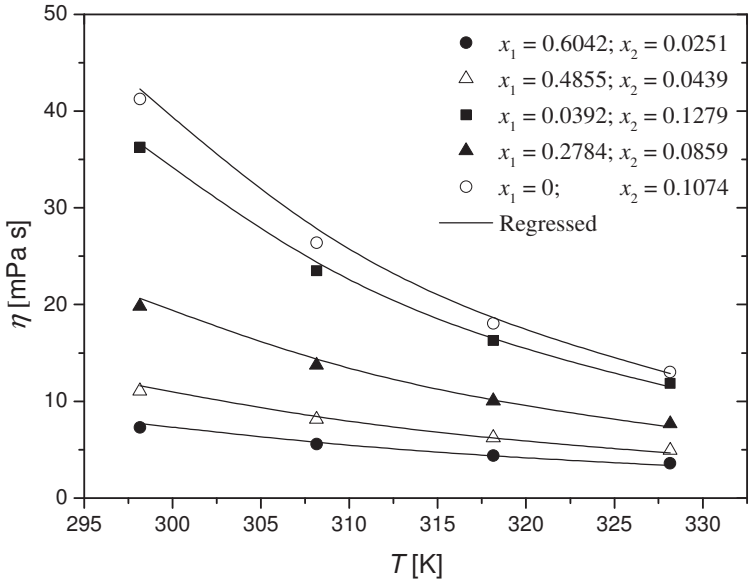

Figure A.6.1. Regression of the experimental data of (x_1 toluene + x_2 methylcyclohexane + x_3[hmim][TCB]) with the Eyring-Patel-Teja model using the GM3 type mixing rule between T = 298.15 K and T = 328.15 K.

List of Publications

Journals

E. Quijada-Maldonado, G.W. Meindersma, A.B. de Haan**,** Ionic liquid effects on mass transfer efficiency in extractive distillation of water – ethanol mixtures, Submitted to *Computers & Chemical Engineering*, 2013.

E. Quijada-Maldonado, T.A.M. Aelmans, G.W. Meindersma, A.B. de Haan, Pilot plant validation of a rate-based extractive distillation model for water-ethanol separation with the ionic liquid [emim][DCA] as solvent. *Chemical Engineering Journal*. 223 (2013), 287-297.

E. Quijada-Maldonado, G.W. Meindersma, A.B. de Haan, Viscosity and density data for the ternary system water(1) – ethanol(2) – ethylene glycol(3) between 298.15 and 328.15K, *Journal of Chemical Thermodynamics*. 57 (2013), 500-505.

E.Quijada-Maldonado, S. van der Boogaart, J.H. Lijbers, G.W. Meindersma, A.B. de Haan, Experimental densities, dynamic viscosities and surface tensions of the ionic liquids series 1-ethyl-3-methylimidazolium acetate and dicyanamide and their binary and ternary mixture with water and ethanol at T = (298.15 to 343.15 K), *Journal of Chemical Thermodynamics*, 51, 51 – 58, 2012.

E. Quijada-Maldonado, G.W. Meindersma, A.B. de Haan, Mass Transfer efficiency in the extractive distillation of toluene + methylcyclohexane mixtures with [hmim][TCB] and NMP as solvents in a pilot plant, (in preparation).

Journal Publications prior PhD thesis

V. Bubnovich, A. Reyes, E. Quijada, A. Mahn, Numerical simulation of lyophilisation of carrot slices at atmospheric pressure in a fluidized bed, *Journal of Food Engineering*, 109, 659 – 667, 2012.

V. Bubnovich, E.Quijada, A. Reyes, Computer Simulation of Atmospheric Freeze Drying of Carrot Slices in a Fluidized Bed*, Numerical Heat Transfer-Part A: Applications*, 56, 170 – 191, 2009.

Book Chapter

G.W. Meidersma, E. Quijada-Maldonado, T.A.M. Aelmans, J.P. Gutierrez-Hernandez, A.B. de Haan, Ionic Liquids in Extractive Distillation of Ethanol/Water: From Laboratory to Pilot Plant, in: A.E.Visser, N.J.Bridges, and R.D.Rogers (Eds.), Ionic liquids: Science and Applications*, ACS Symposium Series*, 2012, pp. 239-257.

Reviewed conference proceeding

E. Quijada-Maldonado; G. W. Meindersma and A. B. de Haan (2014) Mass Transfer efficiency in the extractive distillation of toluene + methylcyclohexane mixtures with [hmim][TCB] and NMP as solvents in a pilot plant. Proceeding of the 10th Distillation & Absorption conference, Friedrichshafen, Germany. Submitted.

E. Quijada, G.W. Meindersma, A.B. de Haan (2010) Rate-Based Mass Transfer Performance Analysis of [EMIM][EtSO4] and Ethylene Glycol in the Extractive Distillation of Water-Ethanol Mixtures. Proceeding of the 9th Distillation & Absorption conference, Eindhoven, The Netherlands, 12 – 15 September 2010, A.B. de Haan, H. Kooijman, A. Górak, 455 - 460

Popular publication

G.W. Meindersma, E. Quijada-Maldonado, J.P. Gutierrez Hernandez, A.B. de Haan (2013) Energie-efficiënt scheiden van azeotropen, NPT procestechnologie, Februari 2013, 18-21.

Conference presentations

Oral presentation

Pilot plant validation of a rate-based extractive distillation model for water-ethanol separation with the ionic liquid [EMIM]DCA as solvent, Chisa 2012, Prague, Czech Republic, 25 – 29 August 2012.

Poster presentations

Rate-Based Mass Transfer Performance Analysis of [EMIM][EtSO4] and Ethylene glycol in the Extractive Distillation of Water-Ethanol Mixtures, CAPE Forum, Aachen, Germany, 11 – 12 March 2010.

Rate Based Mass Tranfer Performance in a Extractive Distillation of water-ethanol Mixture using Ionic Liquids, NPS 9, Velhoven, The Netherlands, 26 – 28 October 2009.

Curriculum Vitae

Esteban de la Cruz Quijada Maldonado was born on the 15th of August 1980 in Providencia, Santiago of Chile. After finishing the high school in 1998 at Guillermo Gonzalez Heinrich in Santiago, He studied Chemical Engineering at the Metropolitan University of Technology from 2000 to 2004. In 2005 He started his internship as Process Engineer at United Breweries Company, abbreviated C.C.U in Spanish (Compañía de Cervecerías Unidas) where for one year developed the project called Quality Assurance of the Process Water. After this internship, in 2008, he graduated at Santiago University of Chile on numerical simulation of the atmospheric freeze drying process in a pulsed fluidized bed. In 2009 Esteban started a PhD project at Eindhoven University of Technology at Eindhoven in the group of Prof.dr.ir André de Haan and under the supervision of Dr.ir. Wytze Meindersma of which results are presented in this thesis. The 1st of October 2013, Esteban was accepted as associate professor at Catholic University of Valparaiso in Chili.